



THE HONG KONG
POLYTECHNIC UNIVERSITY

香港理工大學

Pao Yue-kong Library

包玉剛圖書館

Copyright Undertaking

This thesis is protected by copyright, with all rights reserved.

By reading and using the thesis, the reader understands and agrees to the following terms:

1. The reader will abide by the rules and legal ordinances governing copyright regarding the use of the thesis.
2. The reader will use the thesis for the purpose of research or private study only and not for distribution or further reproduction or any other purpose.
3. The reader agrees to indemnify and hold the University harmless from and against any loss, damage, cost, liability or expenses arising from copyright infringement or unauthorized usage.

IMPORTANT

If you have reasons to believe that any materials in this thesis are deemed not suitable to be distributed in this form, or a copyright owner having difficulty with the material being included in our database, please contact lbsys@polyu.edu.hk providing details. The Library will look into your claim and consider taking remedial action upon receipt of the written requests.

**AKT PATHWAY IN MALIGNANT
PERIPHERAL NERVE SHEATH TUMOR
TREATMENT AND WHITE ADIPOSE
TISSUE METABOLISM**

LI XIAOXIAO

PhD

The Hong Kong Polytechnic University

2019

The Hong Kong Polytechnic University
Department of Applied Biology & Chemical
Technology

**AKT pathway in malignant peripheral
nerve sheath tumor treatment and
white adipose tissue metabolism**

LI XIAOXIAO

**A thesis submitted in partial fulfilment of the
requirements for the degree of Doctor of Philosophy**

Aug 2018

CERTIFICATE OF ORIGINALITY

I hereby declare that this thesis is my own work and that, to the best of my knowledge and belief, it reproduces no material previously published or written, nor material that has been accepted for the award of any other degree or diploma, except where due acknowledgement has been made in the text.

_____ (Signed)

LI XIAOXIAO Name of student

Abstract

There are two projects in this thesis. In the first project, a natural compound named DAW22 was tested *in vitro* and *in vivo* to evaluate its efficacy on malignant peripheral nerve sheath tumor (MPNST) treatment. DAW22 was found to inhibit human MPNST cancer cell line growth viability *in vitro* and reduce tumor growth *in vivo* by targeting AKT/ERK/CTNNB1 pathways and inducing apoptosis in cancer cells. In the second project, the role of Schwann cells (SCs) in the regulation of white adipose tissue (WAT) metabolism was investigated using a transgenic mouse model. SCs-specific *phosphatase and tensin homolog (Pten)* gene inactivation was demonstrated to affect the sympathetic nervous system (SNS) function and subsequently influence SNS-driven lipolysis in WATs.

Publications made during PhD studentship

1. **Li Xiao-Xiao**, Lu Xin-Yi, *et al.* Sodium Tanshinone IIA Sulfonate Ameliorates Hepatic Steatosis by Inhibiting Lipogenesis and Inflammation. *Biomedicine & Pharmacotherapy*, doi.org/10.1016/j.biopha.2018.12.019.
2. **Li Xiao-Xiao**, Zhang Shi-Jie, *et al.* Conditional Mutations of Nf1 and Pten in Schwann Cell Induces Abnormal Neuromuscular Junction Development in Mice. *G3-genes/Genomes/Genetics* 2018 Nov 26. pii: g3.200795.2018. doi: 10.1534/g3.118.200795.
3. **Li Xiao-Xiao**, Zhang Shi-Jie, *et al.* Targeting of AKT/ERK/CTNNB1 by DAW22 as a potential therapeutic compound for malignant peripheral nerve sheath tumor. *Cancer Medicine*. 2018 Sep;7(9):4791-4800. doi: 10.1002/cam4.1732. Epub 2018 Aug 15.

Acknowledgements

Firstly, I would like to express my sincere gratitude to my supervisor Prof Vincent Keng for his continuous support of my PhD study and research. He provided me the chance to join his research team. He is really a nice person with great patience to teach me how to address problems in experiments. His guidance has helped me a lot for doing experiments, writing papers and this thesis, as well as how to be a good presenter.

My sincere thanks also goes to my lab mates, Amy Chiu, Lilian Lo, Jeffrey To, Carlton Wong, Jenny Zhang, Coco Lam, Faa Yu and Cynthia Chiu. Without their precious support and company, it would not be possible for me to fulfil the research. Yoyo Yu and Hening Cui are undergraduate student helpers, who also helped me a lot, especially from Jan 2018 to Jun 2018. I also want to thank Shi Jie Zhang for the stimulating discussions and lab work.

Lastly, I would like to thank my family: my mother and my husband for supporting me spiritually throughout the past three years. My husband is very strict to me, and he always push me to work harder. Sometimes I was unhappy because of what he said, but working hard really helps to become a better researcher. Thank you for his company.

Last but not least, I would like to list the grants that supporting our studies:

- 1) The Shenzhen Science and Technology Innovation Commission (JCYJ20170413154748190);

- 2) Research Grants Council Collaborative Research Fund Scheme (C5012-15E), Hong Kong SAR Government;
- 3) Department of Applied Biology and Chemical Technology, The Hong Kong Polytechnic University, Hong Kong SAR (G-YBTA).

Table of Contents

CERTIFICATE OF ORIGINALITY	3
Abstract.....	4
Publications made during PhD studentship.....	5
Acknowledgements	6
Part 1 Abstract.....	14
CHAPTER 1: Introduction	15
1.1 Malignant peripheral nerve sheath tumors.....	15
1.1.1 Classification of malignant peripheral nerve sheath tumors.....	15
1.1.2 Epidemiology, risk factors and prognosis of MPNSTs	18
1.1.2 General treatment options for MPNSTs patients.....	20
1.1.3 Molecular insights and clinical implications of MPNST	21
1.2 Genetic information of human MPNST cancer cell lines.....	28
1.3 DAW22	31
1.3.1 Purification procedure of DAW22.....	31
1.3.2 Studies about DAW22 and rationale of this study	31
CHAPTER 2: Methodology.....	33
2.1 <i>In vitro</i> studies.....	33
2.1.1 Chemicals.....	33
2.1.2 Cell lines and cell culture	33
2.1.3 Cell proliferation assay.....	34
2.1.4 Colony formation assay	34
2.1.5 Cell cycle assay	35

2.1.6 Western blot analyses	35
2.2 <i>In vivo</i> studies	36
2.2.1 Xenograft mouse model and treatment of DAW22	36
2.2.2 Monitoring of tumor growth and body weight.....	36
2.2.3 Hematoxylin and eosin staining	37
2.3 Statistical analyses.....	37
CHAPTER 3: Results	38
3.1 DAW22 inhibits cell proliferation through induction of apoptosis.....	38
3.1.1 DAW22 inhibits cell proliferation in both sporadic and NF1-related MPNST cell lines	38
3.1.2 DAW22 induces apoptosis in both sporadic and NF1-related MPNST cell lines	40
3.2 DAW22 reduced phosphorylation of AKT, ERK and active CTNNB1 in MPNST cell lines	45
3.2.1 DAW22 reduced phosphorylation of AKT, ERK and non-phospho (active) CTNNB1 in MPNST cell lines	45
3.2.2 AKT inhibitor AZD5363 induced apoptosis in STS-26T, ST8814 and S462 MPNST cancer cell lines	48
3.3 DAW22 reduced tumor growth in xenograft transplanted experiments.....	50
3.3.1 DAW22 treatment delayed the tumor growth of STS-26T cells- transplanted xenograft MPNST model	50
3.3.2 DAW22 reduced phosphorylation of AKT, ERK and non-phospho (active) CTNNB1 in transplanted mice	52
3.3.3 HE staining of tissues from xenografted transplant experiments.....	53

CHAPTER 4: Discussion	55
Reference	60
Part 2 Abstract	75
CHAPTER 5: Introduction	76
5.1 Adipose tissue	76
5.2 The role of sympathetic nervous system in lipolysis	80
5.3 Schwann cells and adipose tissue	83
5.4 PTEN in lipid metabolism	85
5.5 Objectives and significance of this study	85
CHAPTER 6: Methodology	87
6.1 Animal model	87
6.1.1 Establishment of the animal model	87
6.1.2 PCR Genotyping	88
6.1.3 AKT inhibitor treatment	91
6.2 Experimental methods	91
6.2.1 Hematoxylin-Eosin (HE) staining	91
6.2.2 Western blot	92
6.2.3 Immunohistochemistry (IHC) staining	93
6.2.4 UPLC-QQQ-MS based neurotransmitters metabolites	94
CHAPTER 7: Results	96
7.1 SCs-specific <i>Pten</i> inactivation induced bigger iWAT	96
7.2 SCs-specific <i>Pten</i> inactivation results in elevated iWAT fat index	98
7.3 SCs-specific <i>Pten</i> inactivation induced activated AKT signal	101

7.4 SCs-specific <i>Pten</i> inactivation inhibited SNS activity.....	102
7.4.1 SCs-specific <i>Pten</i> inactivation inhibited tyrosine hydroxylase expression	102
7.4.2 SCs-specific <i>Pten</i> inactivation results in decreased NE, dopamine and histamine content	103
7.5 AKT inhibitor AZD5363 improved iWAT hyperplasia	105
7.5.1 AKT inhibitor treatment improved iWAT phenotype.....	105
7.5.2 AKT inhibitor treatment improved SNS activity.....	107
CHAPTER 8: Discussion.....	108
Reference.....	111

LIST OF FIGURES

FIGURE 1 POTENTIAL MOLECULAR TARGETS AND CLINICAL IMPLICATIONS OF MPNST.	27
FIGURE 2 DAW22 INHIBITED CELL PROLIFERATION OF SPORADIC AND NF1-RELATED MPNST CELL LINES.....	39
FIGURE 3 CELL CYCLE ANALYSES AND MORPHOLOGICAL CHANGES IN DAW22- TREATED MPNST CELL LINES.	42
FIGURE 4 LIVE-CELL IMAGING OF INDUCED APOPTOSIS BY DAW22 TREATMENT.....	43
FIGURE 5 INDUCED APOPTOSIS IN DAW22-TREATED MPNST CELLS LINES.	44
FIGURE 6 DAW22 TREATMENT INDUCED CASP3 AND PARP CLEAVAGE IN MPNST CELL LINES IN A TIME-DEPENDENT MANNER.	45
FIGURE 7 DAW22 REDUCED PHOSPHORYLATION OF AKT, ERK AND NON-PHOSPHO (ACTIVE) CTNNB1 IN MPNST CELL LINES.....	47
FIGURE 8 DAW22 TREATMENT REDUCED AKT AND ERK PHOSPHORYLATION IN MPNST CELL LINES IN A TIME-DEPENDENT MANNER.....	48
FIGURE 9 AKT INHIBITOR AZD5363 INDUCED APOPTOSIS IN STS-26T, ST8814 AND S462 MPNST CANCER CELL LINES.	49
FIGURE 10 IN VIVO ANTI-CANCER EFFECT OF DAW22 ON STS-26T TRANSPLANTED XENOGRAFT MOUSE MODEL.	51
FIGURE 11 WESTERN BLOT ANALYSES OF TRANSPLANTED XENOGRAFT TUMORS FROM BOTH VEHICLE- AND DAW22-TREATED GROUPS.	53
FIGURE 12 HE STAINING OF VARIOUS TISSUES TAKEN FROM VEHICLE- AND DAW22- TREATED XENOGRAFT MICE.	54
FIGURE 13 DAW22 TARGETS MULTIPLE SIGNALLING PATHWAYS INVOLVED IN MPNST DISEASE PROGRESSION.....	59

FIGURE 14 THE PHENOTYPE OF THREE DIFFERENT ADIPOCYTES.	77
FIGURE 15 BODY DISTRIBUTION OF WAT AND BAT IN HUMAN (RÀFOLS, 2014).	78
FIGURE 16 ADIPOSE TISSUES INNERVATED BY SYMPATHETIC NERVOUS SYSTEM (SNS) (CARON, LEE, ELMQUIST, & GAUTRON, 2018).	82
FIGURE 17 DETECTION OF SCHWANN CELLS (SCs) IN MOUSE INGUINAL ADIPOSE TISSUE (L. CHEN ET AL., 2017).	84
FIGURE 18 CONDITIONAL INACTIVATION OF PTEN IN SCs.	90
FIGURE 19 SAMPLE PREPARATION PROTOCOL.	95
FIGURE 20 CONDITIONAL INACTIVATION OF PTEN IN SCs INDUCED BIGGER IWAT. .	97
FIGURE 21 ANATOMICAL LOCATIONS OF DIFFERENT WAT AND BAT IN MICE.	99
FIGURE 22 CONDITIONAL INACTIVATION OF PTEN IN SCs RESULT IN IWAT HYPERPLASIA.	100
FIGURE 23 ELEVATED PAKT IN THE SCIATIC NERVES OF DHH-CRE; PTEN ^{F/F} MICE.	101
FIGURE 24 REDUCED TH EXPRESSION IN THE IWAT OF DHH-CRE; PTEN ^{F/F} MICE. ...	103
FIGURE 25 CONTENT OF NEUROTRANSMITTERS WERE DECREASED IN IWAT OF DHH- CRE; PTEN ^{F/F} MICE.	104
FIGURE 26 AKT INHIBITOR IMPROVED HYPERPLASIA OF IWAT IN DHH-CRE; PTEN ^{F/F} MICE.	106
FIGURE 27 AKT INHIBITOR TREATMENT IMPROVED TH EXPRESSION IN DHH-CRE; PTEN ^{F/F} MICE.	107

Part 1

Subtitle: Targeting of AKT/ERK /CTNNB1 by DAW22 as a potential therapeutic compound for malignant peripheral nerve sheath tumor

Part 1 Abstract

Malignant peripheral nerve sheath tumors (MPNSTs) are an aggressive form of soft tissue neoplasm with extremely poor prognosis and no effective medical options currently available. MPNSTs can occur either sporadically or in association with the neurofibromatosis type 1 (NF1) syndrome. Importantly, activation of RAS/RAF/MEK/ERK, PI3K/AKT/mTOR and WNT/CTNNB1 signalling pathways have been reported in both NF1-related MPNSTs and late-stage sporadic MPNSTs. In this study, we found that DAW22, a natural sesquiterpene coumarin compound isolated from *Ferula ferulaeoides* (Steud.) Korov., could inhibit cell proliferation and colony formation in five established human MPNST cancer cell lines. Further molecular mechanism exploration indicated that DAW22 could target the main components in the MPNST tumorigenic pathways: namely suppress phosphorylation of AKT and ERK, and reduce levels of non-phospho (active) CTNNB1. Using nude mice transplanted with human MPNST cancer cells, daily treatment with DAW22 for three weeks was effective in reducing tumor growth. These results support DAW22 as an alternative therapeutic compound for MPNST treatment by affecting multiple signalling transduction pathways in its disease progression.

CHAPTER 1: Introduction

1.1 Malignant peripheral nerve sheath tumors

1.1.1 Classification of malignant peripheral nerve sheath tumors

Malignant peripheral nerve sheath tumors (MPNSTs) are the sixth commonest, biologically aggressive soft-tissue sarcoma (James, Shurell, Singh, Dry, & Eilber, 2016). The specific cell resources of MPNSTs are as yet uncertain, but most of the studies suggested that MPNSTs stem from peripheral nerves, presenting demonstrable features of peripheral nerve differentiation or Schwann differentiation. To be specific, the defined nerve sheath tumors might develop from the differentiation of peripheral nerve to the cellular components of the nerve sheath, including Schwann cells, fibroblasts and perineurial cells (Jo & Fletcher, 2014). MPNSTs can be separated into two types, patients with neurofibromatosis type 1 (NF1) syndrome, which account for about 50% of all MPNST cases, and the remaining are sporadic MPNST patients (Farid et al., 2014).

NF1 syndrome is an autosomal dominantly inherited condition characterized by a various range of clinical symptoms, including learning disabilities, bony dysplasia, cutaneous hyperpigmentation, and the evolution of diverse tumor categories, such as optic glioma, glioblastoma, juvenile monomyelocytic leukaemia, pheochromocytoma, neurofibromas, plexiform neurofibromas and progression to MPNSTs (Gutmann et al., 2017). The incidence of NF1 is approximately 1 in 3500 live births, which is the most common hereditary genomic disorder for the nervous system, and also is the most common genomic predisposition syndrome in human cancer types (Widemann, 2009). NF1 syndrome is caused by an inherited germ line loss-of-function mutation

or acquired *de novo* inactivation of the *neurofibromin 1 (NF1)* tumor suppressor gene on chromosome 17q11.2. The haplo-insufficiency of *NF1* results in an inadequate protein product of neurofibromin, which is a 220-250 kDa cytoplasmic protein that contains regions homology to ubiquitous RAS GTPase-activating proteins (Thangarajh & Gutmann, 2012). Neurofibromin localizes in the cytoplasm, however some studies have found neurofibromin or fragments of it in the nucleus (Scheffzek & Welti, 2012). *NF1* is a negative regulator of the *RAS* proto-oncogenes by hydrolysing the active RAS-GTP to its inactive form of RAS-GDP conformation. This mutation leads to NF1 associated hyperactivation of RAS, and its downstream signal transduction pathways for survival and proliferation (Bollag et al., 1996). The biallelic mutations of *NF1* gene, one hit from the germ line and the second acquired from somatic mutation, was observed in neurofibroma patients. Hence, the RAS activation might be the direct cause for the evolution of NF1 syndrome, with one cell type harbouring the biallelic mutation and subsequently clonally expanded to generate a discrete lesion (Rodriguez, Folpe, Giannini, & Perry, 2012). In an experiment evaluating the NF1 syndrome development, loss of heterozygosity at *NF1* gene locus has been proven to be necessary for neurofibroma formation in both human samples and mouse models (Tucker, Wolkenstein, Revuz, Zeller, & Friedman, 2005). Nevertheless, this loss of heterozygosity at *NF1* gene locus is not sufficient for the transformation of NF1 syndrome to MPNSTs. Genomic alterations other than those at the *NF1* locus have rarely been detected in benign neurofibromas but are commonly found in MPNSTs (Rasmussen et al., 2000). In addition, only about 5% to 13% of NF1 patients eventually develop MPNSTs (Evans et al., 2002). Thus it is hypothesized that the genetic transformation from a benign neurofibroma to its malignant form involves many secondary genetic changes.

Although the NF1 syndrome is almost totally penetrant, its expressivity is highly changeable, with a phenotypic heterogeneity (Pasmant, Vidaud, Vidaud, & Wolkenstein, 2012) that endows tremendous challenges in earlier diagnosis and accurate prediction of clinical manifestations. Superficial skin lesions and cutaneous neurofibromas originated from small peripheral nerve branches are believed to affect almost all NF1 patients. However, these effects are in general asymptomatic, and have a low tendency to give rise to malignancy (Lim, Jaramillo, Poussaint, Chang, & Korf, 2005). By contrast, multiple dermal and/or plexiform neurofibromas are present in less than half patients, and these manifestations are considered as the hallmarks of NF1 syndrome. Importantly, plexiform neurofibromas has been proven to be related with a wide range of severe symptoms and eventually transform to MPNSTs (Farid et al., 2014).

MPNSTs can also occur sporadically in the general population. However, sporadic MPNSTs tend to be overlooked because the misclassification with other soft tissue sarcomas (Harris et al., 1991). Due to distinct genetic initiation profiles in early stage of the NF1-related MPNSTs and sporadic MPNSTs, the median onset age, chemotherapy response and prognosis are unmatched (Shurell et al., 2014). Interestingly, *NF1* mutation can also be found in approximately 40% of sporadic MPNST patients (Perry, Roth, Banerjee, Fuller, & Gutmann, 2001). In addition, *tumor protein p53 (TP53)* mutations (Kim et al., 2017) and *epidermal growth factor (EGFR)* overexpression are commonly found in sporadic patients (Keng, Watson, et al., 2012). Interestingly, patients with advanced stage NF1-associated MPNST cannot be genetically distinguished from advanced sporadic MPNST patients,

indicating that NF1-related and sporadic MPNST patients share similar genetic landscape in the advanced disease stage (Holtkamp et al., 2004).

1.1.2 Epidemiology, risk factors and prognosis of MPNSTs

MPNSTs can occur sporadically or in the context of patients with NF1 syndrome, emerging either *de novo* or arising from the pre-existing benign precursor plexiform neurofibroma (Rubin & Gutmann, 2005). Although MPNSTs are rare worldwide, comprising approximately 5 to 10% of all soft tissue sarcomas, the incidence of MPNSTs has increased due to improved clinical management (Ducatman, Scheithauer, Piegras, Reiman, & Ilstrup, 1986; Evans et al., 2002). MPNSTs affect people with an approximately equal gender distribution. Although MPNSTs may develop at any age, it tends to occur earlier in particular with NF1 patients, compared with other complicated sarcomas, which are normally more frequent over the 60s (Widemann, 2009). More specifically, the median onset age for sporadic MPNST patients ranges from 30s to 70s, with a peak at the 40s to 50s; while for NF1-related MPNSTs, it is between 20s and 40s, with a peak at 20s to 30s, which is significantly younger (Evans et al., 2002; Stucky et al., 2012).

Both NF1 patients and early sporadic patients have a chance to development neurofibromas, which are benign peripheral nerve sheath tumors (Halliday, Sobel, & Martuza, 1991). These patients can develop both superficial and deep neurofibroma tumors (Ferner & Gutmann, 2002). Of great concern, plexiform and intraneural neurofibroma that develop from deeply sited internal nerve bundles, are at a higher risk of undergoing transformation to MPNSTs (Katz, Lazar, & Lev, 2009). This is

supported by clinical data which demonstrated most MPNST patients developed from pre-existing plexiform neurofibroma (Brossier & Carroll, 2012).

MPNSTs develop quite often in the limbs, followed by the trunks, head and neck. Patients have to bear painful and rapidly increasing cellular mass with neurologic deficiency (Stucky et al., 2012). *NF1* gene mutation is the most obvious known risk factor. The lifetime risk of MPNST transformation among patients with NF1 is approximately 5 to 13% (Evans et al., 2002; Tucker et al., 2005). NF1 patients with dermal neurofibromas are not prone to develop malignant tumors, while NF1 patients with plexiform neurofibromas are at a higher risk for malignancy (Ducatman et al., 1986; Tucker et al., 2005). Another primary risk factor for MPNST progression is radiation exposure (Foley, Woodruff, Ellis, & Posner, 1980). Radiation related MPNSTs are uncommon sarcomas and accounts for about 4% of all radiation-induced sarcomas (Cha, Antonescu, Quan, Maru, & Brennan, 2004).

MPNSTs are usually difficult to diagnose at early stages using the current diagnose methods including Computed Tomography (CT) scan and/or (Magnetic Resonance Imaging) MRI scan (Brems, Beert, de Ravel, & Legius, 2009). The five-year survival rates for overall stages vary from 16% to 60%, and 10-year survival rates are around 45% (Dozois et al., 2009; LaFemina et al., 2013). The high rates of local recurrence (greater than 40%), low response of cytotoxic chemotherapy (only 17.6% for NF1 patients and 55.3% for sporadic patients) (Durbin, Ki, He, & Look, 2016), and the tendency of malignancy progression pose immense challenges for effective therapeutic strategies. Poor prognosis is mainly due to large tumor size (> 5cm) and high-grade malignancy. Once metastases occur, MPNSTs are associated with

extremely poor prognosis, with the 5-year survival rate remains at 25% (Turkson, Mamuszka, Grimshaw, & Marshall, 2018).

1.1.2 General treatment options for MPNSTs patients

The general treatment options for MPNST comprises of complete surgical extirpation, adjuvant radiation and chemotherapy, which are identical to soft tissue sarcomas treatment methods. In the context of localized cases, complete surgical excision with wide negative margins offers the best treatment outcome (Grobmyer, Reith, Shahlaee, Bush, & Hochwald, 2008). However, retrospective datasets showed that negative prognostic impacts of margins and local relapse occurred quite often, in a range of 32 to 65% after complete surgical resection, and it is extremely difficult to resect tumors without damaging the around nerves and tissues (Dunn et al., 2013; Gupta, Mammis, & Maniker, 2008). In the context of large tumors (more than 5 cm in diameter) in high-grade MPNSTs, adjuvant radiation is employed to reduce the local recurrence (Stucky et al., 2012). As radiation exposure *per se* is considered as a risk factor to induce MPNST transformation, its application has been highly debated. However, when there is no other treatment options, adjuvant radiation can outweigh the potential risks (Katz et al., 2009). Given the debate over the systemic chemotherapy of MPNSTs, the problems can be attributed to the lack of etiological information underlying the MPNST molecular targets and the lack of correspondingly effective therapeutic regimes. A variety of compounds have been tested for MPNSTs treatment, including vincristine, doxorubicin, cyclophosphamide, dactinomycin, ifosfamide, everolimus, sorafenib, etoposide and pazopanib, with varied responses among patients (Bradford & Kim, 2015; Carli et al., 2005).

With a surge in the genetic pathology information of MPNST in last decade, several targeted agents were tested in clinical trials singly or in combination with other candidate agents. Sorafenib, an inhibitor of Raf kinase and receptor tyrosine kinase, demonstrated no observable response (Maki et al., 2009). mTOR inhibitors and its derivatives (such as everolimus and temstrolimus) obtained varied response on tumor growth inhibition when combined with other candidate drugs (Ghadimi, Lopez, et al., 2012a; Widemann et al., 2016; Yamashita et al., 2014). The MEK inhibitor PD0325901 was reported to reduce tumor growth and prolong survival rate, but it could not induce apoptosis in cancer cells (W. J. Jessen et al., 2013). These agents, either alone or in combination with other chemicals may target multiple pathways and deter any potential cell death resistance leading to better anti-cancer effects (Kim & Pratilas, 2017). Different combinations of compounds targeting main molecules of tumorigenic pathways are still under investigation in order to obtain improved efficacy for MPNST therapy. Currently, there is no FDA-approved drug for MPNST treatment and no promising results released from clinical trial, thus novel small molecule inhibitors are urgently needed to target major pathways and/or induce cancer cell death.

1.1.3 Molecular insights and clinical implications of MPNST

Biallelic mutations of *NF1* tumor suppressor gene were found in about 10 to 15% of dermal neurofibroma, approximately 40% of plexiform neurofibroma and more than 60% of MPNSTs (Durbin et al., 2016). In addition, it has been reported that a portion of sporadic MPNST patients also have *NF1* gene mutation (Ratner & Miller, 2015),

suggesting the central role of *NF1* in MPNST development. Although huge strides have been made in understanding of molecular mechanism of MPNST in the last few years, the current management of the disease are still limited. MPNST is a complicated genetic disease that need further exploration on the pathological molecular path from its early to the advanced stage.

1.1.3.1 RAS-RAF-MEK-ERK pathway

The *RAS* proto-oncogene is the first attractive target as *NF1* loss of function mutations occur in all *NF1*-associated MPNST and about 40% of sporadic MPNST (Bottillo et al., 2009). Farnesylthiosalicylic acid is a *RAS* inhibitor and has been reported to reverse the transformed phenotype of MPNST models but signalling pathways downstream of *RAS* revealed slightly increased activation (Barkan, Starinsky, Friedman, Stein, & Kloog, 2006). Numerous studies support the fact that *RAF-MEK-ERK* pathway, also known as *MAPK* pathway, play an important role in controlling the proliferative capacity of MPNST cancer cells (Johannessen et al., 2005; Mattingly et al., 2006). Cyclin D1 was induced by activated *MAPK* pathway, followed by cyclin-dependent kinase 4 (*CDK4*) activation and retinoblastoma protein (*RB1*) phosphorylation, through which cell cycle progress from *G1* to *S* phase (J. Yang & Du, 2013). Activation of *RAF* by binding with activated *GTP-RAS*, will provoke the mitogenic kinase cascade, first by phosphorylating the *MEK* (*MAPK* kinase) to become *pMEK*, then it will further phosphorylate *ERK* (extracellular-signal regulated kinase, or *MAPK*) (W. J. Jessen et al., 2013). More than 90% of MPNST tissues overexpress *pMEK*, while 21% in benign neurofibromas (C. Zou et al., 2009). Therefore, targeting *RAS/RAF/MEK/ERK* pathway to compromise the sequential phosphorylation reaction seems a rational way to control the mitosis of cancer cells.

Sorafenib, an inhibitor of RAF-dependent MEK phosphorylation reaction, obtained only minor responses in a Phase II clinical trial with 12 MPNST patients (Maki et al., 2009). Instead of being used as a single agent, efficacy of sorafenib together with dacarbazine, an alkylating agent, was tested in order to obtain a synergistic clinical effect for MPNST treatment from 2009 to 2015 (<https://clinicaltrials.gov/ct2/show/results/NCT00837148?term=sorafenib&cond=MPNST&rank=1>). Results from this clinical trial showed only 5/35 patients obtained partial response; 22/35 patients had stable disease development; and 8/35 had progression of disease, indicating a unsatisfactory outcome. MEK blocking agents, such as U0126, PD184352 and PD98059 have been demonstrated to inhibit MPNST cancer cells proliferation *in vitro*, but some of these compounds cannot induce apoptosis (Guertin & Sabatini, 2005; Mattingly et al., 2006).

1.1.3.2 RAS-PI3K-AKT-mTOR pathway

Another pathway exist immediate downstream of RAS is the PI3K-AKT-mTOR pathway, which has been proven to be critical in the tumorigenesis of MPNST (Endo et al., 2012). Expression levels of phosphorylated AKT and activated mTOR were significantly elevated in MPNSTs compared with neurofibromas. Also, this pathway was demonstrated to be highly activated in different MPNST cell lines (C. Y. Zou et al., 2009a). Phosphatase and tension homolog (PTEN), a tumor suppressor gene that inhibit AKT signalling, was demonstrated to be downregulated in MPNST tissue samples compared with neurofibromas (Gregorian et al., 2009). mTOR inhibitors such as RAD001, have shown promising result against MPNST both *in vitro* and *in vivo* (Johannessen et al., 2005; Johansson et al., 2008; Stucky et al., 2012; C. Y. Zou et al., 2009a). Combination of different drugs to target the multiple pathway is

necessary to completely block the signalling transduction and prevent any feedback mechanisms, as this will compromise the desired targeted effect. For example, apoptotic resistance in MPNST cells were observed in xenograft models exposed with PI3K/AKT/mTOR inhibitors, which significantly increased autophagy level to induce growth arrest of MPNST cells under these conditions (Ghadimi, Lopez, et al., 2012b). A promising result was obtained *in vitro* from combination between mTOR and RAS inhibitors, where they demonstrated synergistic effects (Bradtmöller et al., 2012). Also, targeting two different pathways like RAF-MEK-ERK and PI3K/AKT/mTOR showed promising results, with mTOR inhibitor RAD001 and MEK inhibitor PD901, reducing tumor grade and multiplicity using both *in vitro* and *in vivo* MPNST models (Watson et al., 2014). However, there is still no confirmed clinical trials results in terms of the above mentioned combinations for MPNST therapy.

Upstream of the RAS-RAF-MEK-ERK pathway and the PI3K-AKT-mTOR pathway is the tyrosine kinase receptors (TKR), which are a group of cell-surface receptors that regulate cell cycle, cell proliferation, adhesion, migration, invasion and cell survival by releasing positive or negative molecular signals (Schlessinger, 2000). The epidermal growth factor receptor (EGFR) level was significantly higher in MPNST cell lines than normal Schwann cells, which was believed to be closely associated with the development of MPNST (DeClue et al., 2000). In an experiment of genetically engineered MPNST mouse model, overexpression of EGFR was found sufficient to induce transformation of neurofibroma to MPNST through Janus kinase 2 (JAK2)/Signal transducer activator of transcription 3 (STAT3) pathway (Wu et al., 2014b). As a result, EGFR might be an attractive therapeutic target that can be inhibited by small-molecular inhibitors and monoclonal antibodies. For example,

erlotinib inhibits EGFR kinase activity by targeting the cytoplasmic ATP-binding site of the receptor, thus preventing the auto-phosphorylation reaction and downstream activity. Erlotinib has been demonstrated to hamper the proliferation and invasion of MPNST cell lines *in vitro*, showing antiangiogenic effects in established xenograft nude mice (Holtkamp et al., 2008; Mahller et al., 2007; Su, Sin, Darrow, & Sherman, 2003). However, there was no clinical data to support similar effects using erlotinib, as early-stage clinical trial reported no discernible responses and was terminated (Albritton et al., 2006). Combination of monoclonal antibodies and tyrosine kinase inhibitors, which were designed to directly target vascular endothelial growth factor (VEGF) receptors and ligands, has reported mild efficacy, but not specific in MPNST patients in phase II evaluation (D'Adamo et al., 2005). Another TKR that has been studied in MPNST is the MNNG HOS transforming gene (MET). The activation of MET was found to exert regulating effects on MPNST invasion and angiogenesis *in vitro*. Furthermore, its downregulation could reduce the growth of tumors in immunodeficiency mice (Torres et al., 2011).

1.1.3.3 WNT-CTNNB1 and other potential targets

A forward genetic screening using *Sleeping Beauty* insertional mutagenesis system identified several genes related to canonical WNT signalling pathway as candidate driver genes of MPNSTs. This was partly confirmed by evaluating their expression in human neurofibromas and MPNST samples (Rahrmann et al., 2013). Reverse overexpression of *catenin beta 1* (*CTNNB1*) induced transformation of human immortalized Schwann cells (HSC1 λ), further confirming the WNT signalling pathway might be potential therapeutic targets (Watson et al., 2013).

Besides, *tumor protein p53 (TP53)* mutations has been proven associated with MPNST development in different models (Berghmans et al., 2005). However, there are discrepancies in the incidence of *TP53* inactivation in MPNST patients; one study revealed 16 out of 20 tumor samples with inactivated *TP53* while another research demonstrated the incidence was lower than 25% (Subramanian et al., 2010; Verdijk et al., 2010). In addition, sporadic MPNST patients might be more frequently related with *TP53* mutations, while MAPK, PI3K/AKT and EGFR overexpression are more often associated with NF1-related MPNST (Halling et al., 1996). Currently, there are no consistent distinctive gene profiles since MPNST bears complex karyotypes with both inter and intra-tumoral heterogeneity (Thomas, Mautner, Cooper, & Upadhyaya, 2012). In addition, the stem cell factor (SCF) and KIT receptor tyrosine kinase were found to be important in mediating maturation and proliferation of haplo-insufficient *NF1* mast cells which could promote tumor development of plexiform neurofibromas (Jaakkola, Peltonen, Riccardi, Chu, & Uitto, 1989; F.-C. Yang et al., 2006). Agents targeting SCF/KIT was evaluated in a phase II trial in patients with NF1-associated plexiform neurofibroma, but only 20% of patients responded with tumor size reduction after six-months treatment (Robertson et al., 2012).

Several other agents have also been tested preclinically, including histone deacetylase inhibitors (HDACi) and survivin inhibitors. HDACi was proven to trigger cell death exclusively in RAS-enhanced cells. Significant *in vitro* and *in vivo* pro-apoptotic effects of HDACi were observed irrespective of *TP53* mutation status (Klampfer, Huang, Shirasawa, Sasazuki, & Augenlicht, 2007). However, sporadic MPNST cells STS-26T were resistant to HDACi treatment, but could induce autophagy in MPNST cells when combined with autophagy blocking agents (Lopez et al., 2011). Survivin

is involved in cellular survival and division process, as well as cellular stress response. This represents another promising target in human MPNSTs where survivin was highly expressed (Alaggio et al., 2013; Ghadimi, Young, et al., 2012b). Knockdown of survivin could inhibit MPNST cell growth; using small molecule inhibitors could hinder tumor development and metastases in xenograft mouse models (Ghadimi, Young, et al., 2012a; Storlazzi et al., 2006). Popular pathways and targeted agents were summarized in **Figure 1**.

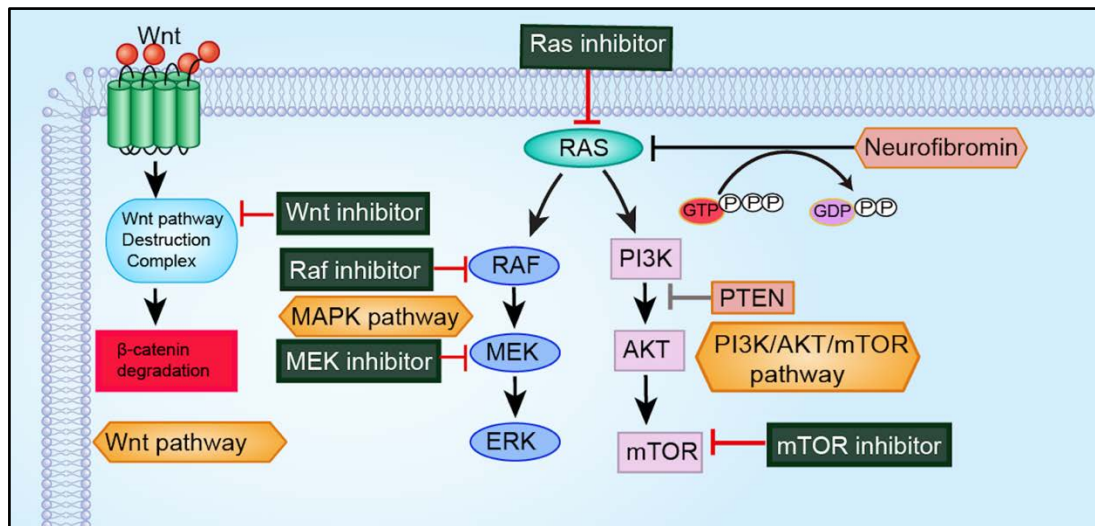


Figure 1 Potential molecular targets and clinical implications of MPNST.

In this diagram, WNT/CTNNB1, MAPK and PI3K-AKT-mTOR pathways are illustrated as well as the corresponding targeted agents. These pathways were demonstrated to be major pathways responsible for MPNST pathogenesis. Abbreviations: MAPK, mitogen-activated protein kinase; RAF, rapidly accelerated fibrosarcoma; MEK, mitogen-activated protein kinase/extracellular signal-regulated kinase kinase; ERK, extracellular-signal-regulated kinase; PI3K, phosphatidyl

inositol 3-kinase; AKT, mouse strain AK thymoma; TOR, target of rapamycin; PTEN, phosphatase and tensin homolog.

1.2 Genetic information of human MPNST cancer cell lines

Human MPNST cancer cell lines can be divided into two groups, the sporadic MPNST cancer cell line and the NF1-related MPNST cancer cell lines. The detailed genetic background information of these human MPNST cell lines was summarized in **Table 1**.

The sporadic cell line STS-26T was derived from a sporadic MPNST cancer patient with functional neurofibromin activity, but the expression of TP53 was completely ablated (Dahlberg, Little, Fletcher, Suit, & Okunieff, 1993; Lopez et al., 2010). Notably, the phosphorylated ERK1/2, AKT and mTOR activities in STS-26T were significantly increased (Sun, Tainsky, & Haddad, 2012; C. Y. Zou et al., 2009b). There are a few NF1-associated MPNST cancer cell lines, including T265, ST8814, S462 and S462-TY. T265 cell strain, which is similar with T265p21 cell line, was derived from a NF1-associated MPNST. This strain has undetectable expression of *NF1* (Sun et al., 2012), with higher phosphorylated ERK1/2, increased EGFR, AKT and mTOR, as well as higher RAS-GTP levels (Lee et al., 2004; C. Y. Zou et al., 2009b). However, the status of *TP53* in T265 was wild-type (Y. Li et al., 2004). ST8814 was also derived from a NF1-associated MPNST patient, with increased AKT/mTOR and phosphorylated ERK1/2 expression levels. As for *NF1*, a heterozygous nonsense mutation in exon 7 was found, which results in dysfunctional *NF1* in ST8814 cells (Barkan et al., 2006). Another two cell strains, S462 and S462-

TY, are similar as S462-TY was created by the passage of S462 as xenografts (Mahller et al., 2008). Notably, the mutant form of *TP53* were highly overexpressed in these two cell lines (Miller et al., 2006).

Table 1 Genetic background information of human MPNST cancer cell lines.

Genetic background information about the MPNST cell lines used in this study.

Expression levels of major genetic components in PI3K/AKT pathway were

compared with immortalized human Schwann cell lines. Data were compiled via

literature review. Major genetic components involved in WNT/CTNNB1 pathway

was performed by our laboratory.

Cell lines	PI3K/AKT				WNT/CTNNB1					
	<i>NFI</i>	<i>TP53</i>	<i>RAS-GTP</i>	<i>PTEN</i>	<i>AKT-mTOR</i>	<i>GSK3B</i>	<i>CDKN2A</i>	<i>MARK2</i>	<i>PPP2R2A</i>	<i>CREBBP</i>
STS-26T	+/+	Absent	Lower	Normal	Higher	Lower	Lower	Higher	Lower	Lower
T265	-/-	Normal	Higher	Lower	Higher	Lower	Absent	Normal	Lower	Lower
ST8814	-/-	Normal	Higher	Lower	Higher	Lower	Absent	Higher	Lower	Higher
S462	-/-	Mutant	Higher	Normal	Lower	Lower	Absent	Higher	Higher	Higher
S462-TY	-/-	Mutant	NA	NA	Lower	Higher	Absent	Higher	Higher	Higher

1.3 DAW22

1.3.1 Purification procedure of DAW22

DAW22 is a sesquiterpene coumarin compound isolated from the roots of *Ferula ferulaeoides* (Steud.) Korov.. This plant has been previously reported to have effective activity in treatment of spasm, digestive disease and arthritis (College, 1986). Roots and rhizomes of this plant were collected in Xinjiang of P.R. of China, followed by identification by Dr. Jimin Xu (National Institutes for Food and Drug Control).

DAW22 was extracted and purified at the School of Pharmacy, Shenyang Pharmaceutical University, China. The procedures were briefly described below: roots were first dried and immersed in EtOH-H₂O (95:5, v/v) for two times under conditions of reflux for 3 hours each time. The extracts were concentrated, and suspended in water, followed by partitioned with EtOAc, to obtain the EtOAc-soluble portion. Silica gel CC with a gradient of petroleum ether (PE)/acetone were used to further separate an aliquot of the EtOAc fraction. Fraction G was further separated via semipreparative high performance liquid chromatography (HPLC) with MeOH-H₂O (78:22, v/v) to generate compound DAW22 (Meng et al., 2013). Structure of DAW22 was verified and analysed by nuclear magnetic resonance spectroscopy assay and physico-chemical approaches with purity higher than 95%.

1.3.2 Studies about DAW22 and rationale of this study

A series of compounds including CANT-1, CANT-2, CANT-3, CANT-4, CANT-5, DAW22 and TAW were tested in terms of their potential anti-cancer effects on

MPNST and hepatocellular carcinoma. DAW22 and TAW were found to be effective to both MPNST cancer cells and HCC cancer cells (*data not shown*). DAW22 has been reported to show anti-proliferative effects on several different tumor cell lines, including HepG2, MCF-7 and C6 glioma cells (Meng et al., 2013). In addition, DAW22 could induce apoptosis and endoplasmic reticulum (ER) stress in C6 glioma cells (L. Zhang, Tong, Zhang, Huang, & Wang, 2015). Given the fact that Schwann cells, glia cells of the peripheral nervous system, are believed to be the major cell source for the initiation of MPNST, we would like to investigate whether DAW22 could affect MPNST cancer cells viability.

MPNST has no effective therapeutically regimes until now, traditional Chinese medicine could be a good resource for the drug screening, especially these chemicals that have been demonstrated to show anti-proliferative effects on cancer cell lines with the preliminary studies. To determine the effect of DAW22 on MPNST tumor development, the anti-cancer effects were evaluated on five human MPNST cancer cell lines. Based on the *in vitro* data, DAW22 could reduce the cell proliferation of these human MPNST cancer cell lines. To further confirm this effect, xenografted nude mice were used to examine the anti-cancer progression effects of DAW22. Both *in vitro* and *in vivo* approaches were used to determine the molecular mechanism of DAW22.

CHAPTER 2: Methodology

2.1 *In vitro* studies

2.1.1 Chemicals

The structure of DAW22 was determined using nuclear magnetic resonance spectroscopy and the purity of this compound was determined by HPLC to be higher than 95%. Finally, DAW22 was dissolved in DMSO as a 10 mM stock solution. AKT inhibitor AZD5363 was commercially purchased and prepared as a 100 mM stock solution in DMSO.

2.1.2 Cell lines and cell culture

The genetic background information about MPNST cancer cell lines were collected and discussed in the above introduction part and summarized in **Table 1**. The whole panel of human MPNST cancer cell lines were kindly provided by Dr Nancy Ratner (Experimental Hematology and Cancer Biology at Cincinnati Children's Hospital Medical Center, Cincinnati, Ohio, USA). The identity of these cell lines was verified by Applied Biological Materials Inc. (British Columbia, Canada) via short tandem repeats (STR) profile comparison (*data not shown*). All the cell lines were detected and found negative for mycoplasma contamination using MycoFluor™ Mycoplasma Detection Kit (Thermo Fisher Scientific, Massachusetts, USA; Cat# M7006). All these cells were cultured in Minimum Essential Media (MEM, Thermo Fisher Scientific, Cat# 11095072) supplemented with 10% fetal bovine serum (Thermo Fisher Scientific, Cat# 10500-064), Antibiotic-Antimycotic (100X) (Thermo Fisher

Scientific, Cat# 15240062) and maintained under standard conditions of 37 °C in a humidified atmosphere with 5% CO₂.

2.1.3 Cell proliferation assay

Human MPNST cancer cells from each cell strain was seeded onto 96-well plates at a density of 6,000 cells per well. After 24 hours, these attached cells were treated with either vehicle control or designated doses of DAW22 for 48 hours. The cell viability was quantified by MTS assay using the CellTiter 96 proliferation kit (Promega, Wisconsin, USA; Cat# G3580). The cell viability assays were performed and analysed using the Opera Phenix high content imaging system (PerkinElmer, Massachusetts, USA). Each experiment were repeated for at least three times.

2.1.4 Colony formation assay

MPNST cell lines were seeded onto 6-well plates at a density of 1,000 cells per well. After 24 hours, when cells were attached to the bottom of the plate, culture medium was removed and replaced with either vehicle control or DAW22-containing medium for 10 days to two weeks, allowing for colony growth. Following 2 weeks, media were removed and cells were fixed with 4% paraformaldehyde in phosphate buffered saline (PBS) for 15 minutes and stained with 0.1% crystal violet solution in PBS for 10 minutes. Followed by washing with PBS until the dotted purple colonies were clearly observed. Images can be taken for each well. Each experiment were repeated for at least three times.

2.1.5 Cell cycle assay

MPNST cancer cells were seeded onto 6-well plates, followed by treatment with indicated concentration of DAW22 for 24 hours. These cells were then fixed with 70% ice-cold ethanol in PBS, stained with propidium iodide (PI, 50 µg/ml, Thermo Fisher Scientific, Cat# P1304MP) and analysed by flow cytometer. Each experiment were repeated for at least three times.

2.1.6 Western blot analyses

Protein was isolated from DAW22-treated MPNST cell lines using the Qproteome Mammalian Protein Prep Kit (Qiagen, Hilden, Germany; Cat# 37901) following the manufacturer's instructions. Concentrations of protein were determined using Bradford Protein Assay (Bio-Rad Laboratories, California, USA; Cat# 5000001) followed by denaturation as described in the product instruction. Protein were separated on a 12% SDS-PAGE gel and transferred to polyvinylidene difluoride (PVDF) membrane (MilliporeSigma, Massachusetts, USA; Cat# IPVH00010). This membrane were first incubated with indicated primary antibodies at 4°C overnight, followed by corresponding secondary antibodies' incubation at room temperature for 1 hour. Targeted proteins were detected using a horseradish peroxidase-conjugated chemiluminescent kit (MilliporeSigma, Cat# WBULS0500). AKT (Cat# 2920), phospho-AKT (Cat# 4060), ERK (Cat# 4695), phospho-ERK (Cat# 4370), poly(ADP-ribose) polymerase 1 (PARP) (Cat# 9532), Non-phospho (Active) CTNNB1 (Cat# 8814), caspase 3 (CASP3) and ACTB (Cat# 4970). With the exception for CASP3 that was purchased from Santa Cruz Biotechnology Inc. (Texas,

USA), remaining primary antibodies were from Cell Signalling Technology (Massachusetts, USA). ACTB was used as the loading control.

2.2 *In vivo* studies

2.2.1 Xenograft mouse model and treatment of DAW22

Six-week old immunocompromised nude mice were obtained from The Chinese University of Hong Kong, Laboratory Animal Services Centre (LASEC), Hong Kong. These mice were kept in the individually ventilated caging area of the Centralised Animal Facilities (CAF), the Hong Kong Polytechnic University. One week after arrival at CAF, the xenografted transplantation was performed. Firstly, the mice were anesthetized with ketamine and each flank injected subcutaneously with 2×10^6 STS-26T cells in 0.1 mL PBS containing 50% Matrigel (Corning Sigma-Aldrich, Missouri, USA; Cat# 356237). One week after cell transplantation, mice were treated with either vehicle or DAW22 at a dose of 60 mg/kg/day for three weeks by daily intraperitoneal injection. All animal studies were approved by the appropriate ethics committee and performed in accordance with the ethical standards stipulated by both CAF (The Hong Kong Polytechnic University) and LASEC (The Chinese University of Hong Kong).

2.2.2 Monitoring of tumor growth and body weight

Body weights and tumor sizes were measured every three days during the treatment period. At the experimental end point, tumor sizes and weights were measured and imaged for each mouse. The formula used for calculation of the tumor volume is: V

= $(L \times W \times W)/2$, where V indicates tumor volume, W indicates tumor width, L indicates tumor length.

2.2.3 Hematoxylin and eosin (HE) staining

Tissues were carefully dissected from the sacrificed animal, washed and placed in cold PBS. Formalin fixed-paraffin embedded sections from various tissues were sectioned at 5 microns using a standard microtome (Leica Biosystems, Wetzlar, Germany), mounted and heat-fixed onto glass slides. Tissue section slides were then processed and stained with hematoxylin-eosin (HE) using standard protocols.

2.3 Statistical analyses

Raw data was analysed using the GraphPad Software (California, USA) Prism (Version 6) and resulting values were expressed as mean \pm standard error of the mean (SEM). Student's t-test and ANOVA in Prism were used for statistical analyses. Value of $P < 0.05$ was considered as statistically significant.

CHAPTER 3: Results

3.1 DAW22 inhibits cell proliferation through induction of apoptosis

3.1.1 DAW22 inhibits cell proliferation in both sporadic and NF1-related MPNST cell lines

The therapeutic potential of DAW22, structure shown in **Figure 2A**, was evaluated using different human MPNST cancer cell lines. Different concentrations of DAW22 were exposed to a panel of five MPNST cell lines for 48 hours: sporadic MPNST cell line STS-26T and four NF1-associated MPNST cell lines S462, S462-TY, ST8814 and T265. Cell proliferation rates were determined by MTS assay. The concentrations that caused a 50% inhibition of cell viability (IC₅₀) in these five cell lines ranged from 30.42 μ M to 46.73 μ M (**Fig. 2B** and **2C**). Among which, the ST8814 and T265 have higher IC₅₀s, which are around 45 μ M, compared with the remaining three cancer cell lines with the IC₅₀ around 30 μ M. This might be due to different genetic background profile, which contributing to distinct responses to cell damage. To further confirm the anti-proliferative effect of DAW22, colony formation assay was conducted to observe if DAW22 could affect cellular attachment, survival and proliferation process. Results from the colony formation assay showed that DAW22 at the doses of 30 μ M and 60 μ M can suppress the formation of MPNST cancer cell colonies (**Fig. 2D**).

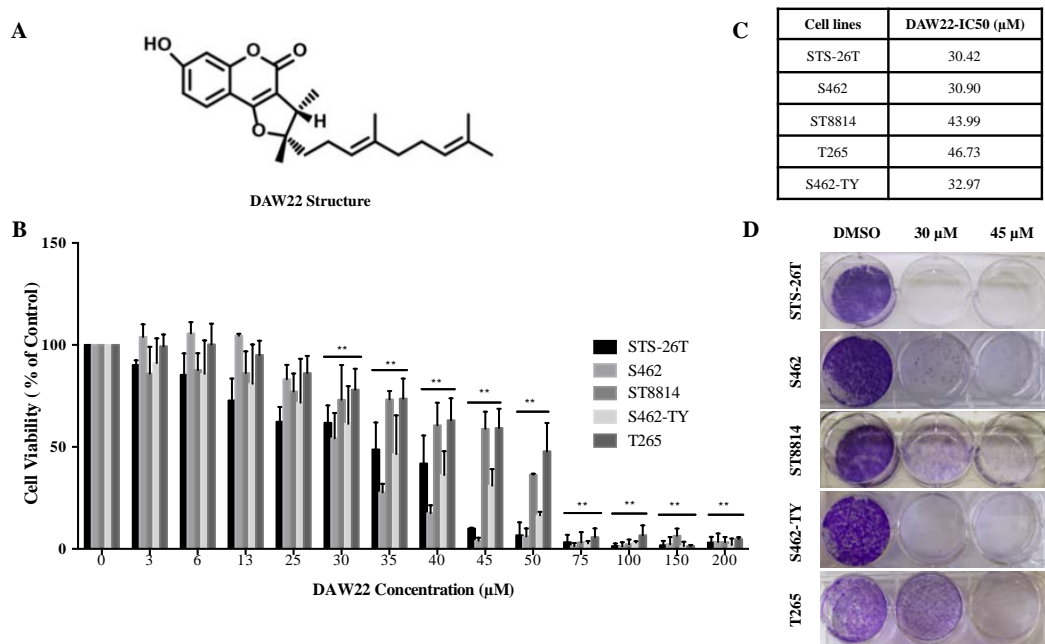


Figure 2 DAW22 inhibited cell proliferation of sporadic and NF1-related MPNST cell lines.

(A) Chemical structure of DAW22. (B) MTS cell viability assay was performed on MPNST cell lines after exposure to indicated concentrations of DAW22 for 48 hours. (C) Concentrations of DAW22 inducing 50% growth inhibition (IC₅₀) in sporadic and NF1-related MPNST cell lines. ST8814 and T265 cell lines were more resistant to DAW22, compared with S462, S462-TY and STS-26T cell lines. DAW22 IC₅₀ values were calculated using GraphPad Software Prism (Version 6). (D) Colony formation analyses of five MPNST cell lines after DAW22 treatment. These five cell lines were seeded on 6-well plate at a density of 1,000 cells per well, treated with 30 µM and 45 µM DAW22 for 2 weeks, and stained with crystal violet. Values were presented as mean ± SEM of three independent experiments. ***P* < 0.01, compared with vehicle control.

3.1.2 DAW22 induces apoptosis in both sporadic and NF1-related MPNST cell lines

Inhibition of cell proliferation is either caused by cell cycle arrest or induction of cell death. In order to explore the anti-cell proliferation effects caused by DAW22, cell cycle assay and cell apoptosis were evaluated using human MPNST cancer cell lines. Firstly, the cell cycle was analysed by flow cytometry using cells that were treated with DAW22 at either 30 μM or 60 μM concentrations for 24 hours. Results indicated that DAW22 could not induce cell cycle arrest, with no significant differences in G2/M phase from two representative cell lines (**Fig. 3A** and **3B**). Meanwhile, MPNST cancer cell lines exposed with either 30 μM or 60 μM of DAW22 showed obvious morphological alterations such as cell shrinkage, rounding and loss of adhesion in culture medium, which indicating cellular damage and death (**Fig. 3C**). As shown on these images, cell viability were decreased in all MPNST cell lines, with T265 and ST8814 cells showed a litter resistant to DAW22-induced cell death, compared with the other three cancer cell strains, which further confirm the MTS assay results and the IC_{50} s trends. Besides, apoptotic buddings were observed in STS-26T cells exposed with 30 μM DAW22 for 48 hrs (**Fig. 4**). With the 5 seconds time intervals, the dynamic changes of the apoptotic bodies can be observed. Upon these observation, our hypothesis is that DAW22 could induce apoptosis in MPNST cancer cells thus exhibiting the anti-cell proliferation effects which has been proven by MTS data (**Fig. 2B**).

To confirm this hypothesis, expression levels of total CASP3 and PARP as well as their cleaved forms were analysed by Western blot analyses. CASP3 and PARP are

cleaved when apoptosis occurred, thus they work as the markers for cell apoptosis process (Bressenot et al., 2009). Exposure of DAW22 for 48 hours induced significant increase of cleaved CASP3 and PARP in a dose-dependent manner in all MPNST cells (**Fig. 5A** and **5B**). The induction of cleaved CASP3 and PARP in each cell line occurred around their IC_{50} concentration, which were consistent with the cell proliferative inhibition data (**Fig. 2B** and **2C**). Furthermore, these apoptotic effects were verified upon DAW22 treatment at different time periods, ranging from 12 hours to 48 hours. These five MPNST cell lines can undergo apoptosis at different time points when treated with DAW22 (**Fig. 6**). Notably, even if DAW22 concentration used for each cell line corresponded with their IC_{50} : 30 μ M in STS-26T, S462 and S462-TY cells; 45 μ M in ST8814 and T265 cells, the apoptosis process in T265 and ST8814 cells were started around 24 hours' treatment, while the other cell lines started at around 12 hours' exposure, which is consistent with the previous MTS data and cell morphological observation. Taken together, the data support that DAW22 could induce programmed cell death in MPNST cell lines by eliciting apoptosis.

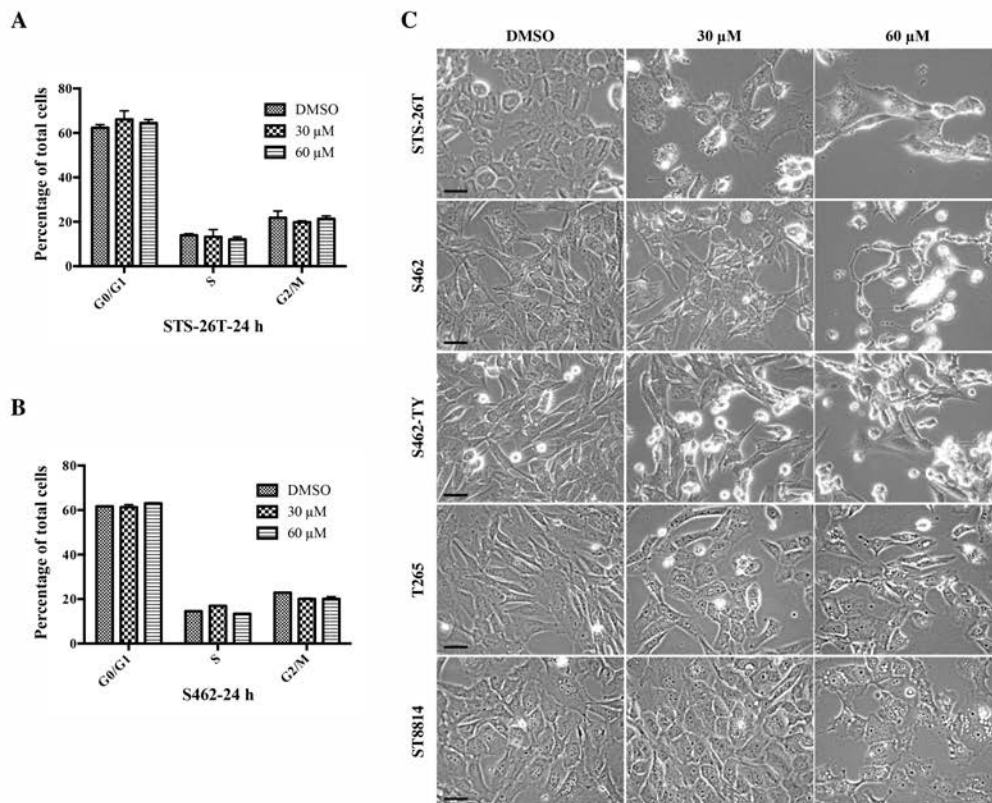


Figure 3 Cell cycle analyses and morphological changes in DAW22-treated MPNST cell lines.

(**A** and **B**) Negative effects of DAW22 on cell cycle of MPNST cancer cell lines. Cells were seeded onto 6-well plates and treated with 30 μ M and 60 μ M of DAW22 for 24 hours. Cell cycle were analysed by propidium iodide staining and flow cytometry. (**C**) Morphological changes observed in DAW22-treated MPNST cell lines. Cell shrinkage, rounding and loss of adhesion in culture medium were observed, indicating cellular damage or cell death. Scale bars, 10 μ m.

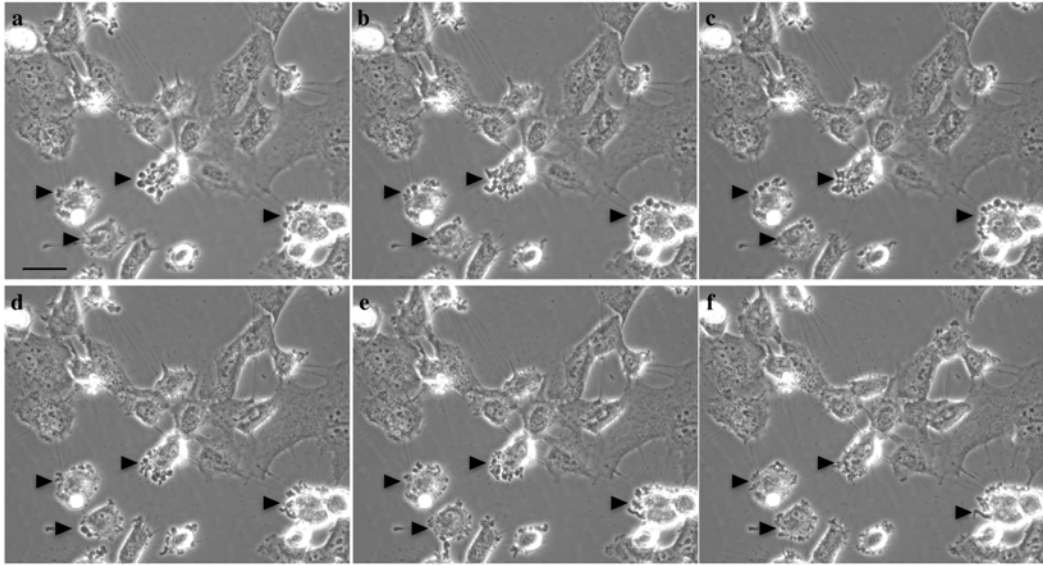


Figure 4 Live-cell imaging of induced apoptosis by DAW22 treatment.

Representative microscopic images of apoptotic budding in STS-26T cells after 30 μ M DAW22 treatment for 48 hours (arrowheads). Images were captured at a time interval of every 5 seconds (**a** to **f**). Scale bar, 10 μ m.

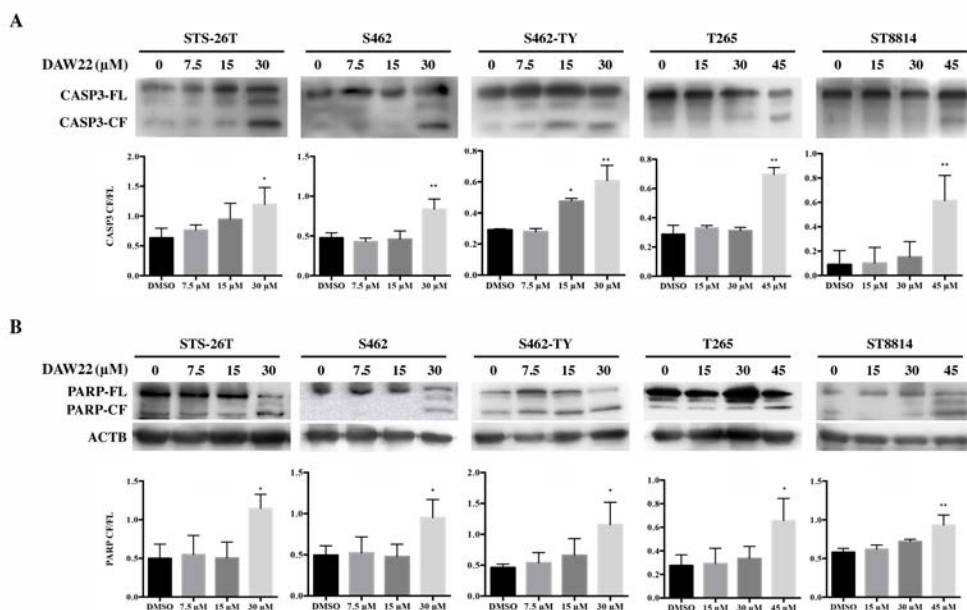


Figure 5 Induced apoptosis in DAW22-treated MPNST cells lines.

Cells were exposed with different concentrations of DAW22 for 48 hours. Western blot analyses were performed to detect levels of both full-length (FL) and cleaved (CF) versions of CASP3 (**A**) and PARP (**B**). Quantitative analyses of CF relative to its FL were shown in (**A**) and (**B**). Values were expressed as mean \pm SEM of three independent blots. * $P < 0.05$; ** $P < 0.01$, compared with vehicle control. ACTB loading only shown in (**B**). Western blot images shown in (**A**) and (**B**) were representative results showing similar trend from at least three independent experiments.

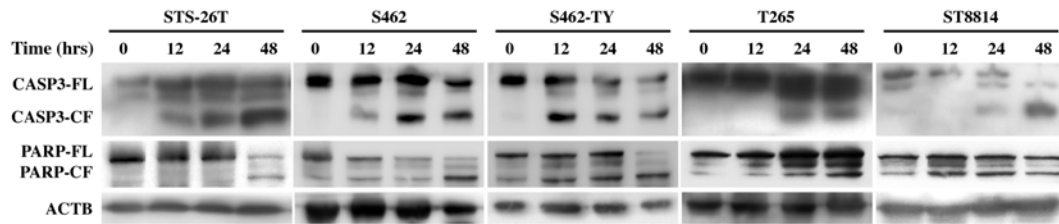


Figure 6 DAW22 treatment induced CASP3 and PARP cleavage in MPNST cell lines in a time-dependent manner.

STS-26T, S462 and S462-TY cells were treated with 30 μ M of DAW22 for indicated time points, while ST8814 and T265 cells were treated with 45 μ M of DAW22 for indicated time points. Western blot analyses were performed to detect levels of both full-length (FL) and cleaved (CF) versions of CASP3 and PARP.

3.2 DAW22 reduced phosphorylation of AKT, ERK and active CTNNB1 in MPNST cell lines

3.2.1 DAW22 reduced phosphorylation of AKT, ERK and non-phospho (active) CTNNB1 in MPNST cell lines

Cooperating genes enriched in the PI3K/AKT/mTOR, mitogen activated protein kinase (MAPK) and WNT/CTNNB1 transduction pathways have been implicated in MPNST disease initiation and progression, as well as the main regulators in mediating cell cycle, cell division and cell death (Endo et al., 2012; Luscan et al., 2013; Rahrmann et al., 2013). RAS activation caused by NF1 mutations induce downstream activation of the AKT/mTOR and RAF/MEK/ERK signalling pathways, whereas the canonical WNT/CTNNB1 signalling pathway has also been demonstrated to be an important genetic driver for cancer progression. Inhibition of WNT and mTOR

signalling pathways could synergistically induce apoptosis in MPNST cancer cells *in vitro* (Watson et al., 2013).

In order to explore the molecular mechanism for the anti-proliferation effects of DAW22, the AKT/mTOR and WNT/CTNNB1 pathways were evaluated in five MPNST cell lines. Total protein lysate from cells treated with either vehicle or different doses of DAW22 were analysed by Western blot. Results showed that DAW22 could remarkably induce a reduction of phosphorylated AKT in both sporadic and NF1-related MPNST cell lines (**Fig. 7A**). To evaluate if DAW22 could also affect the MAPK pathway, total and phosphorylated ERK were analysed. Phosphorylation of ERK was dramatically reduced when treated with DAW22 at their IC₅₀ concentrations (**Fig. 7B**). To obtain a more convincing conclusion, cells treated with certain concentration of DAW22 for different time points were also evaluated. Reduced phosphorylation of AKT and ERK were also observed at different time points when cells were administrated with DAW22 at 30 µM DAW22 in STS-26T, S462 and S462-TY cells, and 45 µM DAW22 in ST8814 and T265 cells (**Fig. 8**). DAW22 also reduced the levels of non-phosphorylated active form of CTNNB1 (**Fig. 7C**).

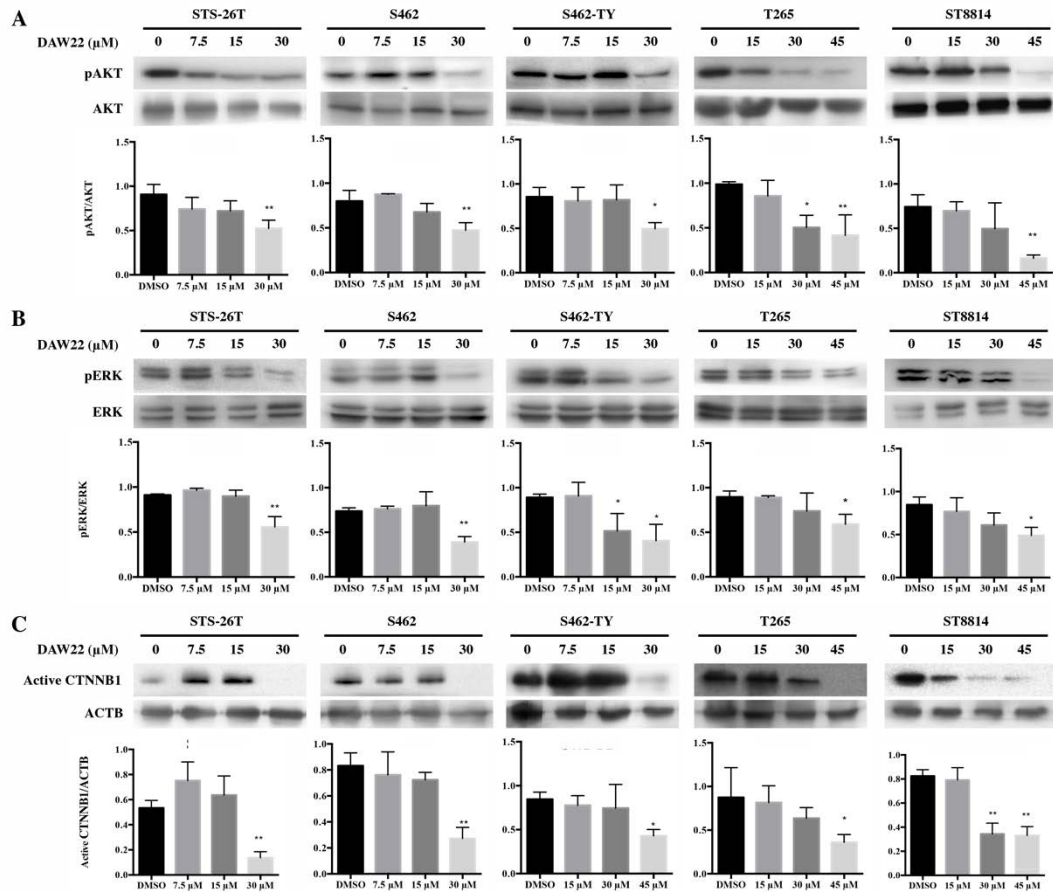


Figure 7 DAW22 reduced phosphorylation of AKT, ERK and non-phospho (active) CTNNB1 in MPNST cell lines.

Cells were treated with different concentrations of DAW22 for 48 hours. Levels of phosphorylated AKT/ERK, total AKT/ERK and active CTNNB1 were detected by Western blot analyses, as shown in (A), (B) and (C). Quantitative analyses of phosphorylated protein relative to its total protein shown in (A) and (B), while active CTNNB1 relative to ACTB was shown in (C). Values were expressed as mean \pm SEM of three independent blots. * $P < 0.05$; ** $P < 0.01$, compared with vehicle control. ACTB loading only shown in (C). Western blot images shown in (A), (B) and (C) were representative results showing similar trend from at least three independent experiments.

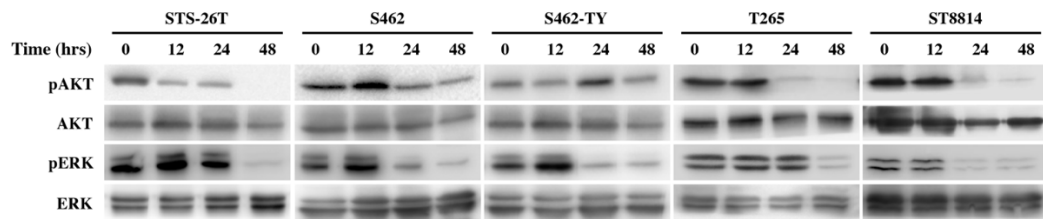


Figure 8 DAW22 treatment reduced AKT and ERK phosphorylation in MPNST cell lines in a time-dependent manner.

STS-26T, S462 and S462-TY cells were treated with 30 μ M of DAW22 for indicated time points, while ST8814 and T265 cells were treated with 45 μ M of DAW22 for indicated time points. Levels of phosphorylated AKT and ERK, as well as total AKT and ERK were detected by Western blot analyses.

3.2.2 AKT inhibitor AZD5363 induced apoptosis in STS-26T, ST8814 and S462 MPNST cancer cell lines

Given that AKT is an important regulatory element in MPNST initiation and progression, and DAW22 could target AKT signalling pathway and induce apoptosis, we wondered whether MPNST cancer cells can undergo apoptosis when they were exposed with AKT inhibitor. A series concentration of AZD5363 were used to treat MPNST cancer cells. Results indicated that AKT inhibitor AZD5363 reduced cell proliferation rates and induced apoptosis in STS-26T, ST8814 and S462 cell lines but at a much higher dosage compared with DAW22 (**Fig. 9**)

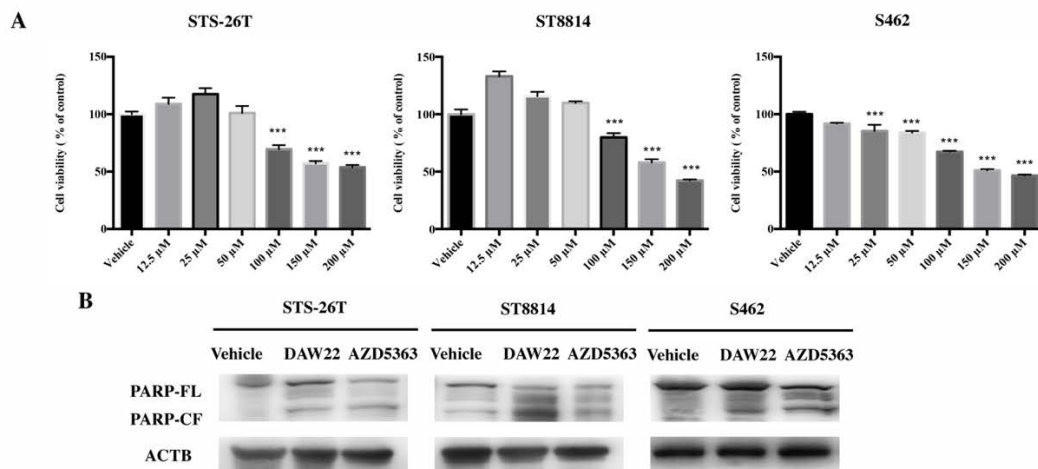


Figure 9 AKT inhibitor AZD5363 induced apoptosis in STS-26T, ST8814 and S462 MPNST cancer cell lines.

(A) STS-26T, ST8814 and S462 cells were treated with different concentration of AZD5363. MTS cell viability assay was performed after exposure for 48 hrs. (B) STS-26T, ST8814 and S462 cells were treated with 150 μM AZD5363 for 48 hrs, while the concentration of DAW22 were 30 μM, 45 μM and 30 μM. Western blot analyses were performed to detect levels of both full-length (FL) and cleaved (CF) versions of PARP.

3.3 DAW22 reduced tumor growth in xenograft transplanted experiments

3.3.1 DAW22 treatment delayed the tumor growth of STS-26T cells-transplanted xenograft MPNST model

In this study, STS-26T cells were subcutaneously injected into nude mice, allowing for tumor formation. One week later, DAW22 (60 mg/kg/day) or vehicle control solution were administered to these nude mice bearing a tumor around 100 mm³ by intraperitoneal injection. During the treatment, tumor size and body weight of mice were measured and recorded every three days. Mice were sacrificed three weeks after DAW22 treatment and the tumors were dissected out for analyses. After comparing the tumor volume between each group, we found that DAW22 significantly inhibited the tumor growth compared with the vehicle control group (**Fig. 10A** and **10C**). During the treatment period, there was no obvious loss of body weight in DAW22-treated group, indicating no gross toxicity effect caused by DAW22 (**Fig. 10B**). At the experimental end point, the average tumor weights in DAW22 treatment group were 1.086 ± 0.1247 g, compared with 1.478 ± 0.1296 g from vehicle control group (**Fig. 10D**). Before this *in vivo* assay, preliminary experiments were performed using DAW22 at a lower dose of 30 mg/kg/day on the same xenograft model. Results indicated that tumor sizes from DAW22-treated mice had a trend to reduce compared with that from vehicle group, but there are no significant difference both in tumor sizes and tumor weight (**Fig. 11**).

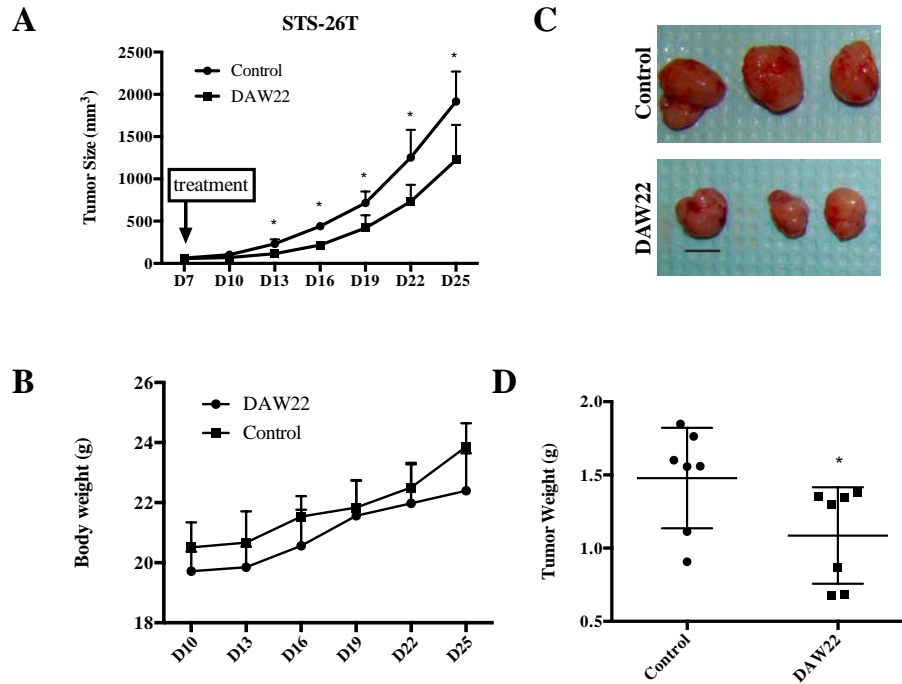


Figure 10 *In vivo* anti-cancer effect of DAW22 (60 mg/kg/day) on STS-26T transplanted xenograft mouse model.

(A) Quantitative analyses of tumor volume in mice from vehicle-treated and DAW22-treated groups. Six-week-old nude mice were engrafted with STS-26T cells and treated with DAW22 (60 mg/kg/day) 1 week after transplantation. DAW22 was introduced by intraperitoneal injection once daily for about three weeks. (B) Body weights from both vehicle-treated and DAW22-treated groups showed no significant differences for the entire treatment period. (C) Representative images of STS-26T subcutaneous tumor xenografts at experimental end point. Scale bar, 1 cm. (D) Significant reduction in tumor weights from DAW22-treated group compared with vehicle-treated animals. Values were expressed as mean \pm SEM; $n = 7$; $*P < 0.05$.

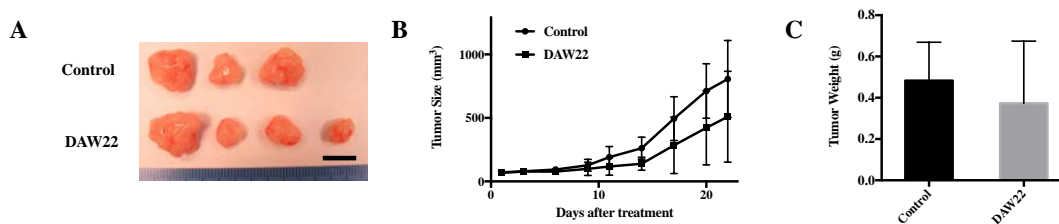


Figure 11 *In vivo* anti-cancer effect of DAW22 (30 mg/kg/day) on STS-26T transplanted xenograft mouse model.

(A) Representative images of STS-26T subcutaneous tumor xenografts at experimental end point. Scale bar, 1 cm. (B) Quantitative analyses of tumor sizes in mice from vehicle-treated and DAW22-treated groups. (C) Tumor weights from DAW22-treated and vehicle-treated mice. Values were expressed as mean \pm SEM; n = 3 for vehicle group and n = 4 for DAW22-treated group.

3.3.2 DAW22 reduced phosphorylation of AKT, ERK and non-phospho (active) CTNNB1 in transplanted mice

In order to confirm that AKT, ERK and CTNNB1 were targets of DAW22 *in vivo*, the protein expression levels of phosphorylated AKT, ERK and active CTNNB1 in xenografted tumors harvested from both vehicle and DAW22 treatment groups were analysed. Reduction of phosphorylated AKT, ERK and active CTNNB1 were observed in tumors from DAW22-treated mice compared with vehicle-treated group (Fig. 12).

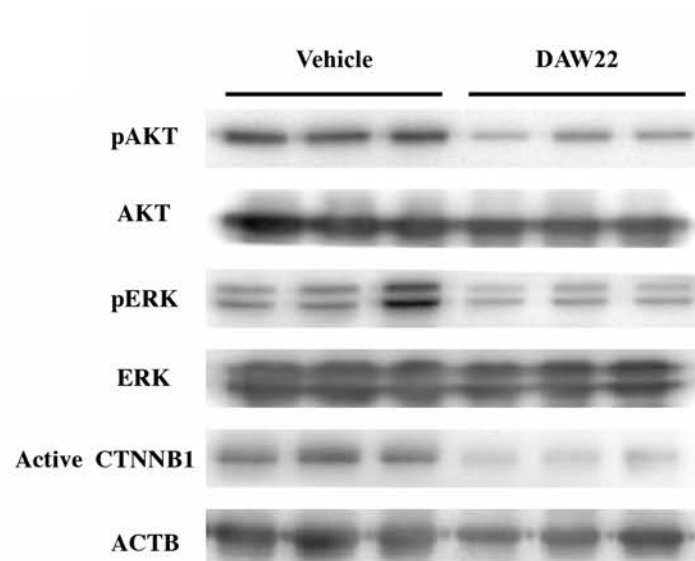


Figure 12 Western blot analyses of transplanted xenograft tumors from both vehicle- and DAW22-treated groups.

Reduction of phosphorylated AKT, ERK and active CTNNB1 levels in DAW22-treated group compared with the vehicle control group.

3.3.3 HE staining of tissues from xenografted transplant experiments

To evaluate if DAW22 induced tissue toxicity *in vivo*, HE staining was performed to visualize any morphological alterations in mouse tissues (liver, kidney, heart, lung, and spleen) isolated from both vehicle- and DAW22-treated mice. This histological method can be used to demonstrate any toxic effects induced by drug treatment *in vivo* (Hwang et al., 2016). Comparison of images from these two groups showed there was no morphological changes induced by DAW22 treatment, indicating no adverse effect caused by DAW22 (**Fig. 13**).

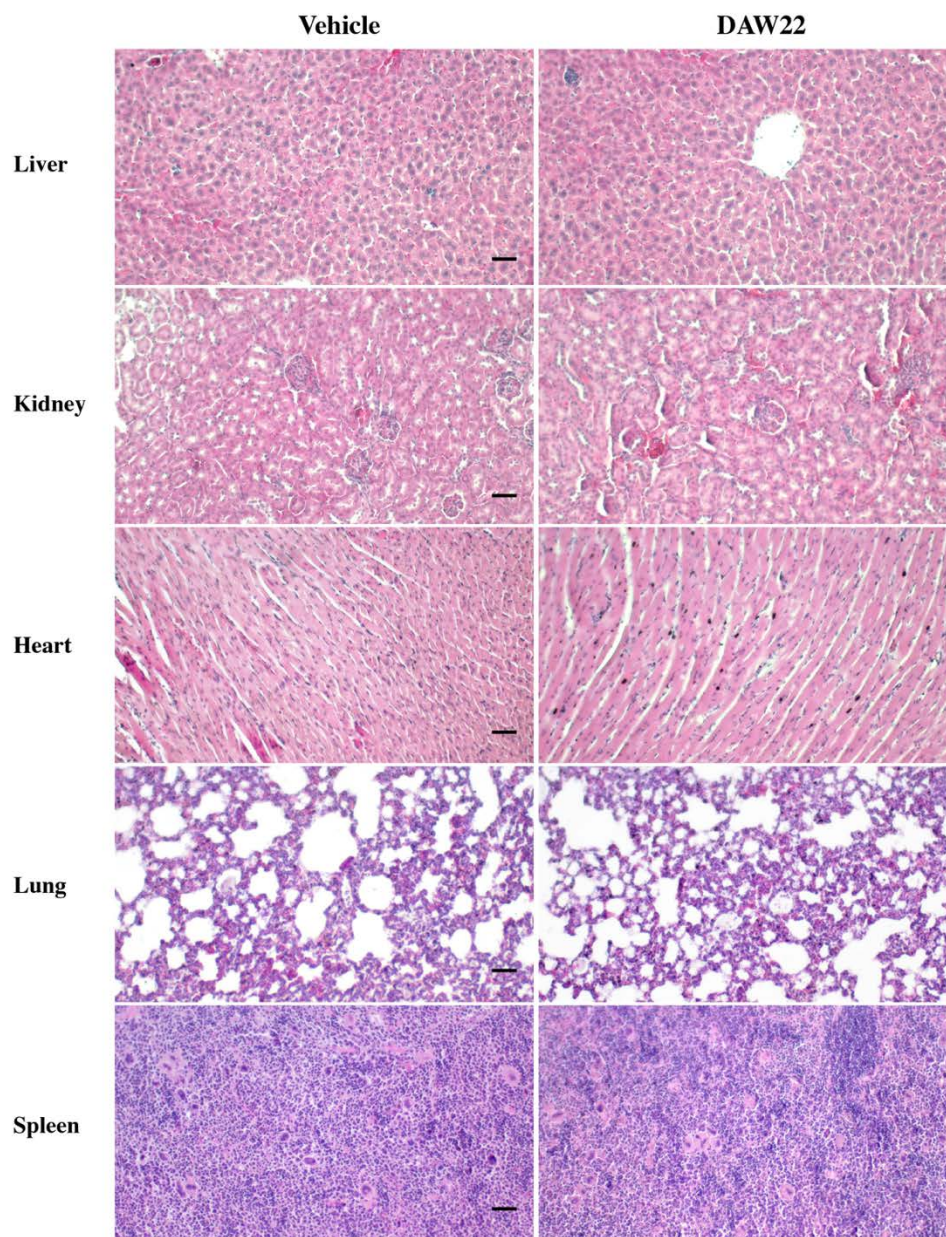


Figure 13 HE staining of various tissues taken from vehicle- and DAW22-treated xenograft mice.

Comparison between two groups showed there was no morphological changes in tissues tested, indicating no adverse effect caused by DAW22. Scale bars, 100 μ M.

CHAPTER 4: Discussion

With a high rate of metastases and extremely poor prognosis, MPNSTs represents one of the most difficult-to-cure sarcoma. Currently, there are no effective drugs for the treatment of MPNST and surgical resection remains the most effective means of therapy, but this method is limited due to the close proximity of the affected peripheral nerves with other tissues. Better therapeutic regimes for MPNST requires a greater understanding of the genetic mechanisms associated with the disease. As precision medicine becomes more important for health care, identification of accurate therapeutic targets and discovery of specific drugs to control cancer development is becoming ever more critical.

In our study, DAW22, a compound isolated from the plant *Ferula ferulaeoides* (Steud.) Korov, inhibited cell proliferation in both sporadic and NF1-related MPNST cell lines at varied doses. ST8814 and T265 cell lines have a IC_{50} of about 45 μ M, compared with STS-26T, S462 and S462-TY cell lines, where the IC_{50} s were around 30 μ M. The differences in the IC_{50} s might be caused by their distinct genetic backgrounds (**Table 1**). The higher IC_{50} s of ST8814 and T265 may result from their normal expression of *TP53* tumor suppressor gene (Y. Li et al., 2004), higher RAS-GTP level caused by NF1 deficiency, and activated AKT-mTOR signaling (Watson et al., 2014), compared with S462 cells. S462-TY cell line has a similar IC_{50} concentration as S462 cells, since S462-TY was derived from a xenograft passage of S462 (Mahller et al., 2008). The *TP53* expression in STS-26T cells was completely absent (Miller et al., 2006), which may have contributed to its relative low IC_{50} concentration. As has been reported that resistance is common in cancers with wild-type *TP53* (Martinez-Rivera

& Siddik, 2012). These may explain the fact that ST8814 and T265 are relatively resistant under DAW22 treatment compared with other cell strains.

Cell cycle was not influenced by DAW22 (**Fig. 3A** and **3B**). The apoptotic budding in STS-26T cells were observed, which suggested that DAW22 could induce apoptosis in MPNST cell lines (**Fig. 4**). Consistent with the apoptotic budding phenotype, the detection of cleaved CASP3 and PARP increased under DAW22 treatment in MPNST cell lines, confirming that DAW22 could indeed trigger apoptotic cell death. The concentration of DAW22 that elicited apoptosis in each cell line was close to their IC_{50s}. Interestingly, DAW22 could induce apoptosis 12 hours after treatment in STS-26T, S462-TY and S462 cell lines at 30 μ M, while it was after 24 hours in ST8814 and T265 cell lines at 45 μ M, which further suggests that varying genetic backgrounds could contribute to distinct cellular responses. Interestingly, cytoplasmic vacuolization was also observed in DAW22-treated MPNST cancer cells (*data not shown*). The presence of cytoplasmic vacuolization may infer that DAW22 could induce methuosis, a kind of non-apoptotic cell death (Maltese & Overmeyer, 2014). Amongst several kinds of non-apoptotic cell death that are characterized by cytoplasmic vacuolization, which includes methuosis, oncosis, paraptosis and necroptosis, only methuosis is characterized by *caspases* and *RAS* expression, which were confirmed in cells exposed with DAW22. Therefore, methuosis may also be induced by DAW22 in addition to apoptosis. However, the molecular mechanism(s) underling methuosis remains to be fully elucidated, and whether and how DAW22 trigger methuosis warrants further exploration.

Accumulating evidence have implicated several pathways are highly related with MPNST transformation. NF1-related MPNST cancer patients have activated RAS signaling, which subsequently cause activation of PI3K/AKT/mTOR and MAPK pathways. Sporadic MPNST patients also showed mutations in these pathways at the advanced disease stages. Moreover, significant activation of WNT/CTNNB1 pathway has been shown to drive human Schwann cell transformation and tumor maintenance in development of MPNST. The important roles of these pathways were further validated using inhibitors targeting AKT, mTOR, MEK and WNT pathways either singly or in combinations (Ahsan, Ge, & Tainsky, 2016; C. Y. Zou et al., 2009b).

Here we demonstrated that DAW22 inhibited phosphorylation of AKT, ERK and active form of CTNNB1, indicating that DAW22 could target multiple signalling pathways involved in MPNST disease progression. Based on these data, we may also speculate that DAW22 can target upstream of AKT/ERK/CTNNB1 pathways, which requires further investigation. AKT has been reported to regulate CTNNB1 phosphorylation and degradation in tumor invasion and development. The effect of AKT on CTNNB1 phosphorylation could be either direct phosphorylation (Fang et al., 2007) or indirectly regulation via the GSK3 β , resulting in the accumulation of CTNNB1 (Nusse, 2005). This interaction between CTNNB1 and AKT conferred resistance to AKT inhibitor in colon cancer (Tenbaum et al., 2012). This could explain the higher IC₅₀s of AKT inhibitor AZD5363 in MPNST cancer cell lines (**Fig. 9**). Whether DAW22 can target AKT directly or indirectly can be examined using computational molecular docking software, which aims to explore the behaviour of small molecules in the binding site of a target protein (Pagadala, Syed, & Tuszynski, 2017). Since AKT, ERK and CTNNB1 are currently the most important components

in the transduction pathways for MPNST disease progression, DAW22 can be used as a potential therapeutic alternatives in fighting against cancer, especially in AKT-resistant cancer types.

STS-26T, S462 and S462-TY were all reported being used as the cancer cell strains for establishing xenograft mouse model (Ghadimi, Lopez, et al., 2012a; Wu et al., 2014a). In advanced stage, NF1-associated MPNST patients cannot be genetically distinguished from sporadic MPNST patients, indicating that they share similar genetic profile (Holtkamp et al., 2004); (Demestre et al., 2013). In our study, we used STS-26T cells to establish the xenografted MPNST cancer model. We found that DAW22 treatment delayed tumor development in STS-26T transplanted xenograft mouse model, resulting in lower tumor growth rate and decreased tumor weight (**Fig. 10**).

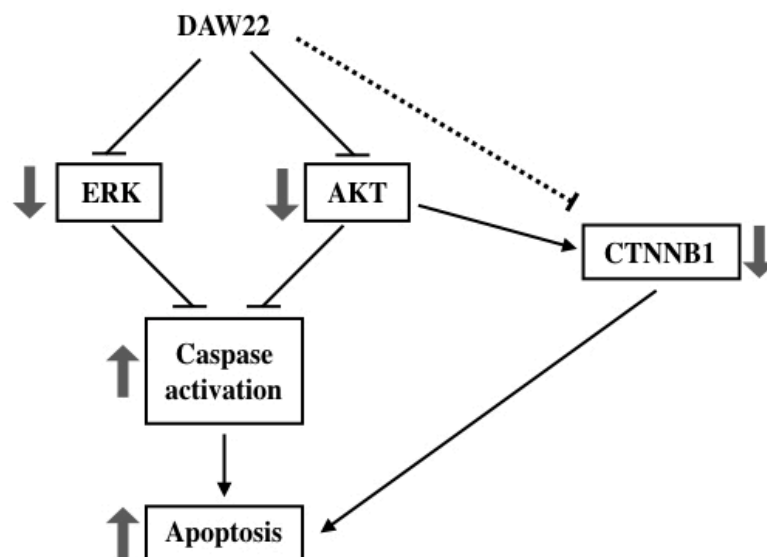


Figure 14 DAW22 targets multiple signalling pathways involved in MPNST disease progression.

DAW22 inhibits expression of phosphorylated ERK, AKT and non-phosphorylated (active) CTNNB1. This contributes to the induction of apoptosis in MPNST cancer cells.

In summary, our current study showed that DAW22 inhibited both sporadic and NF1-related MPNST cancer cell proliferation and induced apoptosis by targeting AKT, ERK and CTNNB1 pathways (**Fig. 14**). In addition, DAW22 delayed tumor growth in STS-26T cells transplanted nude mice, providing strong evidence for DAW22 as a potential novel alternative therapeutic treatment for MPNST treatment.

Reference

- Ahsan, S., Ge, Y., & Tainsky, M. A. (2016). Combinatorial therapeutic targeting of BMP2 and MEK-ERK pathways in NF1-associated malignant peripheral nerve sheath tumors. *Oncotarget*, 7(35), 57171.
- Alaggio, R., Turrini, R., Boldrin, D., Merlo, A., Gambini, C., Ferrari, A., . . . Bonaldi, L. (2013). Survivin expression and prognostic significance in pediatric malignant peripheral nerve sheath tumors (MPNST). *PloS one*, 8(11), e80456.
- Albritton, K., Rankin, C., Coffin, C., Ratner, N., Budd, G., Schuetze, S., . . . Borden, E. (2006). *Phase II study of erlotinib in metastatic or unresectable malignant peripheral nerve sheath tumors (MPNST)*. Paper presented at the ASCO Annual Meeting Proceedings.
- Barkan, B., Starinsky, S., Friedman, E., Stein, R., & Kloog, Y. (2006). The Ras inhibitor farnesylthiosalicylic acid as a potential therapy for neurofibromatosis type 1. *Clinical Cancer Research*, 12(18), 5533-5542.
- Berghmans, S., Murphey, R. D., Wienholds, E., Neuberg, D., Kutok, J. L., Fletcher, C. D., . . . Kanki, J. P. (2005). tp53 mutant zebrafish develop malignant peripheral nerve sheath tumors. *Proceedings of the National Academy of Sciences of the United States of America*, 102(2), 407-412.
- Bollag, G., Clapp, D. W., Shih, S., Adler, F., Zhang, Y. Y., Thompson, P., . . . Jacks, T. (1996). Loss of NF1 results in activation of the Ras signaling pathway and leads to aberrant growth in haematopoietic cells. *Nature genetics*, 12(2), 144.

- Bottillo, I., Ahlquist, T., Brekke, H., Danielsen, S. A., van den Berg, E., Mertens, F., . . . Dallapiccola, B. (2009). Germline and somatic NF1 mutations in sporadic and NF1-associated malignant peripheral nerve sheath tumours. *The Journal of pathology*, *217*(5), 693-701.
- Bradford, D., & Kim, A. (2015). Current treatment options for malignant peripheral nerve sheath tumors. *Current treatment options in oncology*, *16*(3), 12.
- Bradtmöller, M., Hartmann, C., Zietsch, J., Jäschke, S., Mautner, V.-F., Kurtz, A., . . . Reuss, D. (2012). Impaired Pten expression in human malignant peripheral nerve sheath tumours. *PLoS One*, *7*(11), e47595.
- Brems, H., Beert, E., de Ravel, T., & Legius, E. (2009). Mechanisms in the pathogenesis of malignant tumours in neurofibromatosis type 1. *The lancet oncology*, *10*(5), 508-515.
- Bressenot, A., Marchal, S., Bezdetnaya, L., Garrier, J., Guillemin, F., & Plénat, F. (2009). Assessment of apoptosis by immunohistochemistry to active caspase-3, active caspase-7, or cleaved PARP in monolayer cells and spheroid and subcutaneous xenografts of human carcinoma. *Journal of Histochemistry & Cytochemistry*, *57*(4), 289-300.
- Brossier, N. M., & Carroll, S. L. (2012). Genetically engineered mouse models shed new light on the pathogenesis of neurofibromatosis type I-related neoplasms of the peripheral nervous system. *Brain research bulletin*, *88*(1), 58-71.
- Carli, M., Ferrari, A., Mattke, A., Zanetti, I., Casanova, M., Bisogno, G., . . . Koscielniak, E. (2005). Pediatric malignant peripheral nerve sheath tumor: the Italian and German soft tissue sarcoma cooperative group. *Journal of clinical oncology*, *23*(33), 8422-8430.

- Cha, C., Antonescu, C. R., Quan, M. L., Maru, S., & Brennan, M. F. (2004). Long-term results with resection of radiation-induced soft tissue sarcomas. *Annals of surgery, 239*(6), 903.
- College, J. N. M. (1986). Dictionary of traditional Chinese medicine. In: Shanghai Science and Technology Publishing House Shanghai.
- Consortium, E. C. T. S. (1993). Identification and characterization of the tuberous sclerosis gene on chromosome 16. *Cell, 75*(7), 1305-1315.
- D'Adamo, D. R., Anderson, S. E., Albritton, K., Yamada, J., Riedel, E., Scheu, K., . . . Maki, R. G. (2005). Phase II study of doxorubicin and bevacizumab for patients with metastatic soft-tissue sarcomas. *Journal of Clinical Oncology, 23*(28), 7135-7142.
- Dahlberg, W., Little, J., Fletcher, J., Suit, H., & Okunieff, P. (1993). Radiosensitivity in vitro of human soft tissue sarcoma cell lines and skin fibroblasts derived from the same patients. *International journal of radiation biology, 63*(2), 191-198.
- DeClue, J. E., Heffelfinger, S., Benvenuto, G., Ling, B., Li, S., Rui, W., . . . Ratner, N. (2000). Epidermal growth factor receptor expression in neurofibromatosis type 1-related tumors and NF1 animal models. *The Journal of clinical investigation, 105*(9), 1233-1241.
- Dozois, E. J., Wall, J. C., Spinner, R. J., Jacofsky, D. J., Yaszemski, M. J., Sim, F. H., . . . Haddock, M. G. (2009). Neurogenic tumors of the pelvis: clinicopathologic features and surgical outcomes using a multidisciplinary team. *Annals of surgical oncology, 16*(4), 1010-1016.

- Ducatman, B. S., Scheithauer, B. W., Piepgras, D. G., Reiman, H. M., & Ilstrup, D. M. (1986). Malignant peripheral nerve sheath tumors. A clinicopathologic study of 120 cases. *Cancer*, *57*(10), 2006-2021.
- Dunn, G. P., Spiliopoulos, K., Plotkin, S. R., Hornicek, F. J., Harmon, D. C., Delaney, T. F., & Williams, Z. (2013). Role of resection of malignant peripheral nerve sheath tumors in patients with neurofibromatosis type 1. *Journal of neurosurgery*, *118*(1), 142-148.
- Durbin, A. D., Ki, D. H., He, S., & Look, A. T. (2016). Malignant peripheral nerve sheath tumors. In *Cancer and Zebrafish* (pp. 495-530): Springer.
- Endo, M., Yamamoto, H., Setsu, N., Kohashi, K., Takahashi, Y., Ishii, T., . . . Aoki, M. (2012). Prognostic significance of AKT/mTOR and MAPK pathways and antitumor effect of mTOR inhibitor in NF1-related and sporadic malignant peripheral nerve sheath tumors. *Clinical Cancer Research*.
- Evans, D. G. R., Baser, M. E., McGaughran, J., Sharif, S., Howard, E., & Moran, A. (2002). Malignant peripheral nerve sheath tumours in neurofibromatosis 1. *Journal of medical genetics*, *39*(5), 311-314.
- Fang, D., Hawke, D., Zheng, Y., Xia, Y., Meisenhelder, J., Nika, H., . . . Lu, Z. (2007). Phosphorylation of β -catenin by AKT promotes β -catenin transcriptional activity. *Journal of Biological Chemistry*.
- Farid, M., Demicco, E. G., Garcia, R., Ahn, L., Merola, P. R., Cioffi, A., & Maki, R. G. (2014). Malignant peripheral nerve sheath tumors. *The oncologist*, *19*(2), 193-201.
- Ferner, R. E., & Gutmann, D. H. (2002). International consensus statement on malignant peripheral nerve sheath tumors in neurofibromatosis 1. In: AACR.

- Foley, K. M., Woodruff, J. M., Ellis, F. T., & Posner, J. B. (1980). Radiation-induced malignant and atypical peripheral nerve sheath tumors. *Annals of Neurology: Official Journal of the American Neurological Association and the Child Neurology Society*, 7(4), 311-318.
- Ghadimi, M. P., Lopez, G., Torres, K. E., Belousov, R., Young, E. D., Liu, J., . . . Lazar, A. J. (2012a). Targeting the PI3K/mTOR axis, alone and in combination with autophagy blockade, for the treatment of malignant peripheral nerve sheath tumors. *Molecular cancer therapeutics*, 11(8), 1758-1769.
- Ghadimi, M. P., Lopez, G., Torres, K. E., Belousov, R., Young, E. D., Liu, J., . . . Lazar, A. J. (2012b). Targeting the PI3K/mTOR axis, alone and in combination with autophagy blockade, for the treatment of malignant peripheral nerve sheath tumors. *Molecular cancer therapeutics*.
- Ghadimi, M. P., Young, E. D., Belousov, R., Zhang, Y., Lopez, G., Lusby, K., . . . Lazar, A. J. (2012a). Survivin is a viable target for the treatment of malignant peripheral nerve sheath tumors. *Clinical cancer research*, 18(9), 2545-2557.
- Ghadimi, M. P., Young, E. D., Belousov, R., Zhang, Y., Lopez, G., Lusby, K., . . . Lazar, A. J. (2012b). Survivin is a viable target for the treatment of malignant peripheral nerve sheath tumors. *Clinical Cancer Research*.
- Gregorian, C., Nakashima, J., Dry, S. M., Nghiemphu, P. L., Smith, K. B., Ao, Y., . . . Mischel, P. S. (2009). PTEN dosage is essential for neurofibroma development and malignant transformation. *Proceedings of the National Academy of Sciences*, 106(46), 19479-19484.

- Grobmyer, S. R., Reith, J. D., Shahlaee, A., Bush, C. H., & Hochwald, S. N. (2008). Malignant peripheral nerve sheath tumor: molecular pathogenesis and current management considerations. *Journal of surgical oncology*, *97*(4), 340-349.
- Guertin, D. A., & Sabatini, D. M. (2005). An expanding role for mTOR in cancer. *Trends in molecular medicine*, *11*(8), 353-361.
- Gupta, G., Mammis, A., & Maniker, A. (2008). Malignant peripheral nerve sheath tumors. *Neurosurgery Clinics of North America*, *19*(4), 533-543.
- Gutmann, D. H., Ferner, R. E., Listernick, R. H., Korf, B. R., Wolters, P. L., & Johnson, K. J. (2017). Neurofibromatosis type 1. *Nature Reviews Disease Primers*, *3*, 17004.
- Halliday, A. L., Sobel, R. A., & Martuza, R. L. (1991). Benign spinal nerve sheath tumors: their occurrence sporadically and in neurofibromatosis types 1 and 2. *Journal of neurosurgery*, *74*(2), 248-253.
- Halling, K. C., Scheithauer, B. W., Halling, A. C., Nascimento, A. G., Ziesmer, S. C., Roche, P. C., & Wollan, P. C. (1996). p53 expression in neurofibroma and malignant peripheral nerve sheath tumor: an immunohistochemical study of sporadic and NF1-associated tumors. *American journal of clinical pathology*, *106*(3), 282-288.
- Harris, M., Hartley, A. L., Blair, V., Birch, J. M., Banerjee, S. S., Freemont, A., . . . McWilliam, L. (1991). Sarcomas in north west England: I. Histopathological peer review. *British journal of cancer*, *64*(2), 315.
- Holtkamp, N., Malzer, E., Zietsch, J., Okuducu, A. F., Mucha, J., Mawrin, C., . . . von Deimling, A. (2008). EGFR and erbB2 in malignant peripheral nerve

- sheath tumors and implications for targeted therapy. *Neuro-oncology*, 10(6), 946-957.
- Holtkamp, N., Reuß, D. E., Atallah, I., Kuban, R. J., Hartmann, C., Mautner, V. F., . . . Pham, V. A. (2004). Subclassification of nerve sheath tumors by gene expression profiling. *Brain pathology*, 14(3), 258-264.
- Jaakkola, S., Peltonen, J., Riccardi, V., Chu, M.-L., & Uitto, J. (1989). Type 1 neurofibromatosis: selective expression of extracellular matrix genes by Schwann cells, perineurial cells, and fibroblasts in mixed cultures. *The Journal of clinical investigation*, 84(1), 253-261.
- James, A. W., Shurell, E., Singh, A., Dry, S. M., & Eilber, F. C. (2016). Malignant peripheral nerve sheath tumor. *Surgical Oncology Clinics*, 25(4), 789-802.
- Jessen, W. J., Miller, S. J., Jousma, E., Wu, J., Rizvi, T. A., Brundage, M. E., . . . Dombi, E. (2013). MEK inhibition exhibits efficacy in human and mouse neurofibromatosis tumors. *The Journal of clinical investigation*, 123(1), 340-347.
- Jo, V. Y., & Fletcher, C. D. (2014). WHO classification of soft tissue tumours: an update based on the 2013 (4th) edition. *Pathology*, 46(2), 95-104.
- Johannessen, C. M., Reczek, E. E., James, M. F., Brems, H., Legius, E., & Cichowski, K. (2005). The NF1 tumor suppressor critically regulates TSC2 and mTOR. *Proceedings of the National Academy of Sciences of the United States of America*, 102(24), 8573-8578.
- Johansson, G., Mahller, Y. Y., Collins, M. H., Kim, M.-O., Nobukuni, T., Perentesis, J., . . . Thomas, G. (2008). Effective in vivo targeting of the mammalian target of rapamycin pathway in malignant peripheral nerve sheath tumors. *Molecular cancer therapeutics*, 7(5), 1237-1245.

- Katz, D., Lazar, A., & Lev, D. (2009). Malignant peripheral nerve sheath tumour (MPNST): the clinical implications of cellular signalling pathways. *Expert reviews in molecular medicine*, 11.
- Kim, A., & Pratilas, C. A. (2017). The promise of signal transduction in genetically driven sarcomas of the nerve. *Experimental neurology*.
- Klampfer, L., Huang, J., Shirasawa, S., Sasazuki, T., & Augenlicht, L. (2007). Histone deacetylase inhibitors induce cell death selectively in cells that harbor activated kRasV12: The role of signal transducers and activators of transcription 1 and p21. *Cancer research*, 67(18), 8477-8485.
- LaFemina, J., Qin, L.-X., Moraco, N. H., Antonescu, C. R., Fields, R. C., Crago, A. M., . . . Singer, S. (2013). Oncologic outcomes of sporadic, neurofibromatosis-associated, and radiation-induced malignant peripheral nerve sheath tumors. *Annals of surgical oncology*, 20(1), 66-72.
- Lee, P. R., Cohen, J. E., Tendi, E. A., Farrer, R., De Vries, G. H., Becker, K. G., & Fields, R. D. (2004). Transcriptional profiling in an MPNST-derived cell line and normal human Schwann cells. *Neuron glia biology*, 1(2), 135-147.
- Li, Y., Rao, P. K., Wen, R., Song, Y., Muir, D., Wallace, P., . . . Kadesch, T. (2004). Notch and Schwann cell transformation. *Oncogene*, 23(5), 1146.
- Lim, R., Jaramillo, D., Poussaint, T. Y., Chang, Y., & Korf, B. (2005). Superficial neurofibroma: a lesion with unique MRI characteristics in patients with neurofibromatosis type 1. *American Journal of Roentgenology*, 184(3), 962-968.
- Lopez, G., Torres, K., Liu, J., Hernandez, B., Young, E., Belousov, R., . . . McCutcheon, I. E. (2011). Autophagic survival in resistance to histone

deacetylase inhibitors: novel strategies to treat malignant peripheral nerve sheath tumors. *Cancer research*, 71(1), 185-196.

Lopez, G., Torres, K., Liu, J., Hernandez, B., Young, E., Belousov, R., . . .

McCutcheon, I. E. (2010). Autophagic survival in resistance to histone deacetylase inhibitors: novel strategies to treat malignant peripheral nerve sheath tumors. *Cancer research*, canres. 2799.2010.

Luscan, A., Masliah-Planchon, J., Laurendeau, I., Ortonne, N., Varin, J., Lallemand,

F., . . . Borderie, D. (2013). The activation of the WNT signalling pathway is a hallmark in Neurofibromatosis type 1 tumorigenesis. *Clinical Cancer Research*, clincanres. 0780.2013.

Mahller, Y. Y., Vaikunth, S. S., Currier, M. A., Miller, S. J., Ripberger, M. C., Hsu,

Y.-H., . . . Ratner, N. (2007). Oncolytic HSV and erlotinib inhibit tumor growth and angiogenesis in a novel malignant peripheral nerve sheath tumor xenograft model. *Molecular Therapy*, 15(2), 279-286.

Mahller, Y. Y., Vaikunth, S. S., Ripberger, M. C., Baird, W. H., Saeki, Y.,

Cancelas, J. A., . . . Cripe, T. P. (2008). Tissue inhibitor of metalloproteinase-3 via oncolytic herpesvirus inhibits tumor growth and vascular progenitors. *Cancer research*, 68(4), 1170-1179.

Maki, R. G., D'Adamo, D. R., Keohan, M. L., Saulle, M., Schuetze, S. M., Undevia,

S. D., . . . Mita, M. M. (2009). Phase II study of sorafenib in patients with metastatic or recurrent sarcomas. *Journal of clinical oncology*, 27(19), 3133.

Martinez-Rivera, M., & Siddik, Z. H. (2012). Resistance and gain-of-resistance phenotypes in cancers harboring wild-type p53. *Biochemical pharmacology*, 83(8), 1049-1062.

- Mattingly, R. R., Kraniak, J. M., Dilworth, J. T., Mathieu, P., Bealmear, B., Nowak, J. E., . . . Reiners, J. J. (2006). The mitogen-activated protein kinase/extracellular signal-regulated kinase kinase inhibitor PD184352 (CI-1040) selectively induces apoptosis in malignant schwannoma cell lines. *Journal of Pharmacology and Experimental Therapeutics*, *316*(1), 456-465.
- Meng, H., Li, G., Huang, J., Zhang, K., Wang, H., & Wang, J. (2013). Sesquiterpene coumarin and sesquiterpene chromone derivatives from *Ferula ferulaeoides* (Steud.) Korov. *Fitoterapia*, *86*, 70-77.
- Miller, S. J., Rangwala, F., Williams, J., Ackerman, P., Kong, S., Jegga, A. G., . . . Kluwe, L. (2006). Large-scale molecular comparison of human schwann cells to malignant peripheral nerve sheath tumor cell lines and tissues. *Cancer research*, *66*(5), 2584-2591.
- Nusse, R. (2005). Wnt signaling in disease and in development. *Cell research*, *15*(1), 28.
- Packer, R. J., & Rosser, T. (2002). Therapy for plexiform neurofibromas in children with neurofibromatosis 1: an overview. *Journal of child neurology*, *17*(8), 638-641.
- Pasmant, E., Vidaud, M., Vidaud, D., & Wolkenstein, P. (2012). Neurofibromatosis type 1: from genotype to phenotype. *Journal of medical genetics*, *49*(8), 483-489.
- Perry, A., Roth, K. A., Banerjee, R., Fuller, C. E., & Gutmann, D. H. (2001). NF1 deletions in S-100 protein-positive and negative cells of sporadic and neurofibromatosis 1 (NF1)-associated plexiform neurofibromas and malignant peripheral nerve sheath tumors. *The American journal of pathology*, *159*(1), 57-61.

- Rahrmann, E. P., Watson, A. L., Keng, V. W., Choi, K., Moriarity, B. S., Beckmann, D. A., . . . Moertel, C. L. (2013). Forward genetic screen for malignant peripheral nerve sheath tumor formation identifies new genes and pathways driving tumorigenesis. *Nature genetics*, *45*(7), 756.
- Rasmussen, S. A., Overman, J., Thomson, S. A., Colman, S. D., Abernathy, C. R., Trimpert, R. E., . . . Bauer, M. (2000). Chromosome 17 loss-of-heterozygosity studies in benign and malignant tumors in neurofibromatosis type 1. *Genes, Chromosomes and Cancer*, *28*(4), 425-431.
- Ratner, N., & Miller, S. J. (2015). A RASopathy gene commonly mutated in cancer: the neurofibromatosis type 1 tumour suppressor. *Nature Reviews Cancer*, *15*(5), 290.
- Robertson, K. A., Nalepa, G., Yang, F.-C., Bowers, D. C., Ho, C. Y., Hutchins, G. D., . . . Parada, L. F. (2012). Imatinib mesylate for plexiform neurofibromas in patients with neurofibromatosis type 1: a phase 2 trial. *The lancet oncology*, *13*(12), 1218-1224.
- Rodriguez, F. J., Folpe, A. L., Giannini, C., & Perry, A. (2012). Pathology of peripheral nerve sheath tumors: diagnostic overview and update on selected diagnostic problems. *Acta neuropathologica*, *123*(3), 295-319.
- Rubin, J. B., & Gutmann, D. H. (2005). Neurofibromatosis type 1—a model for nervous system tumour formation? *Nature Reviews Cancer*, *5*(7), 557.
- Schlessinger, J. (2000). Cell signaling by receptor tyrosine kinases. *Cell*, *103*(2), 211-225.
- Storlazzi, C., Brekke, H., Mandahl, N., Brosjö, O., Smeland, S., Lothe, R., & Mertens, F. (2006). Identification of a novel amplicon at distal 17q containing the BIRC5/SURVIVIN gene in malignant peripheral nerve sheath

- tumours. *The Journal of Pathology: A Journal of the Pathological Society of Great Britain and Ireland*, 209(4), 492-500.
- Stucky, C.-C. H., Johnson, K. N., Gray, R. J., Pockaj, B. A., Ocal, I. T., Rose, P. S., & Wasif, N. (2012). Malignant peripheral nerve sheath tumors (MPNST): the Mayo Clinic experience. *Annals of surgical oncology*, 19(3), 878-885.
- Su, W., Sin, M., Darrow, A., & Sherman, L. S. (2003). Malignant peripheral nerve sheath tumor cell invasion is facilitated by Src and aberrant CD44 expression. *Glia*, 42(4), 350-358.
- Subramanian, S., Thayanithy, V., West, R. B., Lee, C. H., Beck, A. H., Zhu, S., . . . Hogendoorn, P. C. (2010). Genome-wide transcriptome analyses reveal p53 inactivation mediated loss of miR-34a expression in malignant peripheral nerve sheath tumours. *The Journal of pathology*, 220(1), 58-70.
- Sun, D., Tainsky, M. A., & Haddad, R. (2012). Oncogene mutation survey in MPNST cell lines enhances the dominant role of hyperactive Ras in NF1 associated pro-survival and malignancy. *Translational oncogenomics*, 5, 1.
- Tenbaum, S. P., Ordóñez-Morán, P., Puig, I., Chicote, I., Arqués, O., Landolfi, S., . . . Mendizabal, L. (2012). β -catenin confers resistance to PI3K and AKT inhibitors and subverts FOXO3a to promote metastasis in colon cancer. *Nature medicine*, 18(6), 892.
- Thangarajh, M., & Gutmann, D. (2012). Low-grade gliomas as neurodevelopmental disorders: insights from mouse models of neurofibromatosis-1. *Neuropathology and applied neurobiology*, 38(3), 241-253.
- Thomas, L., Mautner, V.-F., Cooper, D. N., & Upadhyaya, M. (2012). Molecular heterogeneity in malignant peripheral nerve sheath tumors associated with neurofibromatosis type 1. *Human genomics*, 6(1), 1.

- Torres, K. E., Zhu, Q.-S., Bill, K., Lopez, G., Ghadimi, M. P., Xie, X., . . .
- Bolshakov, S. (2011). Activated MET is a molecular prognosticator and potential therapeutic target for malignant peripheral nerve sheath tumors. *Clinical cancer research*, *17*(12), 3943-3955.
- Tucker, T., Wolkenstein, P., Revuz, J., Zeller, J., & Friedman, J. (2005). Association between benign and malignant peripheral nerve sheath tumors in NF1. *Neurology*, *65*(2), 205-211.
- Turkson, L., Mamuszka, H., Grimshaw, K., & Marshall, E. M. (2018). MPNST treatment and diagnosis in NF1: A health economic model. In: AACR.
- Verdijk, R. M., den Bakker, M. A., Dubbink, H. J., Hop, W. C., Dinjens, W. N., & Kros, J. M. (2010). TP53 mutation analysis of malignant peripheral nerve sheath tumors. *Journal of Neuropathology & Experimental Neurology*, *69*(1), 16-26.
- Watson, A. L., Anderson, L. K., Greeley, A. D., Keng, V. W., Rahrman, E. P., Halfond, A. L., . . . Moertel, C. L. (2014). Co-targeting the MAPK and PI3K/AKT/mTOR pathways in two genetically engineered mouse models of schwann cell tumors reduces tumor grade and multiplicity. *Oncotarget*, *5*(6), 1502.
- Watson, A. L., Rahrman, E. P., Moriarity, B. S., Choi, K., Conboy, C. B., Greeley, A. D., . . . Keng, V. W. (2013). Canonical Wnt/ β -catenin signaling drives human Schwann cell transformation, progression, and tumor maintenance. *Cancer discovery*.
- Widemann, B. C. (2009). Current status of sporadic and neurofibromatosis type 1-associated malignant peripheral nerve sheath tumors. *Current oncology reports*, *11*(4), 322-328.

- Widemann, B. C., Meyer, C. F., Cote, G. M., Chugh, R., Milhem, M. M., Van Tine, B. A., . . . Jayaprakash, N. (2016). SARC016: Phase II study of everolimus in combination with bevacizumab in sporadic and neurofibromatosis type 1 (NF1) related refractory malignant peripheral nerve sheath tumors (MPNST). In: American Society of Clinical Oncology.
- Wu, J., Patmore, D. M., Jousma, E., Eaves, D. W., Breving, K., Patel, A. V., . . . Stemmer-Rachamimov, A. O. (2014a). EGFR–STAT3 signaling promotes formation of malignant peripheral nerve sheath tumors. *Oncogene*, *33*(2), 173.
- Wu, J., Patmore, D. M., Jousma, E., Eaves, D. W., Breving, K., Patel, A. V., . . . Stemmer-Rachamimov, A. O. (2014b). EGFR–STAT3 signaling promotes formation of malignant peripheral nerve sheath tumors. *Oncogene*, *33*(2), 173-180.
- Yamashita, A., Baia, G., Ho, J., Velarde, E., Wong, J., Gallia, G., . . . Riggins, G. (2014). Preclinical evaluation of the combination of mTOR and proteasome inhibitors with radiotherapy in malignant peripheral nerve sheath tumors. *Journal of neuro-oncology*, *118*(1), 83-92.
- Yang, F.-C., Chen, S., Clegg, T., Li, X., Morgan, T., Estwick, S. A., . . . Travers, J. (2006). Nf1^{+/-} mast cells induce neurofibroma like phenotypes through secreted TGF- β signaling. *Human molecular genetics*, *15*(16), 2421-2437.
- Yang, J., & Du, X. (2013). Genomic and molecular aberrations in malignant peripheral nerve sheath tumor and their roles in personalized target therapy. *Surgical oncology*, *22*(3), e53-e57.
- Zhang, L., Tong, X., Zhang, J., Huang, J., & Wang, J. (2015). DAW22, a natural sesquiterpene coumarin isolated from *Ferula ferulaeoides* (Steud.) Korov.

that induces C6 glioma cell apoptosis and endoplasmic reticulum (ER) stress. *Fitoterapia*, 103, 46-54.

Zou, C., Smith, K. D., Liu, J., Lahat, G., Myers, S., Wang, W.-L., . . . Lazar, A. J. (2009). Clinical, pathological, and molecular variables predictive of malignant peripheral nerve sheath tumor outcome. *Annals of surgery*, 249(6), 1014-1022.

Zou, C. Y., Smith, K. D., Zhu, Q.-S., Liu, J., McCutcheon, I. E., Slopis, J. M., . . . Mills, G. B. (2009a). Dual targeting of AKT and mammalian target of rapamycin: a potential therapeutic approach for malignant peripheral nerve sheath tumor. *Molecular cancer therapeutics*, 8(5), 1157-1168.

Zou, C. Y., Smith, K. D., Zhu, Q.-S., Liu, J., McCutcheon, I. E., Slopis, J. M., . . . Mills, G. B. (2009b). Dual targeting of AKT and mammalian target of rapamycin: a potential therapeutic approach for malignant peripheral nerve sheath tumor. *Molecular cancer therapeutics*, 1535-7163. MCT-1508-1008.

Part 2

Schwann cell-specific mutation of *Pten* reveals essential roles in sympathetic nervous system-driven lipolysis

Part 2 Abstract

Sympathetic nervous system (SNS) innervation of WAT is believed to be necessary and sufficient to elicit white adipose tissue (WAT) lipolysis. We found that mice with Schwann cell (SC)-specific *Pten* inactivation induces adipocyte hypertrophy in the inguinal WAT (iWAT). This may be due to inhibited SNS activity in iWAT, demonstrated by reduced tyrosine hydroxylase (TH) expression and catecholamine norepinephrine (NE) content. AKT was found to be hyperactivated in sciatic nerves of *Pten*-deficient mice. Moreover, AKT inhibitor AZD5363 treatment improved the iWAT condition in *Pten*-deficient mice. Taken together, we concluded that SCs play an important role in the regulation of SNS-NE stimulated iWAT lipolysis. The concept that SCs affecting SNS functions can provide new insight into peripheral neuropathy associated metabolic diseases.

CHAPTER 5: Introduction

5.1 Adipose tissue

Adipose tissue contains three kinds of adipocytes, including the white adipocytes from WATs, the brown adipocytes from brown adipose tissues (BATs) (Fantuzzi, 2005) and the beige adipocytes (also named inducible brown, or brown-in-white, brite), which exists predominantly in WAT under conditions of increased energy expenditure (Nedergaard & Cannon, 2014). The phenotypes of these three different adipocytes were shown in **Figure 15** (Bartelt & Heeren, 2014).

WATs are the energy storage depot mainly in the form of triglycerides, which is packed as a large and single lipid droplet that take up most of the cytoplasm space in a mature white adipocyte (Bartelt & Heeren, 2014; Zechner et al., 2012) (**Fig. 15**). WAT depots can be found in many parts of human body: abdominal visceral WAT, mesenteric WAT, omental WAT, perirenal areas (retroperitoneal) WAT, and the subcutaneous WAT that are mainly located in the buttocks, thighs, and abdomen. In addition, there are white adipocytes located in pericardial, perivascular, periarterial, periarticular, retroorbital, intramuscular, bone marrow and face areas (Ràfols, 2014). These studies have been summarized in **Figure 16** (Gesta, Tseng, & Kahn, 2007). Interestingly, the distribution of WATs in rodents are different from humans. The subcutaneous WAT in rodents only exist in the haunch area, also named iWAT (T. J. Bartness, Liu, Shrestha, & Ryu, 2014). When energy shortage occurs, lipid storage can be mobilized via lipolysis. This process involves of activation of SNS and subsequent hydrolysis of triglycerides into glycerol and free fatty acids (T. J. Bartness, Shrestha, Vaughan, Schwartz, & Song, 2010).

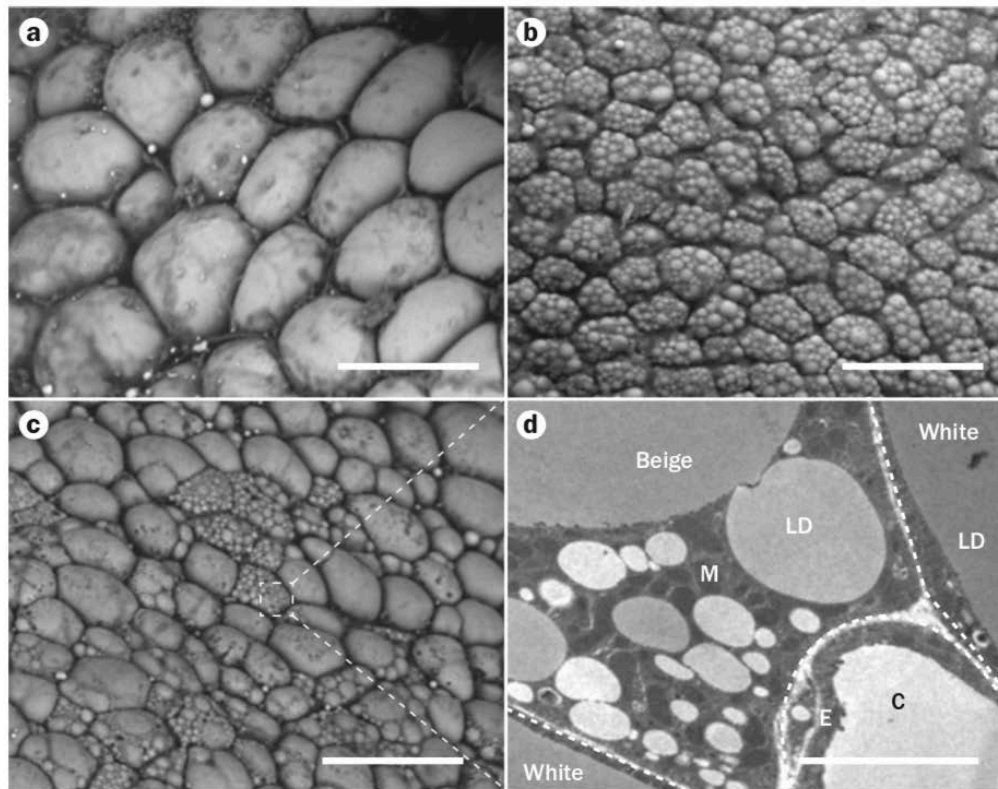


Figure 15 The phenotype of three different adipocytes.

Scanning electron micrographs demonstrating the characteristics of different mouse adipose tissues (Bartelt & Heeren, 2014). (a) White adipocytes from inguinal WAT comprise one single lipid droplet. (b) Brown adipocytes in interscapular brown adipose tissue contain multilocular lipid droplets. (c) Browning of white adipocytes results in formation of multilocular beige adipocytes within inguinal WAT. (d) Transmission electron micrograph of beige adipocytes, showing the high mitochondrial content. Scale bars: a-c, 50 μm . d, 5 μm . Abbreviations: C, capillary; E, endothelial cell; LD, lipid droplet; M, mitochondria; WAT, white adipose tissue.

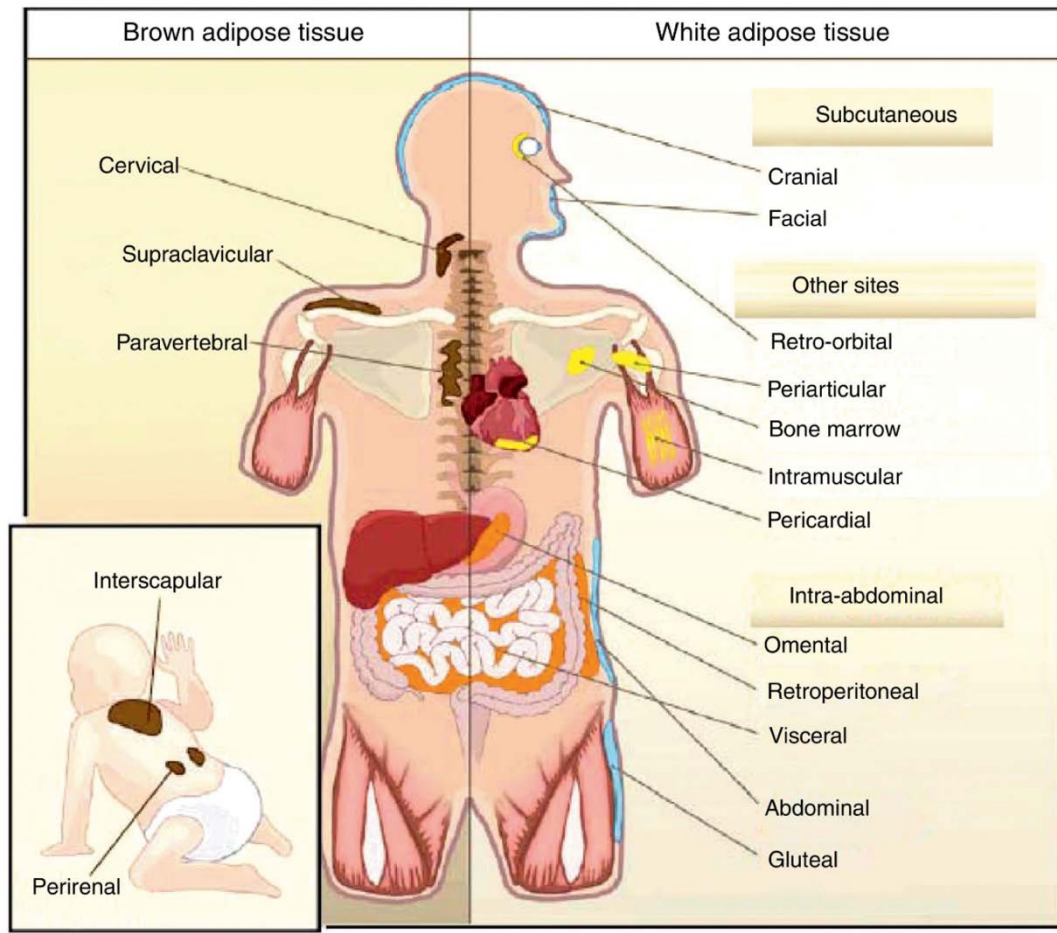


Figure 16 Body distribution of WAT and BAT in humans (Ràfols, 2014).

In contrast to white adipocytes, brown adipocytes contain a few smaller lipid droplets and numerous mitochondria, which confer BAT the multilocular and brown appearance (Enerbäck, 2009) (**Fig. 15**). BAT mainly exist between anterior neck and thorax in humans and their main function is thermoregulation (Rosen & Spiegelman, 2014; Virtanen et al., 2009) (**Fig. 16**). It has also been demonstrated that BAT activity could regulate the triglyceride clearance (Bartelt et al., 2011). Triglycerides are oxidized in the mitochondria of BAT to generate heat, a function for maintaining body warmth under cold temperatures. This process involves the uncoupling protein 1 (UCP1), located in the inner mitochondrial membrane (Cannon & Nedergaard, 2004) (**Fig. 17**). BAT activity can be triggered by cold exposure (Ouellet et al., 2012) or

activation of SNS (Cypess et al., 2015). Activation of BAT has been reported to offer beneficial effects on adiposity, insulin resistance and hyperlipidaemia in mice (Bartelt & Heeren, 2014).

Beige adipocytes are generated either from progenitor cells or trans-differentiated from white adipocytes (Bartelt & Heeren, 2014). This browning phenomenon is an adaptive response to environmental challenges. Cold temperatures can induce browning in white adipocyte (van Marken Lichtenbelt et al., 2009), and adiponectin has been demonstrated to promote this browning effect (Hui et al., 2015). Besides, β 3-adrenergic receptor agonist can also induce browning (Cypess et al., 2015), while knockout of β 3-adrenoceptor repressed the browning of white adipocyte (Jimenez et al., 2003). Interestingly, there are bipotential precursor cells that can develop into beige adipocytes under β 3-adrenergic receptor activation or into white adipocytes under high fat diet conditions in mice (Rosenwald, Perdikari, Rüllicke, & Wolfrum, 2013).

Accumulation of excess WAT has been considered to be a great risk factor for several metabolic health complications, including obesity, cardiovascular disease, diabetes and cancer (Nishida, Ko, & Kumanyika, 2010). WAT mass reduction is an ideal way to prevent these common metabolic disorders. Given the challenges and variable outcomes related with the current suggested methods in fighting against obesity, more accurate molecular mechanism underlying the pathogenesis of adipose tissue accumulation need to be identified.

5.2 The role of sympathetic nervous system in lipolysis

It has been well documented that adrenal medullary catecholamines, especially epinephrine, can induce lipolysis in white adipose tissue. However, controversial results have shown that removal of the circulating epinephrine by bilateral adrenal demedullation did not block lipolysis (Takahashi & Shimazu, 1981). In contrast, innervation of WAT and BAT by the SNS has been well reported and proven to be necessary and sufficient for lipolysis stimulation in WATs (T. J. Bartness et al., 2014; T. J. Bartness et al., 2010; Stojanović, Kieser, & Trajkovski, 2018; Youngstrom & Bartness, 1995). Conventional single neuron tract tracing has demonstrated for the first time that the WAT were innervated by the postganglionic sympathetic neuron (Youngstrom & Bartness, 1995). Recently, the sympathetic neuron-adipose junction, namely the innervation connection, was clearly visualized in *TH-Cre; LSLS-Tomato* mouse WAT (Zeng et al., 2015).

In addition, sympathetic nerve arborizations cover more than 90% of adipocytes in inguinal white adipose tissue (iWAT), indicating a close anatomical and functional interactions (Jiang, Ding, Cao, Wang, & Zeng, 2017; Youngstrom & Bartness, 1995). Electrical or optogenetic stimulation of SNSs activity induces lipolytic effects in WAT and its ablation blocks this effect, suggesting that activity of adipose cells are tightly regulated by the SNS (Correll, 1963; Zeng et al., 2015). Notably, responses of the sympathetic outflow are different in distinct adipose tissues. For example, BAT will has a decreased sympathetic outflow in response to fasting, while WAT demonstrates higher sympathetic activity to allow fatty acid mobilization (Brito, Brito, & Bartness, 2008). In contrast, cold exposure can induce increased sympathetic

outflow in both BAT and WAT to provide substrates for thermogenesis (Labbé et al., 2016). This discrepancy suggests that complicated and different nervous circuits are involved to coordinate adipose tissue metabolism. Moreover, leptin, which is generated and released mainly by adipocytes, play key roles in regulation of the sympathetic outflow to adipose tissues; and also SNS exerts regulatory effects on transcription and secretion of leptin (H. Li, Matheny, & Scarpace, 1997; Y. Zhang, Matheny, Zolotukhin, Tumer, & Scarpace, 2002) (**Fig. 17**).

The catecholamine NE, a principal neurotransmitter released by sympathetic nerves, activates the lipolysis via β 3-adrenergic receptor (β 3-AR) in rodents and β 1, β 2 receptors in humans (Lafontan et al., 1995; Langin, 2006). This initiates the canonical intracellular events that activates protein kinase A (Grove et al.), subsequent hormone sensitive lipase (HSL) and perilipin A phosphorylation in WATs (Holm, 2003; Shen, Patel, Miyoshi, Greenberg, & Kraemer, 2009). HSL catalyses the conversion of diacylglycerol, the products of basal lipolysis produced by triglyceride lipase, into monoacylglycerol, which could serve as an intracellular marker for SNS/NE induced lipolysis (T. J. Bartness et al., 2014; T. J. Bartness et al., 2010; Brasaemle, 2007; Girousse & Langin, 2012) (**Fig. 17**). On the other hand, stimulation of β 3-AR signalling induces expression of key browning transcriptional regulators, such as peroxisome proliferator-activated receptor gamma (PPAR γ) coactivator 1-alpha (PGC1- α) and PR domain containing 16 (PRDM16) (Boström et al., 2012; Ohno, Shinoda, Spiegelman, & Kajimura, 2012; Stojanović et al., 2018).

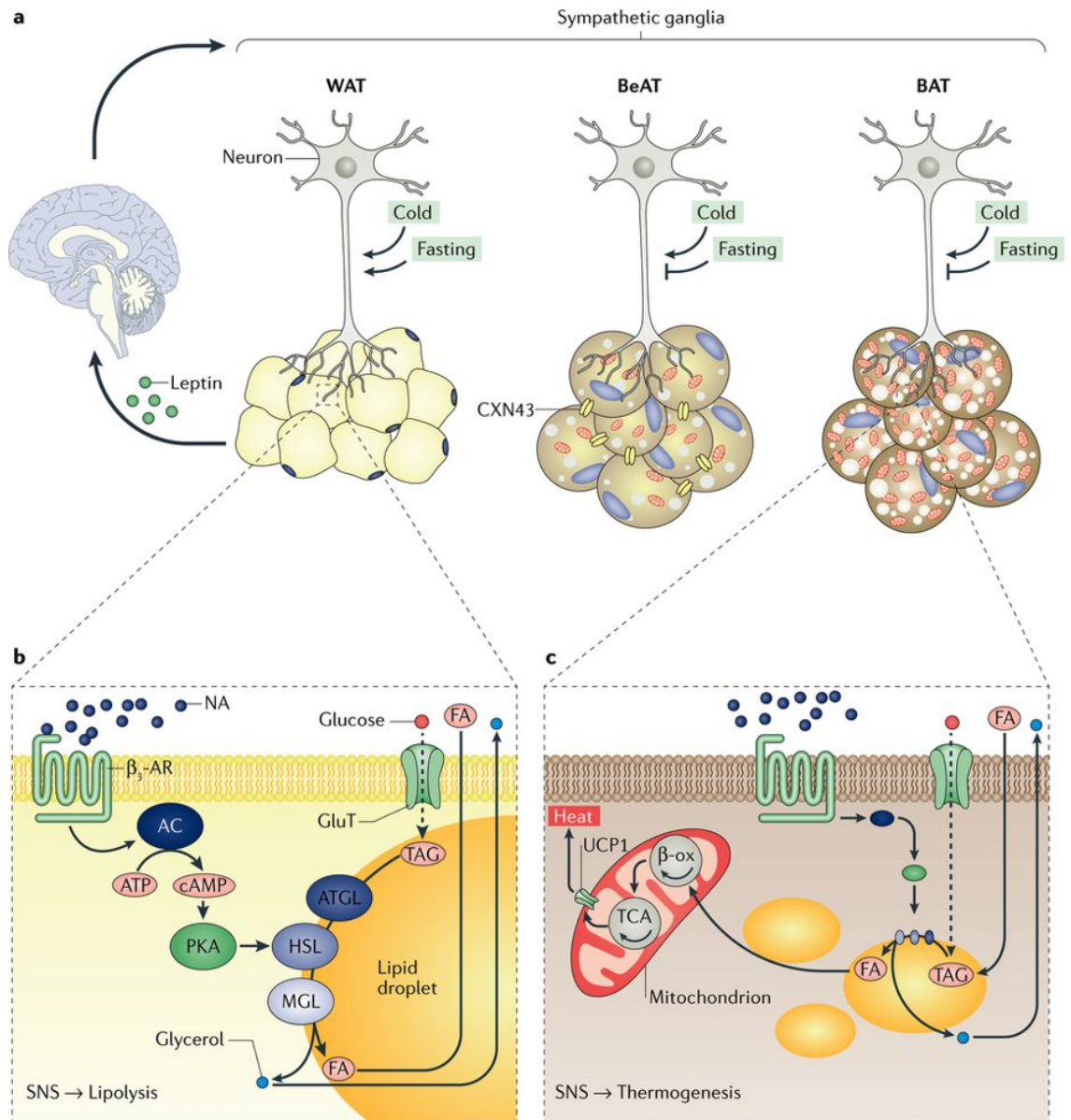


Figure 17 Adipose tissues innervated by sympathetic nervous system (SNS) (Caron, Lee, Elmquist, & Gautron, 2018).

(a) Innervation of white adipose tissue (WAT), beige adipose tissue (BeAT) and brown adipose tissue (Barkan et al.) by sympathetic nerve ganglia. (b) SNS-dependent WAT lipolysis regulatory pathway. (c) SNS-dependent BAT thermogenesis regulatory pathway.

5.3 Schwann cells and adipose tissue

Schwann cells (SCs) are the major glia cells in the peripheral nervous system (PNS). In the SNS, there are two types of neurons contributing to the transmission of signal: preganglionic fibres, which are wrapped by myelinated SCs, and postganglionic fibres, which are surrounded by nonmyelinated SCs (Griffin & Thompson, 2008). SCs are shown to promote nerve regeneration and reinnervation, indicating a role in peripheral nerve repair (K. Jessen & Mirsky, 2016; K. R. Jessen, Mirsky, & Lloyd, 2015; Kalbermatten et al., 2008). However, it is challenging to obtain enough amount of autologous SCs from integrated nerves for research. Instead, derivation of SCs-like cells from adipose-derived stem cells and bone marrow cells have become alternative approaches (Kingham et al., 2007; Lu, Jones, & Tuszynski, 2005; Tohill, Mantovani, Wiberg, & Terenghi, 2004). More recently, SCs-like cells were demonstrated to be directly isolated from marine inguinal adipose tissue (L. Chen et al., 2017) (**Fig. 18**). This phenomenon occurs in patients who undergo liposuction procedures usually experience nerve injury and subsequent regeneration/repair, indicating that SCs also have a role of nerve repair in adipose tissue.

In this study, mice with SCs deficient in *Pten* showed obvious iWAT hyperplasia. This suggests that SCs play a role in regulation of adipocyte homeostasis. However, this concept and relationship of SCs with lipid metabolism remains to be elucidated. In particular, it has not been established whether SCs in WAT could affect SNS activity and mediate SNS-NE induced lipolysis, as well as the mechanism(s) underlying how SCs influence SNS functions. Even though recent studies have

anatomically visualized dense innervation of WAT by SNS, roles of SCs in SNS innervated WAT are largely unknown. In the current study, we tried to explore the molecular mechanism underlying the relationship between SCs abnormality and lipolysis activity in WAT.

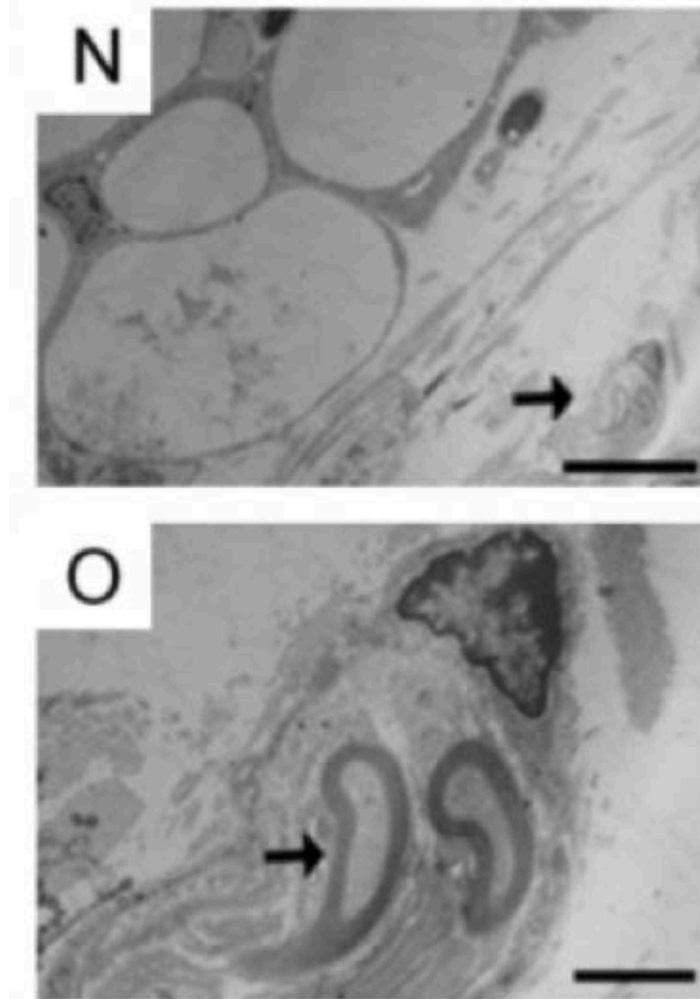


Figure 18 Detection of Schwann cells (SCs) in mouse inguinal adipose tissue (L. Chen et al., 2017).

Detection of SCs in mouse inguinal adipose tissue. (N) Transmission electron microscope images of inguinal adipose tissue in mice. (O) Enlarged picture from figure N. Arrow indicates nerve tissues and SCs. Scale bars, 10 μm and 2 μm in N and O, respectively.

5.4 PTEN in lipid metabolism

Phosphatase and tensin homologue (PTEN) is one of the most commonly identified tumor suppressor gene in different cancer categories. PTEN works as a protein phosphatase that catalysing dephosphorylation 3' phosphate of the inositol ring in phosphatidylinositol (3,4,5)-trisphosphate (PtdIns (3,4,5)P3 or PIP3), resulting in the biphosphate product PIP2 (PtdIns(4,5)P2) (Blero, Payrastra, Schurmans, & Erneux, 2007). This dephosphorylation results in reduced PIP3 and inhibition on AKT signaling pathway, which plays critical roles in regulating cell growth, cell survival and cell migration (Huang & Kontos, 2002). Besides, PTEN also functions as a lipid phosphatase, with a regulatory role in both glucose and lipid metabolism, however, the molecular mechanism on how PTEN affects lipid metabolism remain largely unknown (Cordero-Espinoza & Hagen, 2013; Z. Li et al., 2014). Inactivation of *Pten* specifically in hepatocytes resulted in enhanced fatty acid synthesis, accompanied by fatty liver phenotype, and enhanced liver insulin sensitivity with improved overall glucose tolerance (Stiles et al., 2004). Besides, *MAF1 homolog, negative regulator of RNA polymerase III (Maf1)*, a key downstream target of PTEN, was defined to play a role in lipid metabolism by targeting mTORC1 and forkhead box protein O1 (FOXO1), and it also repressed genes that regulate translational capacity and lipid synthesis (Johnson & Stiles, 2016). Thus, PTEN may serve as a promising target in the regulation of lipid metabolism for therapeutic purpose of obese.

5.5 Objectives and significance of this study

Obesity has become increasingly prevalent and is proven to be related with severe health complications, including fatty liver, type 2 diabetes, cardiovascular disease and cancer (Kopelman, 2000). Molecular biological information in terms of the adipose tissue metabolism is the key to figure out the pathology and therapeutic options for those metabolic diseases. With the discovery of thermogenic beige adipocyte and glycolytic beige adipocyte (Y. Chen et al., 2018; Hattori et al., 2016), our knowledge in lipid metabolism were growing in recent years, but still there are many mysteries remains to be explored. The objective of this study aims to investigate effects of Schwann cells-specific *Pten* gene inactivation on lipid metabolism. Schwann cells are major components in both pre- and post-ganglionic nerve fibres, however, the role of Schwann cells in mediating lipid metabolism was rarely discussed.

Schwann cells-specific *Pten* gene inactivation results in the phenotype of enlarged iWAT in transgenic mouse model, but the underlining mechanism remains unclear. Exploration of this phenomenon can gain insights into the understanding of how Schwann cells influence SNS and subsequent adipocyte activities.

CHAPTER 6: Methodology

6.1 Animal model

6.1.1 Establishment of the animal model

The animal model used in this study were *desert hedgehog* (*Dhh*) promoter driving Cre recombinase (*Dhh-Cre*); *Pten*^{f/f} mice, obtained from the breeding of two mouse strains: *Dhh-Cre* and *Pten*^{f/f} mice. Offsprings will have gene inactivation in Sertoli cell precursors (testes development/male germline), endothelial cells, and Schwann cells of the peripheral nervous system, according to information obtained from The Jackson Laboratory website (<https://www.jax.org/strain/012929>). Strong Cre recombinase activity is reported in *Dhh*-expressing Sertoli cells in the seminiferous tubules of the testis at postnatal day 15 (just before the onset of spermatogenesis when *Gata1* is abundantly expressed), while the enlarged iWAT observed in the experimental mice were shown as early as postnatal day 7, indicating that Sertoli cells are not the major cell source for the bigger iWAT. Endothelial cells are distributed in blood vessels along the whole mouse body, therefore it is not possible to exclude this factor when using *Dhh*-guiding Cre recombinase to limit gene mutations only in SCs. Until now there is no definitive Cre recombinase containing transgenic mouse specific for targeting Schwann cells. Existing transgenic mice used for generating SC-specific gene mutations includes 2',3'-cyclic nucleotide 3' phosphodiesterase (*Cnp*)-Cre, proteolipid protein (myelin) 1 (*Plp1*)-Cre and *Dhh-Cre* (Grove et al., 2017; Keng, Watson, et al., 2012). *Dhh-Cre* activity was observed in SC lineage from mouse embryonic day 12 (E12) and Sertoli cells at postnatal day 15 (Jaegle et al., 2003). In this study, we focused on the SCs, instead of endothelial cells, since SCs

are a major component of the SNS that were reported to be a critical factor in lipolysis of adipose tissues.

The Cre recombinase coding sequence was cloned in-frame with the *Dhh* regulatory sequence and includes a nuclear localization peptide sequence (Jaegle et al., 2003). The floxed *Pten* allele (*Pten*^{f/+}) was generated by cloning one loxP site downstream of exon 5 and the second loxP sites at the upstream of exon 4 (**Fig. 19A**) (Xiao et al., 2005). *Dhh-Cre* mice were crossed with *Pten*^{f/f} strain to generate pups with the genotype *Dhh-Cre*; *Pten*^{f/+}. These mice were further crossed to generate *Dhh-Cre*; *Pten*^{f/f} mice. Mice with the *Dhh-Cre*; *Pten*^{f/f} genotype will have the *Pten* exon 4 and 5 removed under the Cre activation. Representative *Pten* PCR genotyping profile as shown in **Figure 19A**.

6.1.2 PCR Genotyping

PCR genotyping for both *Dhh-Cre* and *Pten* genes were performed for every litter. Firstly, genomic DNA was extracted from mouse tail clippings using proteinase K incubation method, followed by phenol-chloroform isolation, and ethanol precipitation. Genomic DNA was finally dissolved in sterile TE buffer (pH 8) (Ambion Thermo Fisher Scientific, Cat# 1406030) and quantified using a Nanodrop spectrophotometer. PCR genotyping was conducted using 50 ng of diluted genomic DNA as template in a 25 µL PCR reaction volume using GoTaq Green Master Mix (Promega, Cat# M7123). PCR primers used for were shown below:

Dhh-Cre-forward 5'-CTGGCCTGGTCTGGACACAGTGCCC-3',

Dhh-Cre-reverse 5'-CAGGGTCCGCTCGGGCATAC- 3' (amplicon 385 bp);

Pten floxed allele forward 5' - AAAAGTTCCCCTGCTGATTTGT-3',

Pten wild type reverse 5'-TGTTTTTGACCAATTAAAGTAGGCTGT-3' (WT amplicon 310 bp and floxed allele amplicon 435 bp).

PCR program used were based on the instructions suggested by the manufacturer with an initial denaturing step of 95°C for 5 min; 30 or 35 cycles of denaturing at 95°C for 30 seconds, annealing at 55°C for 35 seconds and extension at 72°C for 35 seconds; followed by a final extension at 72°C for 5 minutes. PCR products were visualized on a 2% agarose gel. For *Dhh-Cre*, the genotype results were determined by the absence or presence of the expected band (**Fig. 19B**). For *Pten*, the genotype results were determined by different sizes of expected bands (**Fig. 19B**) and protein expression of PTEN in sciatic nerve were examined (**Fig. 19C**). Co-localization of *Pten* protein and S100 β , which is a marker for SCs, was examined using immunofluorescence staining in order to show *Pten* expression inside SCs (Keng, Rahrman, et al., 2012). Representative images showed that *Pten* inactivation under control of *Dhh* gene resulted in decreased co-localization of *Pten* and S100 β , indicating less *Pten* levels in SCs (**Fig. 19D**).

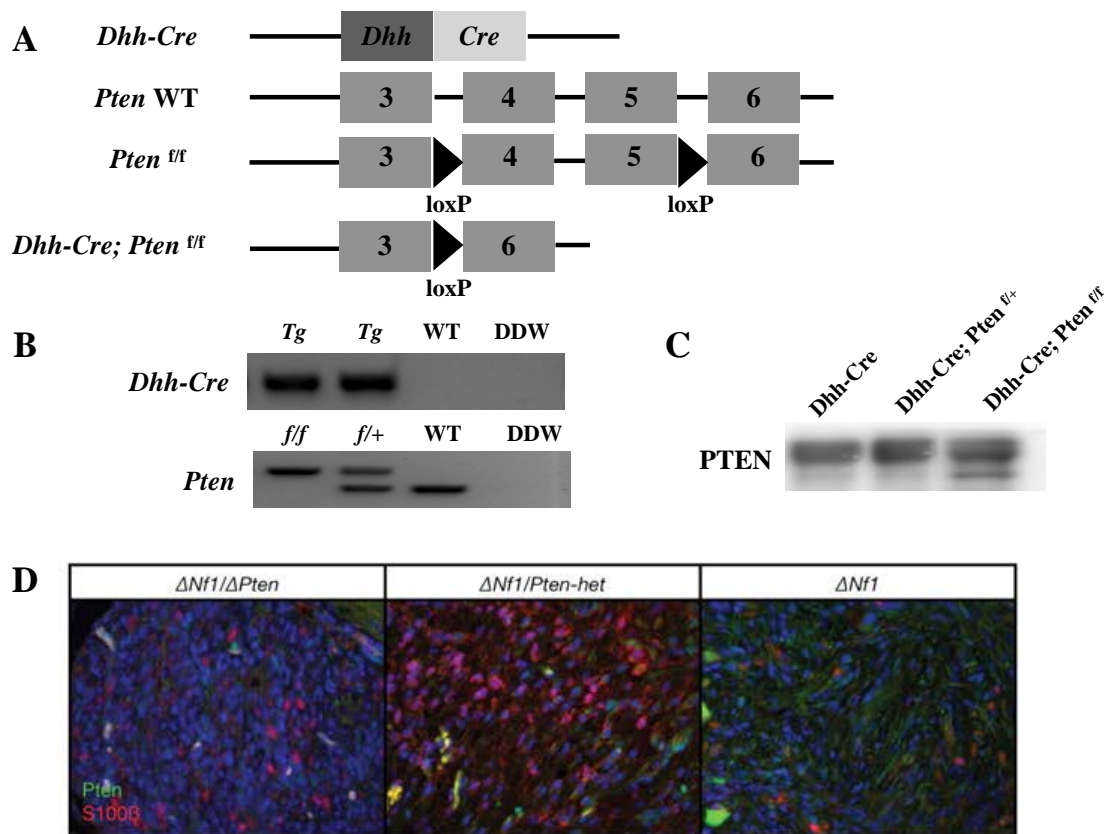


Figure 19 Conditional inactivation of *Pten* in SCs.

(A) Representative transgenes in experimental mice used for the study. The upper line is the *Dhh-Cre* transgene. The following illustrated wild type *Pten* allele (*Pten* WT) and floxed *Pten* allele (*Pten*^{f/f}), where the loxP sites were indicated by black arrowheads. The last line represents the mutated *Pten* in SCs of *Dhh-Cre; Pten*^{f/f} mice after the removal of exons 4 and 5. (B) PCR analysis of the *Dhh-Cre* and *Pten* genotypes. Expected PCR amplicons, *Dhh-Cre* is 385 bp, WT *Pten* is 310 bp, and floxed *Pten* is 435 bp. DDW, double distilled water as negative control. (C) Levels of PTEN in total protein extracts of sciatic nerves were examined by Western blot analyses. (D) Representative immunofluorescent images showing decreased colocalization of Pten (green channel) and S100 β (red channel) proteins in $\Delta Nf1/\Delta Pten$, compared with that in $\Delta Nf1/Pten$ -het, and *Dhh-Cre; Nf1*^{fl/fl} ($\Delta Nf1$)

mice. Peripheral nerves were co-stained with an anti-S100 β to identify Schwann cells, 4', 6-diamidino-2-phenylindole (blue channel) to identify nuclei, and anti-Pten to indicate Pten protein.

6.1.3 AKT inhibitor treatment

AKT inhibitor, AZD5363, was commercially purchased from MedChemExpress company (New Jersey, USA, Cat# HY-15431). AZD5363 was first dissolved in DMSO at a stock concentration of 100 mg/ml. Before injection, the stock solution was diluted into 2 mg/ml using 1X PBS (Gibco Thermo Fisher Scientific, Cat# 1930314). The working concentration of AZD5363 used in this study was 20 mg/kg/day. Mice were weighed before injection, and the injection volume can be calculated using the formula: volume (μ l) = body weight (g) X 10. Mice from control group were injected with same concentration of DMSO as vehicle control treatment. The treatment started at postnatal day (P)-5 and ended at P-30.

6.2 Experimental methods

6.2.1 Hematoxylin-eosin (HE) staining

Mouse iWAT were freshly isolated and frozen in Tissue-Tek® OCT Compound (Sakura Finetek, USA, Cat# 4583) at -80°C overnight, followed by cryosectioning at 10 microns (Leica Biosystems). Glass slides (Marienfeld, Germany, Cat# 32371202) were used to mount the tissue sections. These slides were stained with hematoxylin and eosin using the following protocol: Firstly, the slides were processed by dipping them in water for 2 minutes at room temperature to remove the OCT compound and

twice in 100% ethanol (2 minutes each). This was followed by two changes of 95% ethanol, one change of 70% ethanol, each for 3 minutes. This procedure was meant to rehydrate the tissues. Slides were rinsed with water using 10 to 20 dips before staining with hematoxylin (Gill II hematoxylin, Leica Biosystems, Cat# 041615) for 2.5 minutes. Slides were rinsed under running tap-water for 3 minutes before transferring to 95% ethanol for 1 minute. Slides were treated with blue buffer 8 (Leica Biosystems, Cat# 032615A) for 5 dips before transferring to 95% ethanol for 1 minute. Slides were further stained with eosin (Leica Biosystems, Cat# 021715) for 3 minutes and rinsed with 100% ethanol for three times (1 minute, 3 minutes and 3 minutes, respectively). Lastly, slides were mounted with mounting medium (Leica Biosystems, Cat# 03801982) and glass cover (Marienfeld, Cat# 33228017).

6.2.2 Western blot analyses

Protein was isolated from iWAT and sciatic nerve of experimental mice using the Qproteome Mammalian Protein Prep Kit (Qiagen, Cat#37901) according to the manufacturer's instructions. Concentrations of protein were determined by Bradford Protein Assay (Bio-Rad, Cat#5000001). Protein lysate was separated on an 8% SDS-PAGE gel and transferred to polyvinylidene difluoride (PVDF) membrane (Millipore, Cat# IPVH00010) with 300 ma current for 90 minutes. The membrane was blocked with 5% milk in 1X TBST for 2 hours at room temperature, followed by incubation with primary antibodies at 4°C overnight, and finally the corresponding secondary antibodies' incubation at room temperature for 1.5 hour. Targeted proteins were detected using a horseradish peroxidase-conjugated chemiluminescent kit (Millipore, Cat# WBULS0500). ACTB was used as the loading control. The antibodies used in

this study were obtained from the following companies: PTEN (Cell Signaling Technology, Cat# 9556), phospho-AKT (Cell Signaling Technology, Cat# 4060S), AKT (Cell Signaling Technology, Cat# 4691S), HSL (Cell Signaling Technology, Cat# 4107S), phospho-HSL (Cell Signaling Technology, Cat# 4139S), TH (Merck Millipore, Cat# AB152), and ACTB (Cell Signaling Technology, Cat# 3700).

6.2.3 Immunohistochemistry (IHC) staining

Tissue-Tek® OCT Compound embedded mouse iWAT were sectioned at 10 microns and collected on glass slides (Marienfeld, Cat# 32371202). Firstly, the antigen epitopes on the tissue sections were unmasked using a commercially purchased unmasking solution (Vector Laboratories, California, USA, Cat# H3300) according to the manufacturer's instructions. The tissue section slides were then treated with 3% hydrogen peroxide to remove any endogenous peroxidase activity. Blocking was performed at room temperature using goat serum (5% serum in 1X PBS) in a humidified chamber for 20 minutes. Slides were then incubated with TH primary antibodies (1:500) (Novus Biologicals, Colorado, USA, Cat# NB300-109) at 4°C overnight in a humidified chamber. After primary incubation, slides were washed thoroughly in 1X PBS/0.05% Tween 20 (PBST) before incubating with horseradish peroxidase-secondary antibody raised against the primary antibody. After thorough washing with 1X PBST, the sections were treated with freshly prepared DAB substrate (Invitrogen, Cat# D22187) and allowed for adequate signal to develop before stopping the reaction in water. Finally, sections were then lightly counter stained with haematoxylin before mounted with mounting medium (Leica Biosystems,

Cat# 03801982) and glass cover (Marienfeld, Cat# 33228017) (Keng, Watson, et al., 2012).

6.2.4 UPLC-QQQ-MS based neurotransmitters metabolites

Sample preparation: fresh iWAT was dissected from mice, placed into 1.5 ml Eppendorf tubes and snap frozen immediately in lipid nitrogen. For storage, these samples were kept at -80°C. Before analyses, samples were thawed on ice. Detailed adipose tissue processing procedures were shown in **Figure 20**.

Neurotransmitters metabolites assay: the system used in this study was Agilent 6460 liquid chromatography- triple quadrupole Mass Spectrometer (UPLC-QQQ-MS) equipped with an Electrospray ion (Bugianesi, McCullough, & Marchesini) source. The column used were ACQUITY BEH Amide columns (2.1 mm x 100 mm, 1.7 µm) and ACQUITY BEH Amide pre-columns (2.1 mm x 5 mm, 1.7 µm). Injection volume was 5 µl and sample chamber temperature was set at 4°C. The fragmentor voltages and collision energies were optimized for each neurotransmitter condition. Agilent Mass Hunter software version B.06.00 (quantitative data analysis) were used for data acquisition and processing.

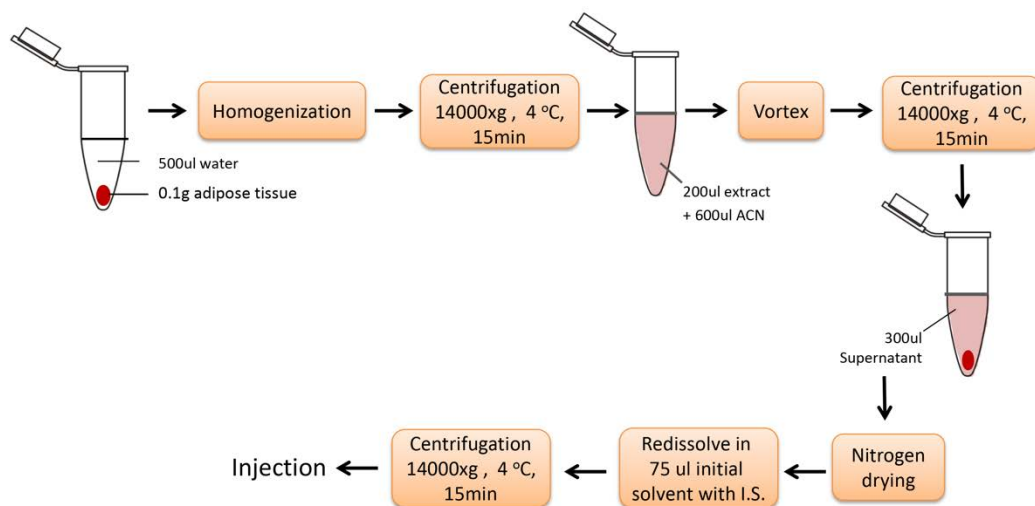


Figure 20 Sample preparation protocol.

Adipose tissue (0.1 g) was immersed with distilled water, homogenized and followed by 4°C centrifugation at 14000g for 15 minutes. Around 200 µl extract was carefully collected and mixed with 600 µl acetonitrile (ACN) and vortex thoroughly. The same centrifugation condition was performed as previously described and around 300 µl supernatant was collected for nitrogen drying. Finally, extract was dissolved in 75 µl initial solvent (acetonitrile: water 85:15% v/v, with 30 mM ammonium formate) and centrifuged as described previously. This image was prepared by Ms Angela Man.

CHAPTER 7: Results

7.1 SCs-specific *Pten* inactivation induced bigger iWAT

Dhh-Cre; Pten^{f/f} mice is an established animal model for malignant peripheral nerve sheath tumors (MPNST) (Keng, Rahrman, et al., 2012; Keng, Watson, et al., 2012). In this MPNST model, two transgenes were introduced in mice either in combination of *Nf1* and *Pten*; or *Egfr* and *Pten* (Keng, Rahrman, et al., 2012; Keng, Watson, et al., 2012). Interestingly, mice with the genotype of *Dhh-Cre; Pten^{f/f}* have bigger lower belly compared with mice with the genotype of *Dhh-Cre* or *Dhh-Cre; Pten^{f/+}* (**Fig. 21A**). The bigger lower belly phenotype has 100% penetrance in every *Dhh-Cre; Pten^{f/f}* mice tested ($n = 7$) and can be observed as early as postnatal day (P)-10 (*data not shown*). At P-30, subcutaneous adipose tissue hyperplasia was identified in *Dhh-Cre; Pten^{f/f}* mice (**Fig. 21B**). Interestingly, this phenomenon has no gender bias as both female and male *Dhh-Cre; Pten^{f/f}* mice display similar adipose tissue hyperplasia.

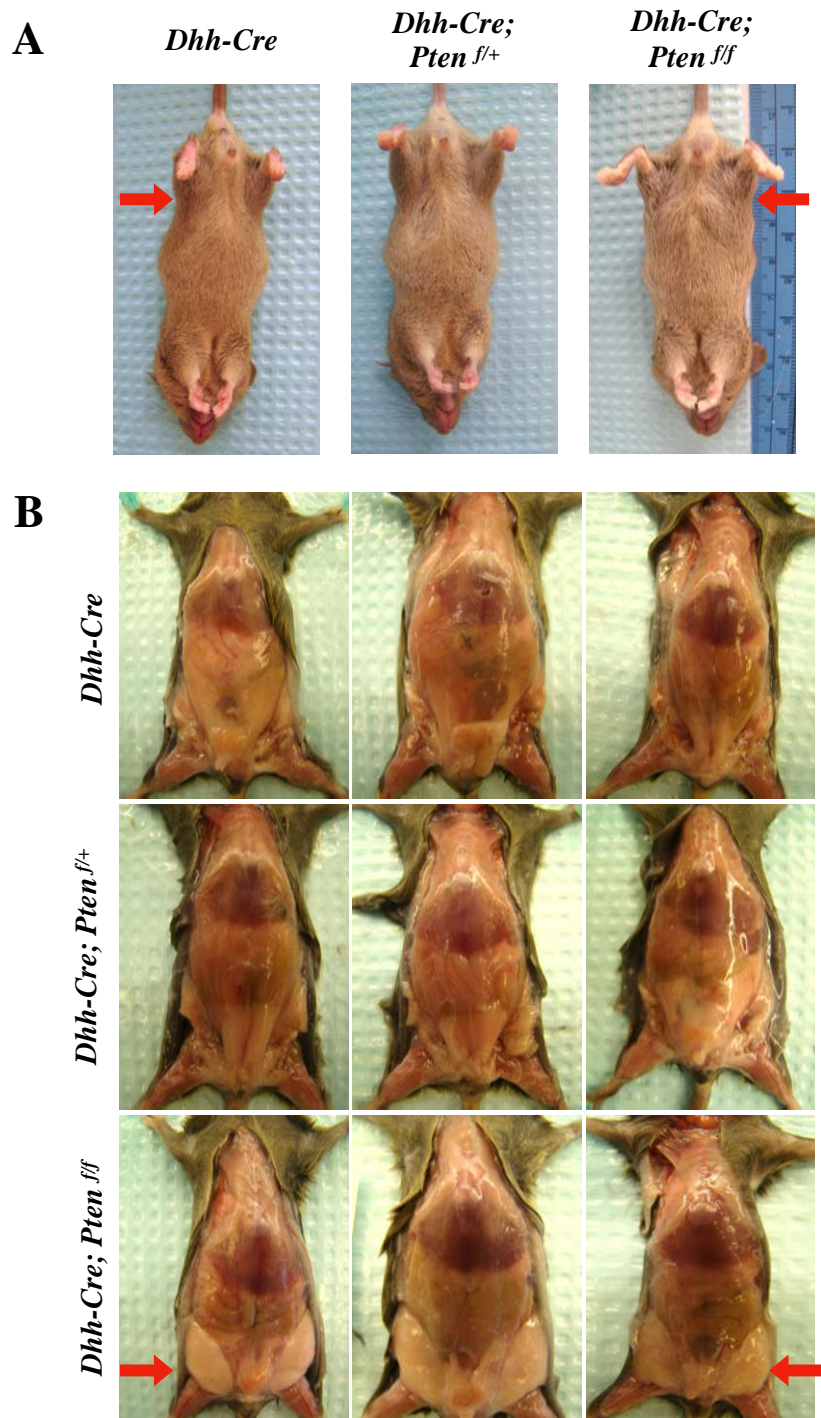


Figure 21 Conditional inactivation of *Pten* in SCs induced bigger iWAT.

(A) Representative images from mice with different genotypes showing the lower belly. (B) Representative images from mice with different genotypes showing the iWAT.

7.2 SCs-specific *Pten* inactivation results in elevated iWAT fat index

Adipose tissues that are commonly studied in mice include iWAT, gonadal white adipose tissue (gWAT) and the interscapular BAT (Barkan et al.; Bartelt & Heeren, 2014), since these adipose tissue represent the subcutaneous white fat tissue, perivisceral fat tissue and brown adipose tissue. The anatomical sites of these adipose tissues in mice have been summarized in **Figure 22** (Bartelt & Heeren, 2014).

In this study, these different kinds of adipose tissues were dissected from mice and weighed to evaluate the fat indexes. Representative images of different fat tissues, including iWAT, gWAT and BAT, were shown in **Figure 23A**. Fat indexes were determined using the following formula: fat tissue weight (g)/body weight (g) X 100. The fat index of iWAT was dramatically increased in *Dhh-Cre; Pten^{f/f}* mice compared with that in control mice *Dhh-Cre*, with the average data 2.372 and 0.6046, respectively. However, the fat index of iWAT in *Dhh-Cre; Pten^{f/+}* mice has no significant difference with that in control mice. In addition, the gWAT and BAT fat index showed no difference among all three experimental mice cohorts (**Fig. 23B**). In order to further confirm the morphology difference of the iWAT between control and *Dhh-Cre; Pten^{f/f}* mice, HE staining was performed. The iWAT adipocytes in *Dhh-Cre; Pten^{f/f}* mice were dramatically increased in size compared with control mouse adipocytes (**Fig. 23C**).

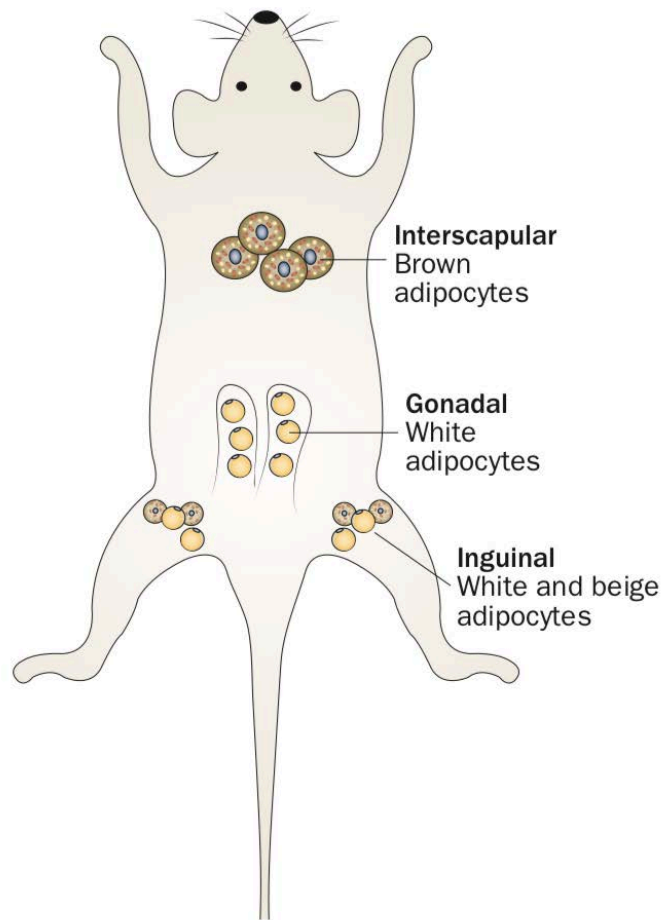


Figure 22 Anatomical locations of different WAT and BAT in mice.

Summary of anatomical locations of different WAT and BAT in mice (Bartelt & Heeren, 2014). The interscapular BAT comprises of classic brown adipocytes.

Gonadal WAT mainly contains white adipocytes, while inguinal WAT contain a mixture of white and beige adipocytes. The proportions of different WAT and BAT depend on energy status.

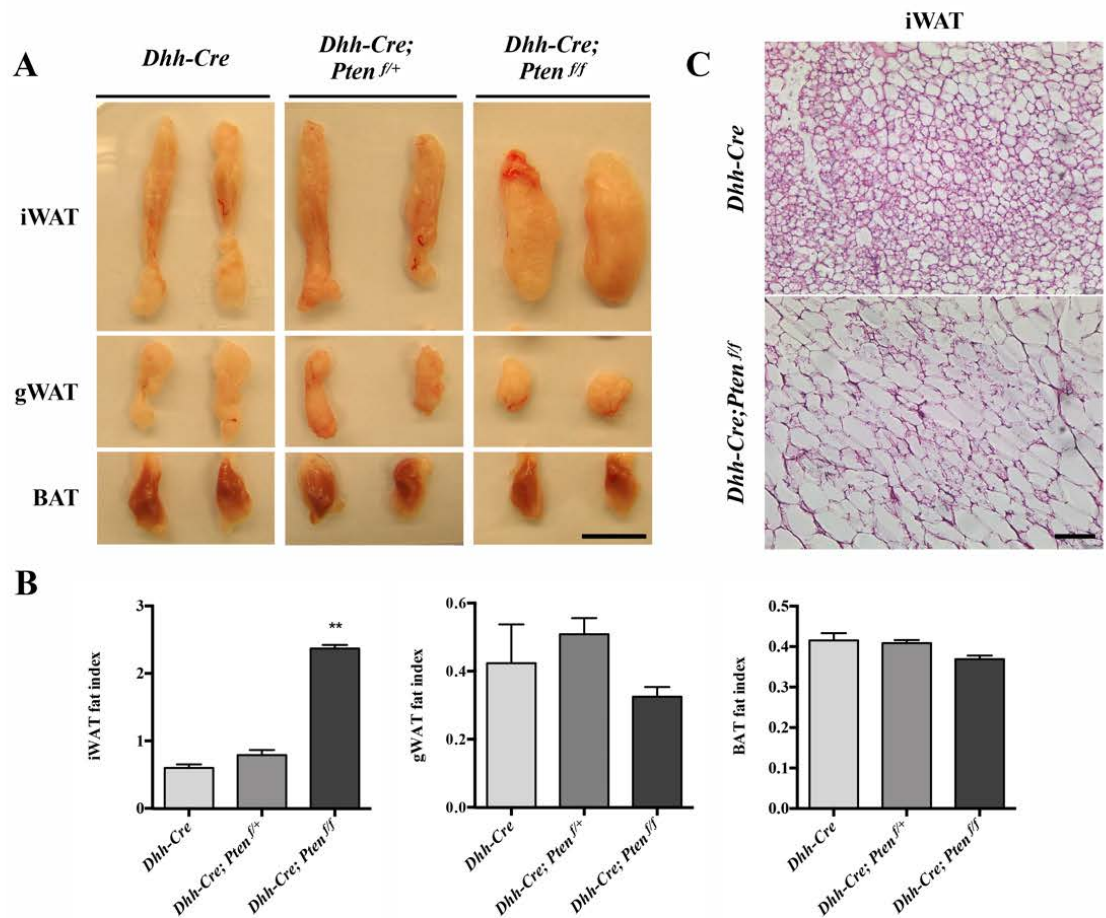


Figure 23 Conditional inactivation of *Pten* in SCs result in iWAT hyperplasia.

(A) Representative images of iWAT, gWAT and BAT from three experimental mouse cohorts. Scale bar, 1 cm. (B) Fat indexes of iWAT, gWAT and BAT from three experimental mouse cohorts, $n = 6$, Values are expressed as mean \pm SEM; ** $P < 0.01$. (C) HE staining images showing adipocytes from iWAT from *Dhh-Cre* control and *Dhh-Cre; Pten^{f/f}* mice. Scale bar, 100 μ M. iWAT indicates inguinal white adipose tissue; gWAT indicates gonadal white adipose tissue; and BAT indicates scapular brown adipose tissue.

7.3 SCs-specific *Pten* inactivation induced activated AKT signal

It has been well reported that PTEN works as a negative regulator in the PI3K/AKT pathway (Carracedo & Pandolfi, 2008). Therefore, we proposed that *Pten* deficiency can result in activation of PI3K/AKT signalling in SCs. The expression level of total AKT and phosphorylated AKT (pAKT) were determined by Western blot analyses. Results showed that pAKT was elevated in sciatic nerve of *Dhh-Cre; Pten^{f/f}* mice, compared with that in *Dhh-Cre* control group (**Fig. 24**). The sciatic nerve lysate was used in order to show relative similar protein expression levels in SCs.

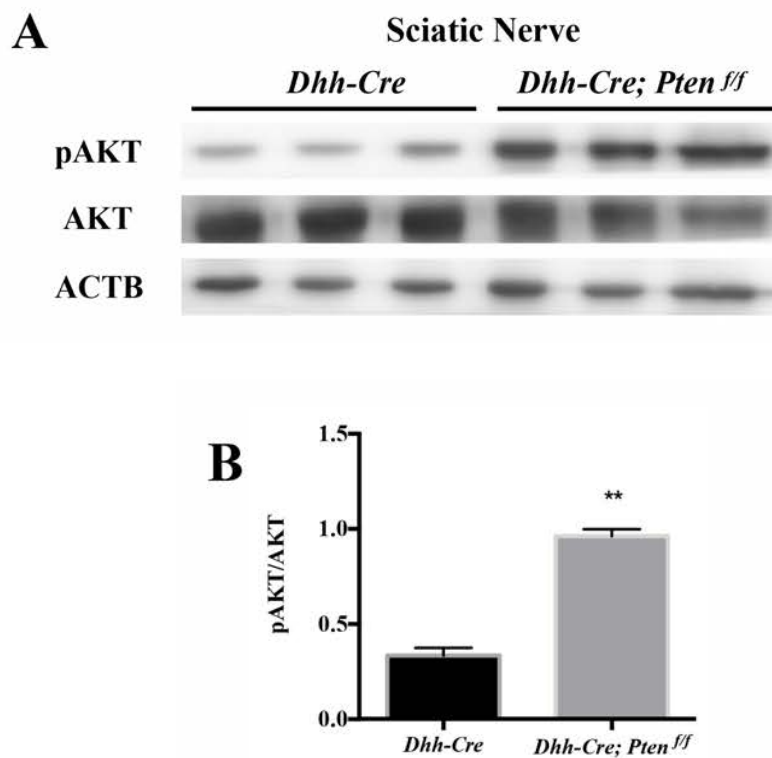


Figure 24 Elevated pAKT in the sciatic nerves of *Dhh-Cre; Pten^{f/f}* mice.

(A) Levels of pAKT and AKT in total protein extracts of sciatic nerves were examined by Western blot analyses. (B) Semi-quantification analyses of pAKT relative to total

AKT in the Western blot bands shown in (A). Values are expressed as mean \pm SEM; ****** $P < 0.01$.

7.4 SCs-specific *Pten* inactivation inhibited SNS activity

Adipocytes are well-innervated by SNS and has been shown to be necessary and sufficient for regulation of lipolysis (T. J. Bartness et al., 2014; T. J. Bartness et al., 2010). Our hypothesis is dysfunctional *Pten* in SCs results in compromised SNS and aberrant lipolysis activities.

7.4.1 SCs-specific *Pten* inactivation inhibited tyrosine hydroxylase expression

Tyrosine Hydroxylase (TH) is a rate-limiting enzyme in catecholamine biosynthesis and a marker for sympathetic neurons (Zeng et al., 2015). Western blot analyses and immunohistochemistry (IHC) staining showed that TH was downregulated in iWAT of *Dhh-Cre; Pten^{f/f}* mice compared with that in control mice (**Fig. 25**). From the IHC images, bigger adipocytes can also be identified in *Dhh-Cre; Pten^{f/f}* mice iWAT, which is similar with the previous HE staining images (**Fig. 23C**). These data suggest that *Pten* mutation in SCs resulted in compromised SNS function.

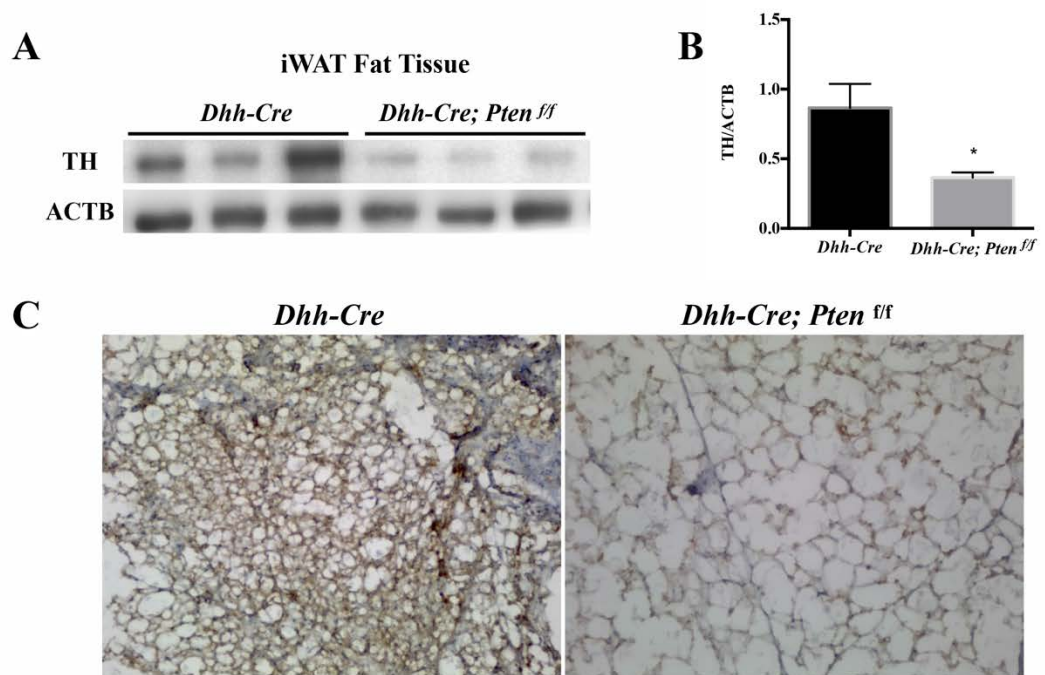


Figure 25 Reduced TH expression in the iWAT of *Dhh-Cre; Pten^{fl/fl}* mice.

(A) TH in protein lysate of iWAT was detected by Western blot analyses in *Dhh-Cre* control mice but reduced in *Dhh-Cre; Pten^{fl/fl}* mice. (B) Semi-quantification analyses of TH relative of ACTB in the Western blot bands shown in (A). Values are expressed as mean \pm SEM; * $P < 0.05$. (C) TH expression was confirmed to be reduced in iWAT of *Dhh-Cre; Pten^{fl/fl}* mice by immunohistochemistry.

7.4.2 SCs-specific *Pten* inactivation results in decreased NE, dopamine and histamine content

NE is the main neurotransmitter released by SNS to control lipolysis (T. J. Bartness et al., 2010). Histamine is another neurotransmitter also believed to accelerate lipolysis in WAT by activating SNS (Jørgensen, Knigge, Warberg, & Kjær, 2007; Sakata, Yoshimatsu, Masaki, & Tsuda, 2003; Tsuda et al., 2002; Yoshimatsu, Hidaka,

Niijima, & Sakata, 2001). To further confirm the inactivated SNS function in *Dhh-Cre; Pten^{ff}* mice, the content of these neurotransmitters in iWAT were analyzed. NE and histamine content were reduced in iWAT of *Dhh-Cre; Pten^{ff}* mice compared with that in control mice (**Fig. 26A** and **26B**). In accordance, dopamine, the direct precursor of NE, was also decreased in *Dhh-Cre; Pten^{ff}* mice (**Fig. 26C**). Besides, the expression level of phosphorylated hormone sensitive lipase (pHSL), a critical downstream enzyme in NE-induced lipolysis, was examined by Western blot analyses and shown to be reduced in iWAT of *Dhh-Cre; Pten^{ff}* mice compared with control mice (**Fig. 26D** and **26E**).

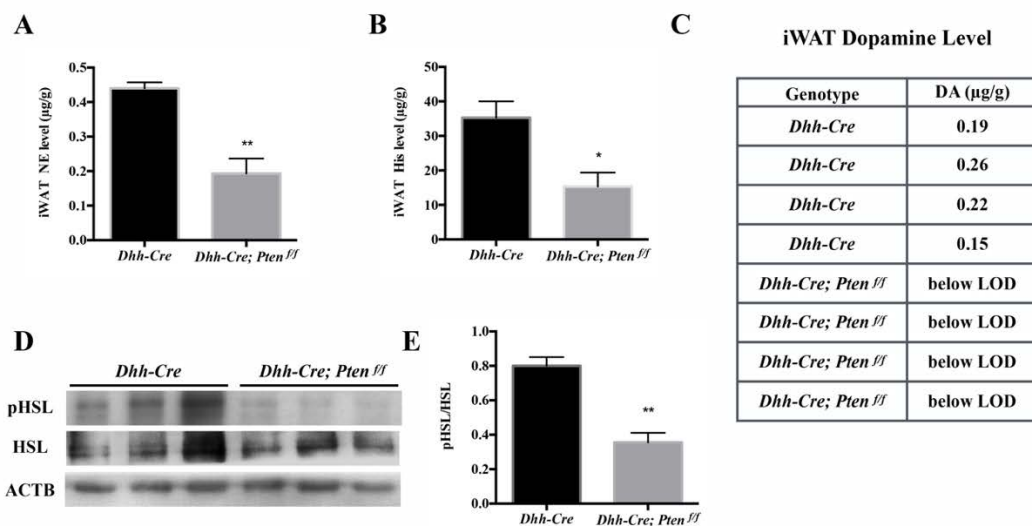


Figure 26 Content of neurotransmitters were decreased in iWAT of *Dhh-Cre; Pten^{ff}* mice.

(**A**, **B** and **C**) Neurotransmitters of NE, histamine (His) and dopamine were detected using UPLC-QQQ-MS method. LOD, limit of detection equals to 0.13 µg/g. (**D**) p-HSL in total protein extracts of iWAT was examined by Western blot analyses. (**E**)

Quantification of Western blot bands shown in (D). Values are expressed as mean \pm SEM; n = 4, ** $P < 0.01$, * $P < 0.05$.

7.5 AKT inhibitor AZD5363 improved iWAT hyperplasia

Previous data has demonstrated that *Pten* inactivation in SCs resulted in activated AKT activity. Furthermore, SNS activity was inhibited in iWAT of *Dhh-Cre; Pten^{ff}* mice. Therefore, we hypothesized that hyperactive AKT may be responsible for the decreased SNS activity and compromised lipolysis in iWAT of *Dhh-Cre; Pten^{ff}* mice.

It has been previously shown that PTEN inactivation could induce hypermyelination in both the central nervous system and peripheral nervous system (PNS) (Goebbels et al., 2010), which is consistent with overexpression of AKT induced enhanced myelination in CNS (Flores et al., 2008). These papers provide strong evidence that AKT could functionally regulate the nervous system. Therefore, inhibiting its function offers a strategy to further explore if AKT is truly the key for SNS activity in iWAT.

7.5.1 AKT inhibitor treatment improved iWAT phenotype

The AKT inhibitor (AZD5363) used in this study can potently inhibits all isoforms of AKT (AKT1/2/3) and phosphorylation of AKT substrates (Davies et al., 2012). Interestingly, the iWAT fat mass from treated mice appear decreased compared with the vehicle control mice (Fig. 27A and 27B). The iWAT fat index from AZD5363 treated mice was reduced to an average number of 1.794, compared with the 2.301 from vehicle group (Fig. 27C).

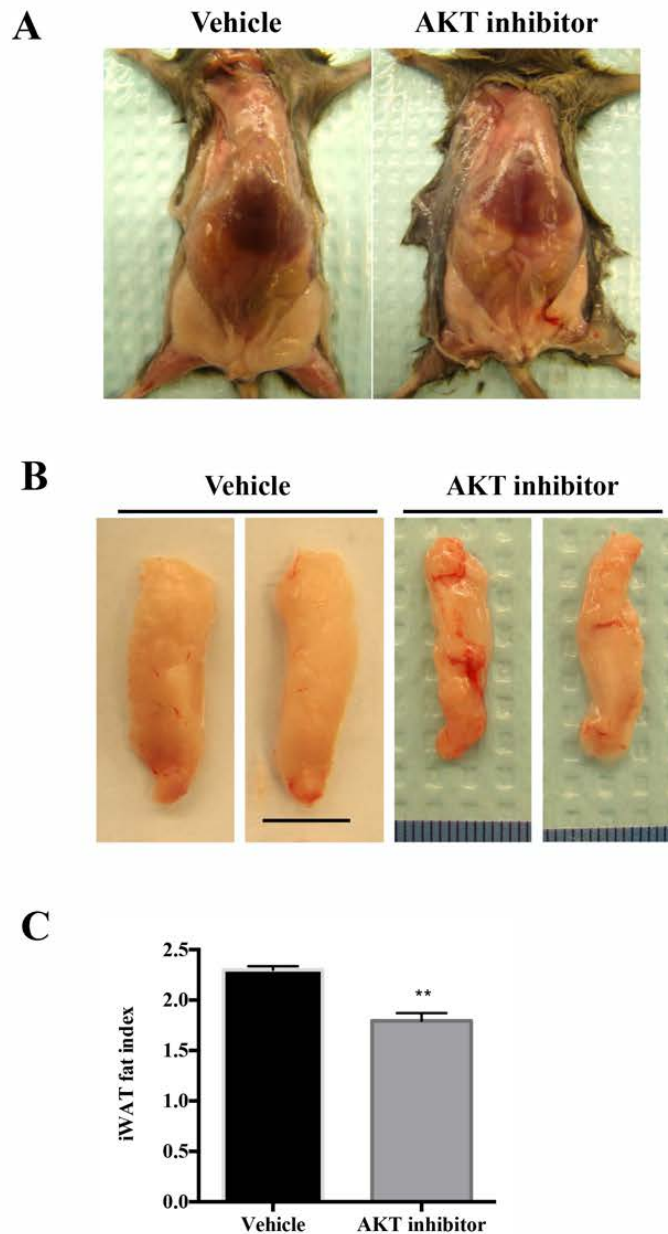


Figure 27 AKT inhibitor improved hyperplasia of iWAT in *Dhh-Cre; Pten^{f/f}* mice.

Dhh-Cre; Pten^{f/f} mice were treated with either 20 mg/kg/day AZD5363 or vehicle solution from P-5 to P-30. iWAT were dissected from mice and weighed. (A) Representative images of opened mice from vehicle or treated group. (B) Representative images of iWAT from vehicle or treated group. Scale bar, 1 cm. (C) Fat index of iWAT from vehicle or treated group. Values are expressed as mean ± SEM; n = 3, ***P* < 0.01.

7.5.2 AKT inhibitor treatment improved SNS activity

Previous data has shown that the iWAT fat index was reduced when mice were treated with AKT inhibitor AZD5363. In order to examine whether the inhibition of AKT function could improve SNS activity and lipolysis, TH and HSL expression were examined by Western blot analyses. Expression levels of TH and total HSL levels in *Dhh-Cre; Pten^{f/f}* iWAT were significantly increased, including a trend towards increased pHSL levels after AZD5363 treatment (**Fig. 28**).

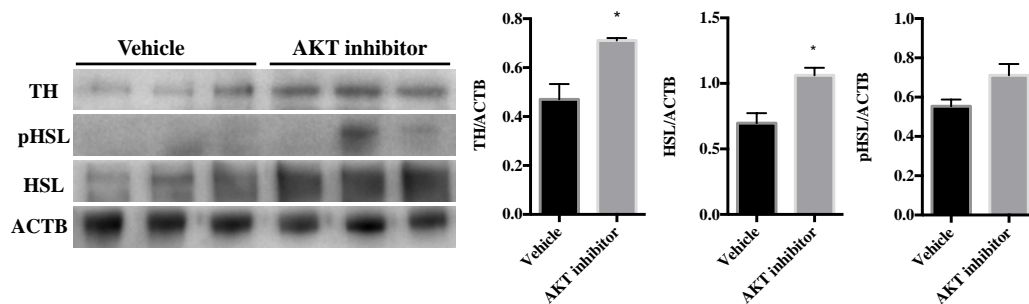


Figure 28 AKT inhibitor treatment improved TH expression in *Dhh-Cre; Pten^{f/f}* mice.

Dhh-Cre; Pten^{f/f} mice were treated with either 20 mg/kg/day AZD5363 or vehicle solution from P-5 to P-30. iWAT were dissected from mice and protein were extracted. TH, HSL, pHSL expression in iWAT were determined by Western blot analyses. Semi-quantification of TH, HSL and pHSL relative to ABCT in Western blot bands were shown. Values are expressed as mean \pm SEM; * $P < 0.05$.

CHAPTER 8: Discussion

SNS is known to stimulate lipolysis and mobilize adipocytes through neuro-adipose junctions in WAT, although the regulatory physiologic mechanisms responsible for this process have not been fully determined. In this study, we found that genetic mutation of *Pten* gene in SCs results in compromised SNS activity and lipolysis in iWAT, leading to iWAT hypertrophy. Moreover, AKT inhibitor AZD5363 treatment partly reversed this phenotype. These data provide evidence confirming the regulatory functions of SCs in mediating SNS-NE stimulated lipolysis in WAT.

The presence of SCs in WAT has been shown by transmission electronic microscope images (L. Chen et al., 2017). However, there is almost no published papers discussing the role of SCs in regulation of WAT metabolism. SNS innervation of WAT has been well studied, indicating the initiator role of SNS innervation in WAT lipolysis (T. Bartness & Ryu, 2015; T. J. Bartness et al., 2010). Given the anatomical relationship of SC in preganglionic and postgenomic SNS, we hypothesized that SCs could play a role in SNS function, as well as lipolysis in iWAT. Most of the published work about SCs focuses on its functions in PNS myelination process and the underlying mechanisms (Pereira, Lebrun-Julien, & Suter, 2012). SCs specific deletion of phosphatidylinositol 4-kinase alpha or fatty acid synthase caused aberrant myelination (Alvarez-Prats et al., 2018; Montani et al., 2018). AKT/mTOR pathway, *Big1/Arfgef1* and *Arf1*, as well as SCs autophagy (myelinophagy) were proven to mediate myelination development in the PNS (Domènech-Estévez et al., 2016; Gomez-Sanchez et al., 2015; Miyamoto et al., 2018; Norrmén & Suter, 2013). Importantly, PTEN reduction in both oligodendrocytes and SCs induced

hypermyelination while activated PTEN terminated myelination (Goebbels et al., 2010; Pereira et al., 2012). However, none of these papers discussing the effects of morphological changes in SCs on SNS activity and WAT metabolism.

In the current study, mice with *Pten* mutation in SCs bear dysfunctional SNS activity, which was proven as reduced TH expression. TH has long been used as a marker for SNS function, since TH is the rate-limiting enzyme for synthesis of NE, one of the major neurotransmitters released by SNS for regulation of target organs (Nagatsu, Levitt, & Udenfriend, 1964; Zeng et al., 2015). SNS-NE driven lipolysis was compromised shown as the decreased neurotransmitters including NE, histamine and dopamine content in iWAT, as well as the reduced pHSL level (**Fig. 26**). Another two lipase, adipose triglyceride lipase (ATGL) and monoglyceride lipase (MGL) can also be examined in the future. In addition, NE was believed to inhibit adipocytes proliferation *in vitro* (T. J. Bartness, Song, Shi, Bowers, & Foster, 2005), which could also contribute to bigger iWAT in the experimental mice compared with the control mice. AKT inhibitor AZD5363 treatment slightly rescued the development of bigger iWAT in *Dhh-Cre; Pten^{fl/fl}* mice, demonstrating as decreased iWAT fat index. This may due to enhanced lipolysis caused by suppressed AKT and subsequent active PKA, which increased the phosphorylation of HSL for lipolysis in iWAT (**Fig. 28**). However, AKT inhibition can activate PKA activity, which further phosphorylates HSL in adipocytes (Choi et al., 2010). Therefore, the improved iWAT phenotype after AKT inhibitor treatment may not be dependent on compromised AKT function in SCs. This confusing issue can be solved by collecting more data evaluating the SNS function in addition to examining TH expression, neurotransmitters content and SCs morphological changes after AKT inhibitor treatment. For example, body

temperature alterations and subsequent evaluation of beta-adrenergic receptor signalling will reflect SNS activity when SCs-specific *Pten* inactivated mice were kept at cold conditions, since cold acclimation stimulates thermogenesis in adipose tissues via activation of SNS and enhanced beta-adrenergic function (Y. Chen et al., 2018).

There are still more mechanism work deserves to be done for further investigation in this study. First of all, *Dhh-Cre* is not absolutely specific for generating SCs gene deletions, and there is currently no SC-specific Cre recombinase commercially available. Another two transgenic mouse strains that are useful for creating SCs-specific gene inactivation including *Cnp-Cre* and *Plp1-Cre* (<http://www.em.mpg.de/index.php?id=233&L=1> and <https://www.jax.org/strain/005975>). Thus, more specific Cre containing transgenic mice targeting SCs are really needed to accurately elucidate and confirm the role of SCs in the SNS-driven iWAT metabolism. Secondly, the question why BAT and gWAT have no altered phenotype like iWAT has not been figured out. This may due to distinct regulatory mechanism of body fat depots, since different responses of fat pads under same environmental stimulus have been reported (T. J. Bartness et al., 2010). SNS can be adaptively stimulated to induce lipolysis in WAT and trigger heat production in BAT in cold environmental temperature, but fasting could results in higher sympathetic activity in iWAT and reduced sympathetic outflow in BAT (Brito et al., 2008; Fenzl & Kiefer, 2014). Thus we wonder whether the SNS can be activated when *Dhh-Cre; Pten^{ff}* mice are exposed with a cold environment. This may gain further insights into the physiological mechanism of SNS function as well as the thermogenesis involved with SCs. Another question is the role of endothelial

cells in development of iWAT, since *Dhh-Cre; Pten^{ff}* mice will have altered endothelial cells along the blood vessels in whole mouse body.

In summary, the current study provides evidence supporting that *Pten* deficiency specifically in SCs play an important role in SNS function and subsequent SNS-NE stimulated lipolysis in iWAT.

Reference

- Ahsan, S., Ge, Y., & Tainsky, M. A. (2016). Combinatorial therapeutic targeting of BMP2 and MEK-ERK pathways in NF1-associated malignant peripheral nerve sheath tumors. *Oncotarget*, 7(35), 57171.
- Alaggio, R., Turrini, R., Boldrin, D., Merlo, A., Gambini, C., Ferrari, A., . . . Bonaldi, L. (2013). Survivin expression and prognostic significance in pediatric malignant peripheral nerve sheath tumors (MPNST). *PloS one*, 8(11), e80456.
- Albritton, K., Rankin, C., Coffin, C., Ratner, N., Budd, G., Schuetze, S., . . . Borden, E. (2006). *Phase II study of erlotinib in metastatic or unresectable malignant peripheral nerve sheath tumors (MPNST)*. Paper presented at the ASCO Annual Meeting Proceedings.
- Alvarez-Prats, A., Bjelobaba, I., Aldworth, Z., Baba, T., Abebe, D., Kim, Y. J., . . . Balla, T. (2018). Schwann-Cell-Specific Deletion of Phosphatidylinositol 4-Kinase Alpha Causes Aberrant Myelination. *Cell reports*, 23(10), 2881-2890.

- Barkan, B., Starinsky, S., Friedman, E., Stein, R., & Kloog, Y. (2006). The Ras inhibitor farnesylthiosalicylic acid as a potential therapy for neurofibromatosis type 1. *Clinical Cancer Research*, *12*(18), 5533-5542.
- Bartelt, A., Bruns, O. T., Reimer, R., Hohenberg, H., Ittrich, H., Peldschus, K., . . . Waurisch, C. (2011). Brown adipose tissue activity controls triglyceride clearance. *Nature medicine*, *17*(2), 200.
- Bartelt, A., & Heeren, J. (2014). Adipose tissue browning and metabolic health. *Nature Reviews Endocrinology*, *10*(1), 24.
- Bartness, T., & Ryu, V. (2015). Neural control of white, beige and brown adipocytes. *International journal of obesity supplements*, *5*(S1), S35.
- Bartness, T. J., Liu, Y., Shrestha, Y. B., & Ryu, V. (2014). Neural innervation of white adipose tissue and the control of lipolysis. *Frontiers in neuroendocrinology*, *35*(4), 473-493.
- Bartness, T. J., Shrestha, Y., Vaughan, C., Schwartz, G., & Song, C. (2010). Sensory and sympathetic nervous system control of white adipose tissue lipolysis. *Molecular and cellular endocrinology*, *318*(1-2), 34-43.
- Bartness, T. J., Song, C. K., Shi, H., Bowers, R. R., & Foster, M. T. (2005). Brain-adipose tissue cross talk. *Proceedings of the Nutrition society*, *64*(1), 53-64.
- Berghmans, S., Murphey, R. D., Wienholds, E., Neuberg, D., Kutok, J. L., Fletcher, C. D., . . . Kanki, J. P. (2005). tp53 mutant zebrafish develop malignant peripheral nerve sheath tumors. *Proceedings of the National Academy of Sciences of the United States of America*, *102*(2), 407-412.
- Blero, D., Payraastre, B., Schurmans, S., & Erneux, C. (2007). Phosphoinositide phosphatases in a network of signalling reactions. *Pflügers Archiv-European Journal of Physiology*, *455*(1), 31-44.

- Bollag, G., Clapp, D. W., Shih, S., Adler, F., Zhang, Y. Y., Thompson, P., . . . Jacks, T. (1996). Loss of NF1 results in activation of the Ras signaling pathway and leads to aberrant growth in haematopoietic cells. *Nature genetics*, *12*(2), 144.
- Boström, P., Wu, J., Jedrychowski, M. P., Korde, A., Ye, L., Lo, J. C., . . . Long, J. Z. (2012). A PGC1- α -dependent myokine that drives brown-fat-like development of white fat and thermogenesis. *Nature*, *481*(7382), 463.
- Bottillo, I., Ahlquist, T., Brekke, H., Danielsen, S. A., van den Berg, E., Mertens, F., . . . Dallapiccola, B. (2009). Germline and somatic NF1 mutations in sporadic and NF1-associated malignant peripheral nerve sheath tumours. *The Journal of pathology*, *217*(5), 693-701.
- Bradford, D., & Kim, A. (2015). Current treatment options for malignant peripheral nerve sheath tumors. *Current treatment options in oncology*, *16*(3), 12.
- Bradtmöller, M., Hartmann, C., Zietsch, J., Jäschke, S., Mautner, V.-F., Kurtz, A., . . . Reuss, D. (2012). Impaired Pten expression in human malignant peripheral nerve sheath tumours. *PLoS One*, *7*(11), e47595.
- Brasaemle, D. L. (2007). Thematic review series: adipocyte biology. The perilipin family of structural lipid droplet proteins: stabilization of lipid droplets and control of lipolysis. *Journal of lipid research*, *48*(12), 2547-2559.
- Brems, H., Beert, E., de Ravel, T., & Legius, E. (2009). Mechanisms in the pathogenesis of malignant tumours in neurofibromatosis type 1. *The lancet oncology*, *10*(5), 508-515.
- Bressenot, A., Marchal, S., Bezdetnaya, L., Garrier, J., Guillemin, F., & Plénat, F. (2009). Assessment of apoptosis by immunohistochemistry to active caspase-3, active caspase-7, or cleaved PARP in monolayer cells and

- spheroid and subcutaneous xenografts of human carcinoma. *Journal of Histochemistry & Cytochemistry*, 57(4), 289-300.
- Brito, N. A., Brito, M. N., & Bartness, T. J. (2008). Differential sympathetic drive to adipose tissues after food deprivation, cold exposure or glucoprivation. *American Journal of Physiology-Regulatory, Integrative and Comparative Physiology*, 294(5), R1445-R1452.
- Brossier, N. M., & Carroll, S. L. (2012). Genetically engineered mouse models shed new light on the pathogenesis of neurofibromatosis type I-related neoplasms of the peripheral nervous system. *Brain research bulletin*, 88(1), 58-71.
- Bugianesi, E., McCullough, A. J., & Marchesini, G. (2005). Insulin resistance: a metabolic pathway to chronic liver disease. *Hepatology*, 42(5), 987-1000.
- Cannon, B., & Nedergaard, J. (2004). Brown adipose tissue: function and physiological significance. *Physiological reviews*, 84(1), 277-359.
- Carli, M., Ferrari, A., Mattke, A., Zanetti, I., Casanova, M., Bisogno, G., . . . Koscielniak, E. (2005). Pediatric malignant peripheral nerve sheath tumor: the Italian and German soft tissue sarcoma cooperative group. *Journal of clinical oncology*, 23(33), 8422-8430.
- Caron, A., Lee, S., Elmquist, J. K., & Gautron, L. (2018). Leptin and brain–adipose crosstalks. *Nature Reviews Neuroscience*, 19(3), 153.
- Carracedo, A., & Pandolfi, P. (2008). The PTEN–PI3K pathway: of feedbacks and cross-talks. *Oncogene*, 27(41), 5527.
- Cha, C., Antonescu, C. R., Quan, M. L., Maru, S., & Brennan, M. F. (2004). Long-term results with resection of radiation-induced soft tissue sarcomas. *Annals of surgery*, 239(6), 903.

- Chen, L., Jin, Y., Yang, X., Liu, Z., Wang, Y., Wang, G., . . . Shen, Z. (2017). Fat tissue, a potential Schwann cell reservoir: isolation and identification of adipose-derived Schwann cells. *American journal of translational research*, 9(5), 2579.
- Chen, Y., Ikeda, K., Yoneshiro, T., Scaramozza, A., Tajima, K., Wang, Q., . . . Brown, Z. (2018). Thermal stress induces glycolytic beige fat formation via a myogenic state. *Nature*.
- Choi, S. M., Tucker, D. F., Gross, D. N., Easton, R. M., DiPilato, L. M., Dean, A. S., . . . Birnbaum, M. J. (2010). Insulin regulates adipocyte lipolysis via an Akt-independent signaling pathway. *Molecular and cellular biology*, 30(21), 5009-5020.
- College, J. N. M. (1986). Dictionary of traditional Chinese medicine. In: Shanghai Science and Technology Publishing House Shanghai.
- Cordero-Espinoza, L., & Hagen, T. (2013). Increased concentrations of Fructose-2, 6-bisphosphate contribute to the Warburg effect in PTEN-deficient cells. *Journal of Biological Chemistry*, jbc. M113. 510289.
- Correll, J. W. (1963). Adipose tissue: ability to respond to nerve stimulation in vitro. *Science*, 140(3565), 387-388.
- Cypess, A. M., Weiner, L. S., Roberts-Toler, C., Elía, E. F., Kessler, S. H., Kahn, P. A., . . . Doria, A. (2015). Activation of human brown adipose tissue by a β 3-adrenergic receptor agonist. *Cell metabolism*, 21(1), 33-38.
- D'Adamo, D. R., Anderson, S. E., Albritton, K., Yamada, J., Riedel, E., Scheu, K., . . . Maki, R. G. (2005). Phase II study of doxorubicin and bevacizumab for patients with metastatic soft-tissue sarcomas. *Journal of Clinical Oncology*, 23(28), 7135-7142.

- Dahlberg, W., Little, J., Fletcher, J., Suit, H., & Okunieff, P. (1993). Radiosensitivity in vitro of human soft tissue sarcoma cell lines and skin fibroblasts derived from the same patients. *International journal of radiation biology*, 63(2), 191-198.
- Davies, B. R., Greenwood, H., Dudley, P., Crafter, C., Yu, D.-H., Zhang, J., . . . Maynard, J. (2012). Preclinical pharmacology of AZD5363, an orally bioavailable inhibitor of AKT: pharmacodynamics, antitumor activity and correlation of monotherapy activity with genetic background. *Molecular cancer therapeutics*, molcanther. 0824.2011.
- DeClue, J. E., Heffelfinger, S., Benvenuto, G., Ling, B., Li, S., Rui, W., . . . Ratner, N. (2000). Epidermal growth factor receptor expression in neurofibromatosis type 1-related tumors and NF1 animal models. *The Journal of clinical investigation*, 105(9), 1233-1241.
- Demestre, M., Terzi, M. Y., Mautner, V., Vajkoczy, P., Kurtz, A., & Piña, A. L. (2013). Effects of pigment epithelium derived factor (PEDF) on malignant peripheral nerve sheath tumours (MPNSTs). *Journal of neuro-oncology*, 115(3), 391-399.
- Domènech-Estévez, E., Baloui, H., Meng, X., Zhang, Y., Deinhardt, K., Dupree, J. L., . . . Salzer, J. L. (2016). Akt regulates axon wrapping and myelin sheath thickness in the PNS. *Journal of Neuroscience*, 36(16), 4506-4521.
- Dozois, E. J., Wall, J. C., Spinner, R. J., Jacofsky, D. J., Yaszemski, M. J., Sim, F. H., . . . Haddock, M. G. (2009). Neurogenic tumors of the pelvis: clinicopathologic features and surgical outcomes using a multidisciplinary team. *Annals of surgical oncology*, 16(4), 1010-1016.

- Ducatman, B. S., Scheithauer, B. W., Piepgras, D. G., Reiman, H. M., & Ilstrup, D. M. (1986). Malignant peripheral nerve sheath tumors. A clinicopathologic study of 120 cases. *Cancer*, *57*(10), 2006-2021.
- Dunn, G. P., Spiliopoulos, K., Plotkin, S. R., Hornicek, F. J., Harmon, D. C., Delaney, T. F., & Williams, Z. (2013). Role of resection of malignant peripheral nerve sheath tumors in patients with neurofibromatosis type 1. *Journal of neurosurgery*, *118*(1), 142-148.
- Durbin, A. D., Ki, D. H., He, S., & Look, A. T. (2016). Malignant peripheral nerve sheath tumors. In *Cancer and Zebrafish* (pp. 495-530): Springer.
- Endo, M., Yamamoto, H., Setsu, N., Kohashi, K., Takahashi, Y., Ishii, T., . . . Aoki, M. (2012). Prognostic significance of AKT/mTOR and MAPK pathways and antitumor effect of mTOR inhibitor in NF1-related and sporadic malignant peripheral nerve sheath tumors. *Clinical Cancer Research*.
- Enerbäck, S. (2009). The origins of brown adipose tissue. *New England Journal of Medicine*, *360*(19), 2021-2023.
- Evans, D. G. R., Baser, M. E., McGaughran, J., Sharif, S., Howard, E., & Moran, A. (2002). Malignant peripheral nerve sheath tumours in neurofibromatosis 1. *Journal of medical genetics*, *39*(5), 311-314.
- Fang, D., Hawke, D., Zheng, Y., Xia, Y., Meisenhelder, J., Nika, H., . . . Lu, Z. (2007). Phosphorylation of β -catenin by AKT promotes β -catenin transcriptional activity. *Journal of Biological Chemistry*.
- Fantuzzi, G. (2005). Adipose tissue, adipokines, and inflammation. *Journal of Allergy and Clinical Immunology*, *115*(5), 911-919.

- Farid, M., Demicco, E. G., Garcia, R., Ahn, L., Merola, P. R., Cioffi, A., & Maki, R. G. (2014). Malignant peripheral nerve sheath tumors. *The oncologist, 19*(2), 193-201.
- Fenzl, A., & Kiefer, F. W. (2014). Brown adipose tissue and thermogenesis. *Hormone molecular biology and clinical investigation, 19*(1), 25-37.
- Ferner, R. E., & Gutmann, D. H. (2002). International consensus statement on malignant peripheral nerve sheath tumors in neurofibromatosis 1. In: AACR.
- Flores, A. I., Narayanan, S. P., Morse, E. N., Shick, H. E., Yin, X., Kidd, G., . . . Macklin, W. B. (2008). Constitutively active Akt induces enhanced myelination in the CNS. *Journal of Neuroscience, 28*(28), 7174-7183.
- Foley, K. M., Woodruff, J. M., Ellis, F. T., & Posner, J. B. (1980). Radiation-induced malignant and atypical peripheral nerve sheath tumors. *Annals of Neurology: Official Journal of the American Neurological Association and the Child Neurology Society, 7*(4), 311-318.
- Gesta, S., Tseng, Y.-H., & Kahn, C. R. (2007). Developmental origin of fat: tracking obesity to its source. *Cell, 131*(2), 242-256.
- Ghadimi, M. P., Lopez, G., Torres, K. E., Belousov, R., Young, E. D., Liu, J., . . . Lazar, A. J. (2012a). Targeting the PI3K/mTOR axis, alone and in combination with autophagy blockade, for the treatment of malignant peripheral nerve sheath tumors. *Molecular cancer therapeutics*.
- Ghadimi, M. P., Lopez, G., Torres, K. E., Belousov, R., Young, E. D., Liu, J., . . . Lazar, A. J. (2012b). Targeting the PI3K/mTOR axis, alone and in combination with autophagy blockade, for the treatment of malignant peripheral nerve sheath tumors. *Molecular cancer therapeutics, 11*(8), 1758-1769.

- Ghadimi, M. P., Young, E. D., Belousov, R., Zhang, Y., Lopez, G., Lusby, K., . . . Lazar, A. J. (2012a). Survivin is a viable target for the treatment of malignant peripheral nerve sheath tumors. *Clinical cancer research*, *18*(9), 2545-2557.
- Ghadimi, M. P., Young, E. D., Belousov, R., Zhang, Y., Lopez, G., Lusby, K., . . . Lazar, A. J. (2012b). Survivin is a viable target for the treatment of malignant peripheral nerve sheath tumors. *Clinical Cancer Research*.
- Girousse, A., & Langin, D. (2012). Adipocyte lipases and lipid droplet-associated proteins: insight from transgenic mouse models. *International Journal of Obesity*, 581.
- Goebbels, S., Oltrogge, J. H., Kemper, R., Heilmann, I., Bormuth, I., Wolfer, S., . . . Lappe-Siefke, C. (2010). Elevated phosphatidylinositol 3, 4, 5-trisphosphate in glia triggers cell-autonomous membrane wrapping and myelination. *Journal of Neuroscience*, *30*(26), 8953-8964.
- Gomez-Sanchez, J. A., Carty, L., Iruarrizaga-Lejarreta, M., Palomo-Irigoyen, M., Varela-Rey, M., Griffith, M., . . . Aurrekoetxea, I. (2015). Schwann cell autophagy, myelinophagy, initiates myelin clearance from injured nerves. *J Cell Biol*, *210*(1), 153-168.
- Gregorian, C., Nakashima, J., Dry, S. M., Nghiemphu, P. L., Smith, K. B., Ao, Y., . . . Mischel, P. S. (2009). PTEN dosage is essential for neurofibroma development and malignant transformation. *Proceedings of the National Academy of Sciences*, *106*(46), 19479-19484.
- Griffin, J. W., & Thompson, W. J. (2008). Biology and pathology of nonmyelinating Schwann cells. *Glia*, *56*(14), 1518-1531.

- Grobmyer, S. R., Reith, J. D., Shahlaee, A., Bush, C. H., & Hochwald, S. N. (2008). Malignant peripheral nerve sheath tumor: molecular pathogenesis and current management considerations. *Journal of surgical oncology*, *97*(4), 340-349.
- Grove, M., Kim, H., Santerre, M., Krupka, A. J., Han, S. B., Zhai, J., . . . Kim, S. (2017). YAP/TAZ initiate and maintain Schwann cell myelination. *Elife*, *6*, e20982.
- Guertin, D. A., & Sabatini, D. M. (2005). An expanding role for mTOR in cancer. *Trends in molecular medicine*, *11*(8), 353-361.
- Gupta, G., Mammis, A., & Maniker, A. (2008). Malignant peripheral nerve sheath tumors. *Neurosurgery Clinics of North America*, *19*(4), 533-543.
- Gutmann, D. H., Ferner, R. E., Listernick, R. H., Korf, B. R., Wolters, P. L., & Johnson, K. J. (2017). Neurofibromatosis type 1. *Nature Reviews Disease Primers*, *3*, 17004.
- Halliday, A. L., Sobel, R. A., & Martuza, R. L. (1991). Benign spinal nerve sheath tumors: their occurrence sporadically and in neurofibromatosis types 1 and 2. *Journal of neurosurgery*, *74*(2), 248-253.
- Halling, K. C., Scheithauer, B. W., Halling, A. C., Nascimento, A. G., Ziesmer, S. C., Roche, P. C., & Wollan, P. C. (1996). p53 expression in neurofibroma and malignant peripheral nerve sheath tumor: an immunohistochemical study of sporadic and NF1-associated tumors. *American journal of clinical pathology*, *106*(3), 282-288.
- Harris, M., Hartley, A. L., Blair, V., Birch, J. M., Banerjee, S. S., Freemont, A., . . . McWilliam, L. (1991). Sarcomas in north west England: I. Histopathological peer review. *British journal of cancer*, *64*(2), 315.

- Hattori, K., Naguro, I., Okabe, K., Funatsu, T., Furutani, S., Takeda, K., & Ichijo, H. (2016). ASK1 signalling regulates brown and beige adipocyte function. *Nature communications*, 7, 11158.
- Holm, C. (2003). Molecular mechanisms regulating hormone-sensitive lipase and lipolysis. In: Portland Press Limited.
- Holtkamp, N., Malzer, E., Zietsch, J., Okuducu, A. F., Mucha, J., Mawrin, C., . . . von Deimling, A. (2008). EGFR and erbB2 in malignant peripheral nerve sheath tumors and implications for targeted therapy. *Neuro-oncology*, 10(6), 946-957.
- Holtkamp, N., Reuß, D. E., Atallah, I., Kuban, R. J., Hartmann, C., Mautner, V. F., . . . Pham, V. A. (2004). Subclassification of nerve sheath tumors by gene expression profiling. *Brain pathology*, 14(3), 258-264.
- Huang, J., & Kontos, C. D. (2002). Inhibition of vascular smooth muscle cell proliferation, migration, and survival by the tumor suppressor protein PTEN. *Arteriosclerosis, thrombosis, and vascular biology*, 22(5), 745-751.
- Hui, X., Gu, P., Zhang, J., Nie, T., Pan, Y., Wu, D., . . . Lam, K. S. (2015). Adiponectin enhances cold-induced browning of subcutaneous adipose tissue via promoting M2 macrophage proliferation. *Cell metabolism*, 22(2), 279-290.
- Hwang, M. H., Cho, M., Lee, D. G., Go, E. B., Park, Y. S., & Chung, N. (2016). Single-and repeated-dose oral toxicity tests of deep sea water mineral extracts in ICR mice. *Journal of Applied Biological Chemistry*, 59(3), 227-231.
- Jaakkola, S., Peltonen, J., Riccardi, V., Chu, M.-L., & Uitto, J. (1989). Type 1 neurofibromatosis: selective expression of extracellular matrix genes by

- Schwann cells, perineurial cells, and fibroblasts in mixed cultures. *The Journal of clinical investigation*, 84(1), 253-261.
- Jaegle, M., Ghazvini, M., Mandemakers, W., Piirsoo, M., Driegen, S., Levavasseur, F., . . . Meijer, D. (2003). The POU proteins Brn-2 and Oct-6 share important functions in Schwann cell development. *Genes & development*, 17(11), 1380-1391.
- James, A. W., Shurell, E., Singh, A., Dry, S. M., & Eilber, F. C. (2016). Malignant peripheral nerve sheath tumor. *Surgical Oncology Clinics*, 25(4), 789-802.
- Jessen, K., & Mirsky, R. (2016). The repair Schwann cell and its function in regenerating nerves. *The Journal of physiology*, 594(13), 3521-3531.
- Jessen, K. R., Mirsky, R., & Lloyd, A. C. (2015). Schwann cells: development and role in nerve repair. *Cold Spring Harbor perspectives in biology*, 7(7), a020487.
- Jessen, W. J., Miller, S. J., Jousma, E., Wu, J., Rizvi, T. A., Brundage, M. E., . . . Dombi, E. (2013). MEK inhibition exhibits efficacy in human and mouse neurofibromatosis tumors. *The Journal of clinical investigation*, 123(1), 340-347.
- Jiang, H., Ding, X., Cao, Y., Wang, H., & Zeng, W. (2017). Dense Intra-adipose Sympathetic Arborizations Are Essential for Cold-Induced Beiging of Mouse White Adipose Tissue. *Cell metabolism*, 26(4), 686-692. e683.
- Jimenez, M., Barbatelli, G., Allevi, R., Cinti, S., Seydoux, J., Giacobino, J. P., . . . Preitner, F. (2003). β 3-Adrenoceptor knockout in C57BL/6J mice depresses the occurrence of brown adipocytes in white fat. *European Journal of Biochemistry*, 270(4), 699-705.

- Jo, V. Y., & Fletcher, C. D. (2014). WHO classification of soft tissue tumours: an update based on the 2013 (4th) edition. *Pathology*, 46(2), 95-104.
- Johannessen, C. M., Reczek, E. E., James, M. F., Brems, H., Legius, E., & Cichowski, K. (2005). The NF1 tumor suppressor critically regulates TSC2 and mTOR. *Proceedings of the National Academy of Sciences of the United States of America*, 102(24), 8573-8578.
- Johansson, G., Mahller, Y. Y., Collins, M. H., Kim, M.-O., Nobukuni, T., Perentesis, J., . . . Thomas, G. (2008). Effective in vivo targeting of the mammalian target of rapamycin pathway in malignant peripheral nerve sheath tumors. *Molecular cancer therapeutics*, 7(5), 1237-1245.
- Johnson, D. L., & Stiles, B. L. (2016). Maf1, a new PTEN target linking RNA and lipid metabolism. *Trends in Endocrinology & Metabolism*, 27(10), 742-750.
- Jørgensen, E. A., Knigge, U., Warberg, J., & Kjær, A. (2007). Histamine and the regulation of body weight. *Neuroendocrinology*, 86(3), 210-214.
- Kalbermatten, D. F., Erba, P., Mahay, D., Wiberg, M., Pierer, G., & Terenghi, G. (2008). Schwann cell strip for peripheral nerve repair. *Journal of Hand Surgery (European Volume)*, 33(5), 587-594.
- Katz, D., Lazar, A., & Lev, D. (2009). Malignant peripheral nerve sheath tumour (MPNST): the clinical implications of cellular signalling pathways. *Expert reviews in molecular medicine*, 11.
- Keng, V. W., Rahrman, E. P., Watson, A. L., Tschida, B. R., Moertel, C. L., Jessen, W. J., . . . Largaespada, D. A. (2012). PTEN and NF1 inactivation in Schwann cells produces a severe phenotype in the peripheral nervous system that promotes the development and malignant progression of peripheral nerve sheath tumors. *Cancer research*, 72(13), 3405-3413.

- Keng, V. W., Watson, A. L., Rahrman, E. P., Li, H., Tschida, B. R., Moriarity, B. S., . . . Wallace, M. R. (2012). Conditional inactivation of Pten with EGFR overexpression in Schwann cells models sporadic MPNST. *Sarcoma, 2012*.
- Kim, A., & Pratilas, C. A. (2017). The promise of signal transduction in genetically driven sarcomas of the nerve. *Experimental neurology*.
- Kim, A., Stewart, D. R., Reilly, K. M., Viskochil, D., Miettinen, M. M., & Widemann, B. C. (2017). Malignant peripheral nerve sheath tumors state of the science: leveraging clinical and biological insights into effective therapies. *Sarcoma, 2017*.
- Kingham, P. J., Kalbermatten, D. F., Mahay, D., Armstrong, S. J., Wiberg, M., & Terenghi, G. (2007). Adipose-derived stem cells differentiate into a Schwann cell phenotype and promote neurite outgrowth in vitro. *Experimental neurology, 207(2)*, 267-274.
- Klampfer, L., Huang, J., Shirasawa, S., Sasazuki, T., & Augenlicht, L. (2007). Histone deacetylase inhibitors induce cell death selectively in cells that harbor activated kRasV12: The role of signal transducers and activators of transcription 1 and p21. *Cancer research, 67(18)*, 8477-8485.
- Kopelman, P. G. (2000). Obesity as a medical problem. *Nature, 404(6778)*, 635.
- Labbé, S. M., Caron, A., Chechi, K., Laplante, M., Lecomte, R., & Richard, D. (2016). Metabolic activity of brown, “beige,” and white adipose tissues in response to chronic adrenergic stimulation in male mice. *American Journal of Physiology-Endocrinology and Metabolism, 311(1)*, E260-E268.
- LaFemina, J., Qin, L.-X., Moraco, N. H., Antonescu, C. R., Fields, R. C., Crago, A. M., . . . Singer, S. (2013). Oncologic outcomes of sporadic,

neurofibromatosis-associated, and radiation-induced malignant peripheral nerve sheath tumors. *Annals of surgical oncology*, 20(1), 66-72.

Lafontan, M., Bousquet-Melou, A., Galitzky, J., Barbe, P., Carpené, C., Langin, D., . . . Bouloumié, A. (1995). Adrenergic receptors and fat cells: differential recruitment by physiological amines and homologous regulation. *Obesity*, 3(S4).

Langin, D. (2006). Adipose tissue lipolysis as a metabolic pathway to define pharmacological strategies against obesity and the metabolic syndrome. *Pharmacological Research*, 53(6), 482-491.

Lee, P. R., Cohen, J. E., Tendi, E. A., Farrer, R., De Vries, G. H., Becker, K. G., & Fields, R. D. (2004). Transcriptional profiling in an MPNST-derived cell line and normal human Schwann cells. *Neuron glia biology*, 1(2), 135-147.

Li, H., Matheny, M., & Scarpace, P. J. (1997). beta 3-Adrenergic-mediated suppression of leptin gene expression in rats. *American Journal of Physiology-Endocrinology and Metabolism*, 272(6), E1031-E1036.

Li, Y., Rao, P. K., Wen, R., Song, Y., Muir, D., Wallace, P., . . . Kadesch, T. (2004). Notch and Schwann cell transformation. *Oncogene*, 23(5), 1146.

Li, Z., Li, J., Bi, P., Lu, Y., Burcham, G., Elzey, B. D., . . . Kuang, S. (2014). Plk1 phosphorylation of PTEN causes a tumor-promoting metabolic state. *Molecular and cellular biology*, MCB. 00814-00814.

Lim, R., Jaramillo, D., Poussaint, T. Y., Chang, Y., & Korf, B. (2005). Superficial neurofibroma: a lesion with unique MRI characteristics in patients with neurofibromatosis type 1. *American Journal of Roentgenology*, 184(3), 962-968.

- Lopez, G., Torres, K., Liu, J., Hernandez, B., Young, E., Belousov, R., . . .
McCutcheon, I. E. (2011). Autophagic survival in resistance to histone
deacetylase inhibitors: novel strategies to treat malignant peripheral nerve
sheath tumors. *Cancer research*, 71(1), 185-196.
- Lopez, G., Torres, K., Liu, J., Hernandez, B., Young, E., Belousov, R., . . .
McCutcheon, I. E. (2010). Autophagic survival in resistance to histone
deacetylase inhibitors: novel strategies to treat malignant peripheral nerve
sheath tumors. *Cancer research*, canres. 2799.2010.
- Lu, P., Jones, L., & Tuszynski, M. (2005). BDNF-expressing marrow stromal cells
support extensive axonal growth at sites of spinal cord injury. *Experimental
neurology*, 191(2), 344-360.
- Luscan, A., Masliah-Planchon, J., Laurendeau, I., Ortonne, N., Varin, J., Lallemand,
F., . . . Borderie, D. (2013). The activation of the WNT signalling pathway is
a hallmark in Neurofibromatosis type 1 tumorigenesis. *Clinical Cancer
Research*, clincanres. 0780.2013.
- Mahller, Y. Y., Vaikunth, S. S., Currier, M. A., Miller, S. J., Ripberger, M. C., Hsu,
Y.-H., . . . Ratner, N. (2007). Oncolytic HSV and erlotinib inhibit tumor
growth and angiogenesis in a novel malignant peripheral nerve sheath tumor
xenograft model. *Molecular Therapy*, 15(2), 279-286.
- Mahller, Y. Y., Vaikunth, S. S., Ripberger, M. C., Baird, W. H., Saeki, Y.,
Cancelas, J. A., . . . Cripe, T. P. (2008). Tissue inhibitor of
metalloproteinase-3 via oncolytic herpesvirus inhibits tumor growth and
vascular progenitors. *Cancer research*, 68(4), 1170-1179.

- Maki, R. G., D'Adamo, D. R., Keohan, M. L., Saulle, M., Schuetze, S. M., Undevia, S. D., . . . Mita, M. M. (2009). Phase II study of sorafenib in patients with metastatic or recurrent sarcomas. *Journal of clinical oncology*, 27(19), 3133.
- Maltese, W. A., & Overmeyer, J. H. (2014). Methuosis: nonapoptotic cell death associated with vacuolization of macropinosome and endosome compartments. *The American journal of pathology*, 184(6), 1630-1642.
- Martinez-Rivera, M., & Siddik, Z. H. (2012). Resistance and gain-of-resistance phenotypes in cancers harboring wild-type p53. *Biochemical pharmacology*, 83(8), 1049-1062.
- Mattingly, R. R., Kraniak, J. M., Dilworth, J. T., Mathieu, P., Bealmear, B., Nowak, J. E., . . . Reiners, J. J. (2006). The mitogen-activated protein kinase/extracellular signal-regulated kinase inhibitor PD184352 (CI-1040) selectively induces apoptosis in malignant schwannoma cell lines. *Journal of Pharmacology and Experimental Therapeutics*, 316(1), 456-465.
- Meng, H., Li, G., Huang, J., Zhang, K., Wang, H., & Wang, J. (2013). Sesquiterpene coumarin and sesquiterpene chromone derivatives from *Ferula ferulaeoides* (Steud.) Korov. *Fitoterapia*, 86, 70-77.
- Miller, S. J., Rangwala, F., Williams, J., Ackerman, P., Kong, S., Jegga, A. G., . . . Kluwe, L. (2006). Large-scale molecular comparison of human schwann cells to malignant peripheral nerve sheath tumor cell lines and tissues. *Cancer research*, 66(5), 2584-2591.
- Miyamoto, Y., Torii, T., Tago, K., Tanoue, A., Takashima, S., & Yamauchi, J. (2018). BIG1/Arfgef1 and Arf1 regulate the initiation of myelination by Schwann cells in mice. *Science advances*, 4(4), eaar4471.

- Montani, L., Pereira, J. A., Norrmén, C., Pohl, H. B., Tinelli, E., Trötz Müller, M., . . . Schwager, R. (2018). De novo fatty acid synthesis by Schwann cells is essential for peripheral nervous system myelination. *J Cell Biol*, *217*(4), 1353-1368.
- Nagatsu, T., Levitt, M., & Udenfriend, S. (1964). Tyrosine hydroxylase the initial step in norepinephrine biosynthesis. *Journal of Biological Chemistry*, *239*(9), 2910-2917.
- Nedergaard, J., & Cannon, B. (2014). The browning of white adipose tissue: some burning issues. *Cell metabolism*, *20*(3), 396-407.
- Nishida, C., Ko, G., & Kumanyika, S. (2010). Body fat distribution and noncommunicable diseases in populations: overview of the 2008 WHO Expert Consultation on Waist Circumference and Waist–Hip Ratio. *European journal of clinical nutrition*, *64*(1), 2.
- Norrmén, C., & Suter, U. (2013). Akt/mTOR signalling in myelination. In: Portland Press Limited.
- Nusse, R. (2005). Wnt signaling in disease and in development. *Cell research*, *15*(1), 28.
- Ohno, H., Shinoda, K., Spiegelman, B. M., & Kajimura, S. (2012). PPAR γ agonists induce a white-to-brown fat conversion through stabilization of PRDM16 protein. *Cell metabolism*, *15*(3), 395-404.
- Ouellet, V., Labbé, S. M., Blondin, D. P., Phoenix, S., Guérin, B., Haman, F., . . . Carpentier, A. C. (2012). Brown adipose tissue oxidative metabolism contributes to energy expenditure during acute cold exposure in humans. *The Journal of clinical investigation*, *122*(2), 545-552.

- Pagadala, N. S., Syed, K., & Tuszynski, J. (2017). Software for molecular docking: a review. *Biophysical reviews*, 9(2), 91-102.
- Pasmant, E., Vidaud, M., Vidaud, D., & Wolkenstein, P. (2012). Neurofibromatosis type 1: from genotype to phenotype. *Journal of medical genetics*, 49(8), 483-489.
- Pereira, J. A., Lebrun-Julien, F., & Suter, U. (2012). Molecular mechanisms regulating myelination in the peripheral nervous system. *Trends in neurosciences*, 35(2), 123-134.
- Perry, A., Roth, K. A., Banerjee, R., Fuller, C. E., & Gutmann, D. H. (2001). NF1 deletions in S-100 protein-positive and negative cells of sporadic and neurofibromatosis 1 (NF1)-associated plexiform neurofibromas and malignant peripheral nerve sheath tumors. *The American journal of pathology*, 159(1), 57-61.
- Ràfols, M. E. (2014). Adipose tissue: cell heterogeneity and functional diversity. *Endocrinología y Nutrición (English Edition)*, 61(2), 100-112.
- Rahrmann, E. P., Watson, A. L., Keng, V. W., Choi, K., Moriarity, B. S., Beckmann, D. A., . . . Moertel, C. L. (2013). Forward genetic screen for malignant peripheral nerve sheath tumor formation identifies new genes and pathways driving tumorigenesis. *Nature genetics*, 45(7), 756.
- Rasmussen, S. A., Overman, J., Thomson, S. A., Colman, S. D., Abernathy, C. R., Trimpert, R. E., . . . Bauer, M. (2000). Chromosome 17 loss-of-heterozygosity studies in benign and malignant tumors in neurofibromatosis type 1. *Genes, Chromosomes and Cancer*, 28(4), 425-431.

- Ratner, N., & Miller, S. J. (2015). A RASopathy gene commonly mutated in cancer: the neurofibromatosis type 1 tumour suppressor. *Nature Reviews Cancer*, *15*(5), 290.
- Robertson, K. A., Nalepa, G., Yang, F.-C., Bowers, D. C., Ho, C. Y., Hutchins, G. D., . . . Parada, L. F. (2012). Imatinib mesylate for plexiform neurofibromas in patients with neurofibromatosis type 1: a phase 2 trial. *The lancet oncology*, *13*(12), 1218-1224.
- Rodriguez, F. J., Folpe, A. L., Giannini, C., & Perry, A. (2012). Pathology of peripheral nerve sheath tumors: diagnostic overview and update on selected diagnostic problems. *Acta neuropathologica*, *123*(3), 295-319.
- Rosen, E. D., & Spiegelman, B. M. (2014). What we talk about when we talk about fat. *Cell*, *156*(1-2), 20-44.
- Rosenwald, M., Perdikari, A., Rüllicke, T., & Wolfrum, C. (2013). Bi-directional interconversion of brite and white adipocytes. *Nature cell biology*, *15*(6), 659.
- Rubin, J. B., & Gutmann, D. H. (2005). Neurofibromatosis type 1—a model for nervous system tumour formation? *Nature Reviews Cancer*, *5*(7), 557.
- Sakata, T., Yoshimatsu, H., Masaki, T., & Tsuda, K. (2003). Anti-obesity actions of mastication driven by histamine neurons in rats. *Experimental biology and medicine*, *228*(10), 1106-1110.
- Scheffzek, K., & Welte, S. (2012). Neurofibromin: protein domains and functional characteristics. In *Neurofibromatosis Type 1* (pp. 305-326): Springer.
- Schlessinger, J. (2000). Cell signaling by receptor tyrosine kinases. *Cell*, *103*(2), 211-225.

- Shen, W.-J., Patel, S., Miyoshi, H., Greenberg, A. S., & Kraemer, F. B. (2009). Functional interaction of hormone-sensitive lipase and perilipin in lipolysis. *Journal of lipid research*, *50*(11), 2306-2313.
- Shurell, E., Tran, L. M., Nakashima, J., Smith, K. B., Tam, B. M., Li, Y., . . . Wu, H. (2014). Gender dimorphism and age of onset in malignant peripheral nerve sheath tumor preclinical models and human patients. *BMC cancer*, *14*(1), 827.
- Stiles, B., Wang, Y., Stahl, A., Bassilian, S., Lee, W. P., Kim, Y.-J., . . . Magnuson, M. A. (2004). Liver-specific deletion of negative regulator Pten results in fatty liver and insulin hypersensitivity. *Proceedings of the National Academy of Sciences*, *101*(7), 2082-2087.
- Stojanović, O., Kieser, S., & Trajkovski, M. (2018). Common traits between the beige fat-inducing stimuli. *Current Opinion in Cell Biology*, *55*, 67-73.
- Storlazzi, C., Brekke, H., Mandahl, N., Brosjö, O., Smeland, S., Lothe, R., & Mertens, F. (2006). Identification of a novel amplicon at distal 17q containing the BIRC5/SURVIVIN gene in malignant peripheral nerve sheath tumours. *The Journal of Pathology: A Journal of the Pathological Society of Great Britain and Ireland*, *209*(4), 492-500.
- Stucky, C.-C. H., Johnson, K. N., Gray, R. J., Pockaj, B. A., Ocal, I. T., Rose, P. S., & Wasif, N. (2012). Malignant peripheral nerve sheath tumors (MPNST): the Mayo Clinic experience. *Annals of surgical oncology*, *19*(3), 878-885.
- Su, W., Sin, M., Darrow, A., & Sherman, L. S. (2003). Malignant peripheral nerve sheath tumor cell invasion is facilitated by Src and aberrant CD44 expression. *Glia*, *42*(4), 350-358.

- Subramanian, S., Thayanithy, V., West, R. B., Lee, C. H., Beck, A. H., Zhu, S., . . .
Hogendoorn, P. C. (2010). Genome-wide transcriptome analyses reveal p53
inactivation mediated loss of miR-34a expression in malignant peripheral
nerve sheath tumours. *The Journal of pathology*, 220(1), 58-70.
- Sun, D., Tainsky, M. A., & Haddad, R. (2012). Oncogene mutation survey in
MPNST cell lines enhances the dominant role of hyperactive Ras in NF1
associated pro-survival and malignancy. *Translational oncogenomics*, 5, 1.
- Takahashi, A., & Shimazu, T. (1981). Hypothalamic regulation of lipid metabolism
in the rat: effect of hypothalamic stimulation on lipolysis. *Journal of the
autonomic nervous system*, 4(3), 195-206.
- Tenbaum, S. P., Ordóñez-Morán, P., Puig, I., Chicote, I., Arqués, O., Landolfi,
S., . . . Mendizabal, L. (2012). β -catenin confers resistance to PI3K and AKT
inhibitors and subverts FOXO3a to promote metastasis in colon cancer.
Nature medicine, 18(6), 892.
- Thangarajh, M., & Gutmann, D. (2012). Low-grade gliomas as neurodevelopmental
disorders: insights from mouse models of neurofibromatosis-1.
Neuropathology and applied neurobiology, 38(3), 241-253.
- Thomas, L., Mautner, V.-F., Cooper, D. N., & Upadhyaya, M. (2012). Molecular
heterogeneity in malignant peripheral nerve sheath tumors associated with
neurofibromatosis type 1. *Human genomics*, 6(1), 1.
- Tohill, M., Mantovani, C., Wiberg, M., & Terenghi, G. (2004). Rat bone marrow
mesenchymal stem cells express glial markers and stimulate nerve
regeneration. *Neuroscience letters*, 362(3), 200-203.
- Torres, K. E., Zhu, Q.-S., Bill, K., Lopez, G., Ghadimi, M. P., Xie, X., . . .
Bolshakov, S. (2011). Activated MET is a molecular prognosticator and

- potential therapeutic target for malignant peripheral nerve sheath tumors. *Clinical cancer research*, 17(12), 3943-3955.
- Tsuda, K., Yoshimatsu, H., Nijjima, A., Chiba, S., Okeda, T., & Sakata, T. (2002). Hypothalamic histamine neurons activate lipolysis in rat adipose tissue. *Experimental biology and medicine*, 227(3), 208-213.
- Tucker, T., Wolkenstein, P., Revuz, J., Zeller, J., & Friedman, J. (2005). Association between benign and malignant peripheral nerve sheath tumors in NF1. *Neurology*, 65(2), 205-211.
- Turkson, L., Mamuszka, H., Grimshaw, K., & Marshall, E. M. (2018). MPNST treatment and diagnosis in NF1: A health economic model. In: AACR.
- van Marken Lichtenbelt, W. D., Vanhommelrig, J. W., Smulders, N. M., Drossaerts, J. M., Kemerink, G. J., Bouvy, N. D., . . . Teule, G. J. (2009). Cold-activated brown adipose tissue in healthy men. *New England Journal of Medicine*, 360(15), 1500-1508.
- Verdijk, R. M., den Bakker, M. A., Dubbink, H. J., Hop, W. C., Dinjens, W. N., & Kros, J. M. (2010). TP53 mutation analysis of malignant peripheral nerve sheath tumors. *Journal of Neuropathology & Experimental Neurology*, 69(1), 16-26.
- Virtanen, K. A., Lidell, M. E., Orava, J., Heglind, M., Westergren, R., Niemi, T., . . . Enerbäck, S. (2009). Functional brown adipose tissue in healthy adults. *New England Journal of Medicine*, 360(15), 1518-1525.
- Watson, A. L., Anderson, L. K., Greeley, A. D., Keng, V. W., Rahrmann, E. P., Halfond, A. L., . . . Moertel, C. L. (2014). Co-targeting the MAPK and PI3K/AKT/mTOR pathways in two genetically engineered mouse models of

- schwann cell tumors reduces tumor grade and multiplicity. *Oncotarget*, 5(6), 1502.
- Watson, A. L., Rahrman, E. P., Moriarity, B. S., Choi, K., Conboy, C. B., Greeley, A. D., . . . Keng, V. W. (2013). Canonical Wnt/ β -catenin signaling drives human Schwann cell transformation, progression, and tumor maintenance. *Cancer discovery*.
- Widemann, B. C. (2009). Current status of sporadic and neurofibromatosis type 1-associated malignant peripheral nerve sheath tumors. *Current oncology reports*, 11(4), 322-328.
- Widemann, B. C., Meyer, C. F., Cote, G. M., Chugh, R., Milhem, M. M., Van Tine, B. A., . . . Jayaprakash, N. (2016). SARC016: Phase II study of everolimus in combination with bevacizumab in sporadic and neurofibromatosis type 1 (NF1) related refractory malignant peripheral nerve sheath tumors (MPNST). In: American Society of Clinical Oncology.
- Wu, J., Patmore, D. M., Jousma, E., Eaves, D. W., Breving, K., Patel, A. V., . . . Stemmer-Rachamimov, A. O. (2014a). EGFR–STAT3 signaling promotes formation of malignant peripheral nerve sheath tumors. *Oncogene*, 33(2), 173.
- Wu, J., Patmore, D. M., Jousma, E., Eaves, D. W., Breving, K., Patel, A. V., . . . Stemmer-Rachamimov, A. O. (2014b). EGFR–STAT3 signaling promotes formation of malignant peripheral nerve sheath tumors. *Oncogene*, 33(2), 173-180.
- Xiao, A., Yin, C., Yang, C., Di Cristofano, A., Pandolfi, P. P., & Van Dyke, T. (2005). Somatic induction of Pten loss in a preclinical astrocytoma model

- reveals major roles in disease progression and avenues for target discovery and validation. *Cancer research*, 65(12), 5172-5180.
- Yamashita, A., Baia, G., Ho, J., Velarde, E., Wong, J., Gallia, G., . . . Riggins, G. (2014). Preclinical evaluation of the combination of mTOR and proteasome inhibitors with radiotherapy in malignant peripheral nerve sheath tumors. *Journal of neuro-oncology*, 118(1), 83-92.
- Yang, F.-C., Chen, S., Clegg, T., Li, X., Morgan, T., Estwick, S. A., . . . Travers, J. (2006). Nf1^{+/-} mast cells induce neurofibroma like phenotypes through secreted TGF- β signaling. *Human molecular genetics*, 15(16), 2421-2437.
- Yang, J., & Du, X. (2013). Genomic and molecular aberrations in malignant peripheral nerve sheath tumor and their roles in personalized target therapy. *Surgical oncology*, 22(3), e53-e57.
- Yoshimatsu, H., Hidaka, S., Nijima, A., & Sakata, T. (2001). Histamine neurons down-regulate ob gene expression in rat white adipose tissue. *Inflammation Research*, 50(2), 72-73.
- Youngstrom, T. G., & Bartness, T. J. (1995). Catecholaminergic innervation of white adipose tissue in Siberian hamsters. *American Journal of Physiology-Regulatory, Integrative and Comparative Physiology*, 268(3), R744-R751.
- Zechner, R., Zimmermann, R., Eichmann, T. O., Kohlwein, S. D., Haemmerle, G., Lass, A., & Madeo, F. (2012). FAT SIGNALS-lipases and lipolysis in lipid metabolism and signaling. *Cell metabolism*, 15(3), 279-291.
- Zeng, W., Pirzgalska, R. M., Pereira, M. M., Kubasova, N., Barateiro, A., Seixas, E., . . . Martins, G. G. (2015). Sympathetic neuro-adipose connections mediate leptin-driven lipolysis. *Cell*, 163(1), 84-94.

- Zhang, L., Tong, X., Zhang, J., Huang, J., & Wang, J. (2015). DAW22, a natural sesquiterpene coumarin isolated from *Ferula ferulaeoides* (Steud.) Korov. that induces C6 glioma cell apoptosis and endoplasmic reticulum (ER) stress. *Fitoterapia*, *103*, 46-54.
- Zhang, Y., Matheny, M., Zolotukhin, S., Tumer, N., & Scarpace, P. J. (2002). Regulation of adiponectin and leptin gene expression in white and brown adipose tissues: influence of β 3-adrenergic agonists, retinoic acid, leptin and fasting. *Biochimica et Biophysica Acta (BBA)-Molecular and Cell Biology of Lipids*, *1584*(2), 115-122.
- Zou, C., Smith, K. D., Liu, J., Lahat, G., Myers, S., Wang, W.-L., . . . Lazar, A. J. (2009). Clinical, pathological, and molecular variables predictive of malignant peripheral nerve sheath tumor outcome. *Annals of surgery*, *249*(6), 1014-1022.
- Zou, C. Y., Smith, K. D., Zhu, Q.-S., Liu, J., McCutcheon, I. E., Slopis, J. M., . . . Mills, G. B. (2009a). Dual targeting of AKT and mammalian target of rapamycin: a potential therapeutic approach for malignant peripheral nerve sheath tumor. *Molecular cancer therapeutics*, *8*(5), 1157-1168.
- Zou, C. Y., Smith, K. D., Zhu, Q.-S., Liu, J., McCutcheon, I. E., Slopis, J. M., . . . Mills, G. B. (2009b). Dual targeting of AKT and mammalian target of rapamycin: a potential therapeutic approach for malignant peripheral nerve sheath tumor. *Molecular cancer therapeutics*, 1535-7163. MCT-1508-1008.